MycoKeys 57: 1–30 (2019)
doi: 10.3897/mycokeys.57.33267
http://mycokeys.pensoft.net

RESEARCH ARTICLE

A peer-reviewed open-access journal
MycoKeys
Launched to accelerate biodiversity research

Understanding the evolution of phenotypical characters in the *Micarea prasina* group (Pilocarpaceae) and descriptions of six new species within the group

Beata Guzow-Krzemińska[1], Emmanuël Sérusiaux[2], Pieter P.G. van den Boom[3], A. Maarten Brand[4], Annina Launis[5], Anna Łubek[6], Martin Kukwa[1]

1 *University of Gdańsk, Faculty of Biology, Department of Plant Taxonomy and Nature Conservation, Wita Stwosza 59, PL-80-308 Gdańsk, Poland* **2** *Evolution and Conservation Biology Unit, University of Liège, Sart Tilman B22, B-4000 Liège, Belgium* **3** *Arafura 16, NL-5691 JA Son, The Netherlands* **4** *Klipperwerf 5, NL-2317 DX Leiden, The Netherlands* **5** *Botany unit, Finnish Museum of Natural History, P.O. Box 7, FI-00014 University of Helsinki, Finland* **6** *The Jan Kochanowski University in Kielce, Institute of Biology, Świętokrzyska 15, PL-25-406 Kielce, Poland*

Corresponding author: *Beata Guzow-Krzemińska* (beata.guzow@biol.ug.edu.pl)

Academic editor: *Pradeep Divakar* | Received 22 January 2019 | Accepted 9 July 2019 | Published 31 July 2019

Citation: Guzow-Krzemińska B, Sérusiaux E, van den Boom PPG, Brand AM, Launis A, Łubek A, Kukwa M (2019) Understanding the evolution of phenotypical characters in the *Micarea prasina* group (Pilocarpaceae) and descriptions of six new species within the group. MycoKeys 57: 1–30. https://doi.org/10.3897/mycokeys.57.33267

Abstract

Six new *Micarea* species are described from Europe. Phylogenetic analyses, based on three loci, i.e. mtSSU rDNA, *Mcm7* and ITS rDNA and ancestral state reconstructions, were used to evaluate infra-group divisions and the role of secondary metabolites and selected morphological characters on the taxonomy in the *M. prasina* group. Two main lineages were found within the group. The *Micarea micrococca* clade consists of twelve species, including the long-known *M. micrococca* and the newly described *M. microsorediata*, *M. nigra* and *M. pauli*. Within this clade, most species produce methoxymicareic acid, with the exceptions of *M. levicula* and *M. viridileprosa* producing gyrophoric acid. The *M. prasina* clade includes the newly described *M. azorica* closely related to *M. prasina* s.str., *M. aeruginoprasina* sp. nov. and *M. isidioprasina* sp. nov. The species within this clade are characterised by the production of micareic acid, with the exception of *M. herbarum* which lacks any detectable substances and *M. subviridescens* that produces prasinic acid. Based on our reconstructions, it was concluded that the ancestor of the *M. prasina* group probably had a thallus consisting of goniocysts, which were lost several times during evolution, while isidia and soredia evolved independently at multiple times. Our research supported the view that the ancestor of *M. prasina* group did not produce any secondary substances, but they were gained independently in different lineages, such as methoxymicareic acid which is restricted to *M. micrococca* and allied species or micareic acid present in the *M. prasina* clade.

Keywords
Ancestral state reconstruction, lichenised fungi, morphology, mtSSU rDNA, secondary metabolites, taxonomy

Introduction

Traditionally, morpho-anatomical characters, together with secondary metabolites, have played an important role in the lichen classification (e.g. Brodo 1978, 1986; Lumbsch 1998). With the introduction of molecular data, powerful tools for reconstructing phylogenetic relationships have become available. Furthermore, molecular phylogenies can serve as a backbone for tracing the evolution of morphological and chemical characters by reconstructing their ancestral states. Such interpretations of character evolution usually open new perspectives to the evolutionary history (Lumbsch et al. 2006).

Secondary metabolites have been traditionally used in the taxonomy of lichens at different taxonomic levels, although their values have been questioned by many authors (Lumbsch et al. 2006; Leavitt et al. 2011; Lutsak et al. 2017). In many cases, molecular data do not correspond with the chemical variation and, therefore, the correlation between them has to be evaluated for each taxonomic group *de novo* (e.g. Goffinet and Miadlikowska 1999; Kroken and Taylor 2001; Molina et al. 2004; Divakar et al. 2005, 2006; Elix et al. 2009; Buschbom and Mueller 2006; Nelsen and Gargas 2008; Nelsen et al. 2008; Lendemer et al. 2015; Ossowska et al. 2018). Moreover, the production of certain secondary metabolites might be triggered by the environment (e.g. climate, edaphic factors, associated symbionts) (Spribille et al. 2016; Lutsak et al. 2017).

The genus *Micarea* Fr., comprising ca. 100 species, is a cosmopolitan group of lichens which has been extensively studied in Europe by Coppins (1983) and Czarnota (2007). Phenotypical diversity in this group of lichens is not limited to morphological characters, but also includes diverse secondary metabolites and, hence, chemical variation plays an important role in their taxonomy. Recently, *Micarea* has received more attention and numerous species have been described based on anatomical, morphological and chemical characters and, in some cases, also molecular data (e.g. Czarnota and Guzow-Krzemińska 2010; Svensson and Thor 2011; Cáceres et al. 2013; Aptroot and Cáceres 2014; Brand et al. 2014; van den Boom and Ertz 2014; Guzow-Krzemińska et al. 2016; McCarthy and Elix 2016; van den Boom et al. 2017; Kantvilas 2018; Launis et al. 2019a, b).

Species delimitation within *Micarea* has been especially difficult in the *M. prasina* group which was first characterised by Coppins (1983) based on morphological, anatomical and chemical features. At first, the group included *M. prasina* Fr., the type species of the genus, as well as *M. hedlundii* Coppins and *M. levicula* (Nyl.). Coppins (1983) also suggested that *M. misella* (Nyl.) Hedl., *M. melanobola* (Nyl.) Coppins and *M. synotheoides* (Nyl.) Coppins might be related to *M. prasina*; however, as supported by recent molecular studies, *M. misella* and *M. synotheoides* do not belong to this group (Czarnota and Guzow-Krzemińska 2010; van den Boom et al. 2017; Launis et al. 2019a). *Micarea melanobola* was synonymised with *M. prasina* (Czarnota 2007), but recently found to be a distinct species (Launis et al. 2019b).

Coppins (1983) treated *M. prasina* in a wide sense including specimens with variable morphology and chemistry, which later were distinguished as distinct species, i.e. *M. micrococca* (Körb.) Gams ex Coppins for the methoxymicareic acid chemotype, *M. prasina* s.str. for the micareic acid chemotype and *M. subviridescens* (Nyl.) Hedl. for the prasinic acid chemotype (Coppins 2009). Further studies showed even higher chemical variation within the *M. prasina* group and *M. xanthonica* Coppins & Tønsberg with xanthones (thiophanic acid with satellites) and *M. viridileprosa* Coppins & van den Boom containing gyrophoric acid (Coppins and Tønsberg 2001; van den Boom and Coppins 2001) were recognised. Later, more new species were discovered, such as *M. nowakii* Czarnota & Coppins, *M. soralifera* Guzow-Krzemińska, Czarnota, Łubek & Kukwa and *M. meridionalis* van den Boom, Brand, Coppins & Sérus. producing micareic acid. Moreover, *M. byssacea* (Th. Fr.) Czarnota, Guzow-Krzemińska & Coppins, *M. czarnotae* Launis, van den Boom, Sérusiaux & Myllys, *M. laeta* Launis & Myllys, *M. microareolata* Launis, Pykälä & Myllys and *M. pseudomicrococca* Launis & Myllys containing methoxymicareic acid, as well as *M. tomentosa* Czarnota & Coppins and *M. herbarum* Brand, Coppins, Sérus. & van den Boom lacking any lichen substances detectable by thin layer chromatography (TLC), were added to this group (Czarnota 2007; Czarnota and Guzow-Krzemińska 2010; Guzow-Krzemińska et al. 2016; van den Boom et al. 2017; Launis et al. 2019a). These species were described, based on phenotypic characters and molecular data. Recently crystalline granules studied in polarised light were also presented as a novel species-level character for *Micarea* spp. (Launis et al. 2019b). During the preparation of the final version of this paper, several other species within *M. prasina* group have also been described (Launis et al. 2019b), but those have not been included in our analyses.

Moreover, several other new species likely to belong to the *M. prasina* group have been described. Two such species were described from Réunion, i.e. *M. melanoprasina* Brand, van den Boom & Sérus. producing a substance probably related to micareic acid and *M. hyalinoxanthonica* Brand, van den Boom & Sérus. containing a xanthone (probably thiophanic acid) (Brand et al. 2014). Furthermore, one species was described from Brazil, i.e. *M. corallothallina* M. Cáceres, D. A. Mota & Aptroot lacking any lichen substances (Cáceres et al. 2013) and yet another from South Australia, i.e. *M. kartana* Kantvilas & Coppins containing gyrophoric acid (Kantvilas 2018). However, the phylogenetic relationships of these species are still uncertain due to the lack of molecular data. These studies also show that phenotypical variation within the *M. prasina* group may still be underestimated and requires further studies.

This study is based on specimens from years of collection in Belgium, France, Germany, Portugal (including Madeira and the Azores), Poland, Romania and the Netherlands. Using these collections for a phylogenetic reconstruction, six new species, belonging to the *M. prasina* group, are described by means of morphological, anatomical, chemical and molecular data. Moreover, by reconstructing ancestral states, the evolution of diagnostic traits, that are traditionally used for the taxonomic classification of species belonging to the *M. prasina* group, were investigated. Infra-group divisions and

the role of secondary metabolites for species taxonomy within the *M. prasina* group were also evaluated. The production of selected secondary metabolites is further analysed (i.e. gyrophoric, methoxymicareic, micareic, prasinic and thiophanic acids), as well as the presence of several pigments in the apothecia commonly used in lichen taxonomy (Meyer and Printzen 2000) (i.e. Sedifolia-grey, Elachista-brown, Cinereorufa-green and Superba-brown). Ancestral state reconstruction of morphological characters i.e. goniocysts, isidia and soredia is also performed.

Materials and methods

Materials

Material of the new species, including samples used for DNA analyses, is deposited in KTC, UGDA and LG, with additional specimens stored in private herbaria of van den Boom and Brand.

Morphology and chemistry

Apothecial sections and squashed thallus preparations were studied in tap water with or without the addition of C (commercial bleach) and K (water solution of potassium hydroxide) (Orange et al. 2001). Dimensions of all anatomical features were measured in water. Thin layer chromatography (TLC) was used for the determination of lichen substances according to the standard methods (Orange et al. 2001). All samples were studied in solvent C. The nomenclature of apothecial pigments follows Meyer and Printzen (2000). Crystalline granules were studied in polarised light (see Launis et al. 2019a, b).

Taxon sampling for DNA

A total of 63 new sequences were generated for this study (Suppl. material 2, Table S1). Additional sequences of mtSSU, *Mcm7* and ITS rDNA from specimens of the *Micarea prasina* group were obtained from GenBank (Suppl. material 2, Table S1). Moreover, sequences of the above-mentioned markers from specimens of *M. adnata* Coppins, *M. elachista* (Körb.) Coppins & R. Sant., *M. globulosella* (Nyl.) Coppins, *M. misella*, *M. peliocarpa* (Anzi) Coppins & R. Sant., *M. pycnidiophora* Coppins & P. James, *M. stipitata* Coppins & P. James and *M. synotheoides* (Suppl. material 2, Table S1), which were shown to be outside the group (e.g. Launis et al. 2019a) were also obtained from GenBank. In total, sequences of 119 specimens were subjected to analyses. *Micarea peliocarpa* (Anzi) Coppins & R. Sant. was chosen as the outgroup, based on the study of Launis et al. (2019a).

DNA extraction, PCR amplification and DNA sequencing

DNA was extracted directly from pieces of thalli using a modified CTAB method (Guzow-Krzemińska and Węgrzyn 2000). DNA extracts were used for PCR amplification and 25 µl of PCR mix contained 1U of Taq polymerase (Thermo Scientific) or 1U of DreamTaq polymerase (Thermo Scientific) and appropriate buffer, 0.2 mM of each of the four dNTPs, 0.5 µM of each primer and 10–50 ng of genomic DNA. PCR amplifications were performed using a Mastercycler (Eppendorf).

Amplifications of mtSSU rDNA, employing mrSSU1 and mrSSU3R primers (Zoller et al. 1999), were performed using the following conditions: initial denaturation at 95 °C for 10 min followed by 6 cycles at 95 °C for 1 min, 62 °C for 1 min and 72 °C for 105 s and then 30 cycles at 95 °C for 1 min, 56 °C for 1 min and 72 °C for 1 min, with a final extension step at 72 °C for 10 min.

Amplifications of the *Mcm7* region employing Mcm7_AL1r and Mcm7_AL2f primers (Launis et al. 2019a) were performed using the following conditions: initial denaturation at 94 °C for 5 min, followed by 38 cycles at 94 °C for 45 s (denaturation), 56 °C for 50 s (annealing) and 72 °C for 1 min (extension), with the final extension at 72 °C for 5 min.

Amplifications of the ITS region employed the following primer pairs: ITS1F (Gardes and Bruns 1993) and ITS4 (White et al. 1990) or ITS 5 and ITS4A (Kroken and Taylor 2001) or nu-SSU-1626-5' (Gargas and DePriest 1996) and nu-LSU-136-3' (Döring et al. 2000). The following PCR cycling parameters were applied to amplify nuclear ITS region: an initial denaturation at 94 °C for 3 min, followed by 35 cycles at 94 °C for 30 s, 54 °C for 30 s (for ITS1F and ITS4 or nu-SSU-1626-5' and nu-LSU-136-3' primers) or 62 °C for 30 s (for ITS5 and ITS4A primers) and 72 °C for 1 min, with a final extension at 72 °C for 7 min. PCR products were visualised on agarose gels in order to determine DNA fragment lengths. Subsequently, PCR products were purified using Clean-up Concentrator (A&A Biotechnology) following the manufacturer's protocol or 10 µl of PCR products were treated with a mixture of 20 units of Exonuclease I and 2 units of FastAP Thermosensitive Alkaline Phosphatase enzymes (Thermo Scientific) to remove unincorporated primers and nucleotides. Treatment with those enzymes was carried out at 37 °C for 15 min, followed by incubation at 85 °C for 15 min to completely inactivate both enzymes. Sequencing of each PCR product was performed in Macrogen (www.macrogen.com) using the PCR primers.

Sequence alignment and phylogenetic analysis

The newly generated sequences (GenBank accession numbers are given in Suppl. material 2, Table S1) were compared to the sequences available in the GenBank database (http://www.ncbi.nlm.nih.gov/BLAST/) using BLASTn search (Altschul et al. 1990) in order to confirm their identity. The sequences of each marker were aligned with se-

quences of selected representatives of the genus *Micarea* obtained from GenBank (list of specimens and GenBank Accession Numbers are given in Suppl. material 2, Table S1). Alignment was performed using Seaview software (Galtier et al. 1996; Gouy et al. 2010) employing the Muscle option, followed by manual optimisation. Portions of the alignment with ambiguous positions that might not have been homologous and terminal ends were excluded from the analyses. As the gene trees for each marker did not show any strongly supported conflicts, three datasets were combined into a concatenated matrix in the Seaview software (Galtier et al. 1996; Gouy et al. 2010) and the final alignment was deposited in Treebase (Accession No. S24731).

Partition Finder 2 (Lanfear et al. 2016), implemented at CIPRES Science Gateway (Miller et al. 2010), was used to determine the best substitution model for each partition under Akaike Information Criterion (AIC) and greedy search algorithm (Lanfear et al. 2012). The following models were found: TVM+I+G+X for mtSSU, TRN+I+G+X for *Mcm7* and GTR+I+G+X for ITS regions.

The data were analysed using a Bayesian approach (MCMC) in MrBayes 3.2 (Huelsenbeck and Ronquist 2001; Ronquist and Huelsenbeck 2003) and best models determined by Partition Finder 2 were employed. Two parallel runs were performed, each using four independent chains and 10 million generations, sampling trees every 1,000th generation. Tracer v. 1.5 (Rambaut and Drummond 2007) was used to ensure that stationarity was reached by plotting the log-likelihood values of the sample points against generation time. Posterior probabilities (PP) were determined by calculating a majority-rule consensus tree generated from the 15,002 post-burn-in trees of the 20,002 trees sampled by the two MCMC runs, using the sumt option of MrBayes.

Maximum likelihood analyses were performed using RaxML HPC v.8 on XSEDE (Stamatakis 2014) under the GTRGAMMAI model on CIPRES Science Gateway (Miller et al. 2010). Rapid bootstrap analyses were performed with 1,000 bootstrap replicates (BS). The RAxML tree did not contradict the Bayesian tree topology for the strongly supported branches. Therefore, only the maximum likelihood tree is shown with the posterior probabilities (PP) of the Bayesian analysis and the bootstrap support values added near the internal branches. BS ≥ 70 and PP ≥ 0.95 were considered significant. Phylogenetic trees were visualised using FigTree v. 1.4.2, in which the clades for previously described taxa are collapsed (Rambaut 2012).

Ancestral character state reconstruction

Morphological and chemical characters from taxa of the *Micarea prasina* group and selected outgroup taxa were obtained from herbarium material and complemented with data from literature. In order to reduce the number of missing data in our dataset, we did not include *M. pycnidiophora*, *M. stipitata* and *M. synotheoides*, which do not belong to the *M. prasina* group and for which mtSSU sequences were only available and *Micarea* sp. lineage A, which represents a single specimen that has not been formally described. The following secondary metabolites were analysed: gyrophoric,

methoxymicareic, micareic, prasinic and thiophanic acids. The presence of apothecial pigmentation was also analysed and the following pigments were noted: Sedifolia-grey, Elachista-brown, Cinereorufa-green and Superba-brown. The presence of selected morphological characters was also analysed, i.e. goniocysts, isidia and soredia. The morphological and chemical characters were coded as a multistate data matrix (Suppl. material 2, Table S2) and a binary dataset (Suppl. material 2, Table S3) and subjected to ancestral character state reconstruction using the parsimony model with characters treated as unordered and the likelihood method (Mk1 model) in Mesquite v.3.5 (Maddison and Maddison 2018). Ancestral state reconstructions were based on the topology of the consensus tree obtained using Mr Bayes 3.2 (Huelsenbeck and Ronquist 2001; Ronquist and Huelsenbeck 2003)

Results

The final DNA alignment consisted of sequences obtained from 119 individual specimens and three markers, i.e. mtSSU, *Mcm7* and ITS rDNA, with a total of 1784 characters. Since the topologies from the maximum likelihood and Bayesian analyses did not show any strongly supported conflict, the maximum likelihood tree (RaxML Optimisation Likelihood was -14426.795913) is presented in Figure 1 with added posteriori probabilities from Bayesian analysis (Harmonic mean was -13101.16). In order to reduce the size of the tree, highly supported clades were collapsed for previously described taxa.

The phylogenetic reconstruction (Fig. 1) shows that the *M. prasina* group is highly supported and monophyletic (100 BS and 1 PP) and it agrees with previous phylogenies based on a mtSSU marker (e.g. Czarnota and Guzow-Krzemińska 2010; Guzow-Krzemińska et al. 2016) or three loci (Launis et al. 2019a). Two main lineages are further distinguished, i.e. the *M. micrococca* clade and the *M. prasina* clade with sequences of *M. tomentosa* forming a highly supported lineage, basal to the two clades (Fig. 1). Moreover, *M. hedlundii* and *M. xanthonica* are closely related (82 BS) and sister to the *M. micrococca* clade (Fig. 1).

The *Micarea micrococca* clade in Figure 1 (99 BS and 1 PP) consists mostly of species containing methoxymicareic acid. This group accommodates the newly described species *M. microsorediata*, *M. nigra* and *M. pauli*, as well as *M. byssacea*, *M. czarnotae*, *M. laeta*, *M. levicula*, *M. microareolata*, *M. micrococca*, *M. pseudomicrococca*, *M. viridileprosa* and an undescribed *Micarea* sp. (lineage A in Launis et al. 2019a). The closest relatives to *M. pauli* are *M. viridileprosa* and *M. levicula* (99 BS and 1 PP), while the relationships of *M. micrococca*, *M. microsorediata* and *M. nigra* remain unresolved.

The *Micarea prasina* clade (93 BS and 1 PP) consists mostly of species containing micareic acid and accommodates the newly described *M. aeruginoprasina*, *M. azorica* and *M. isidioprasina*, as well as *M. herbarum*, *M. meridionalis*, *M. nowakii*, *M. prasina*, *M. soralifera* and *M. subviridescens.* Several highly supported lineages are further distinguished within this clade. The newly described *M. azorica* forms a highly

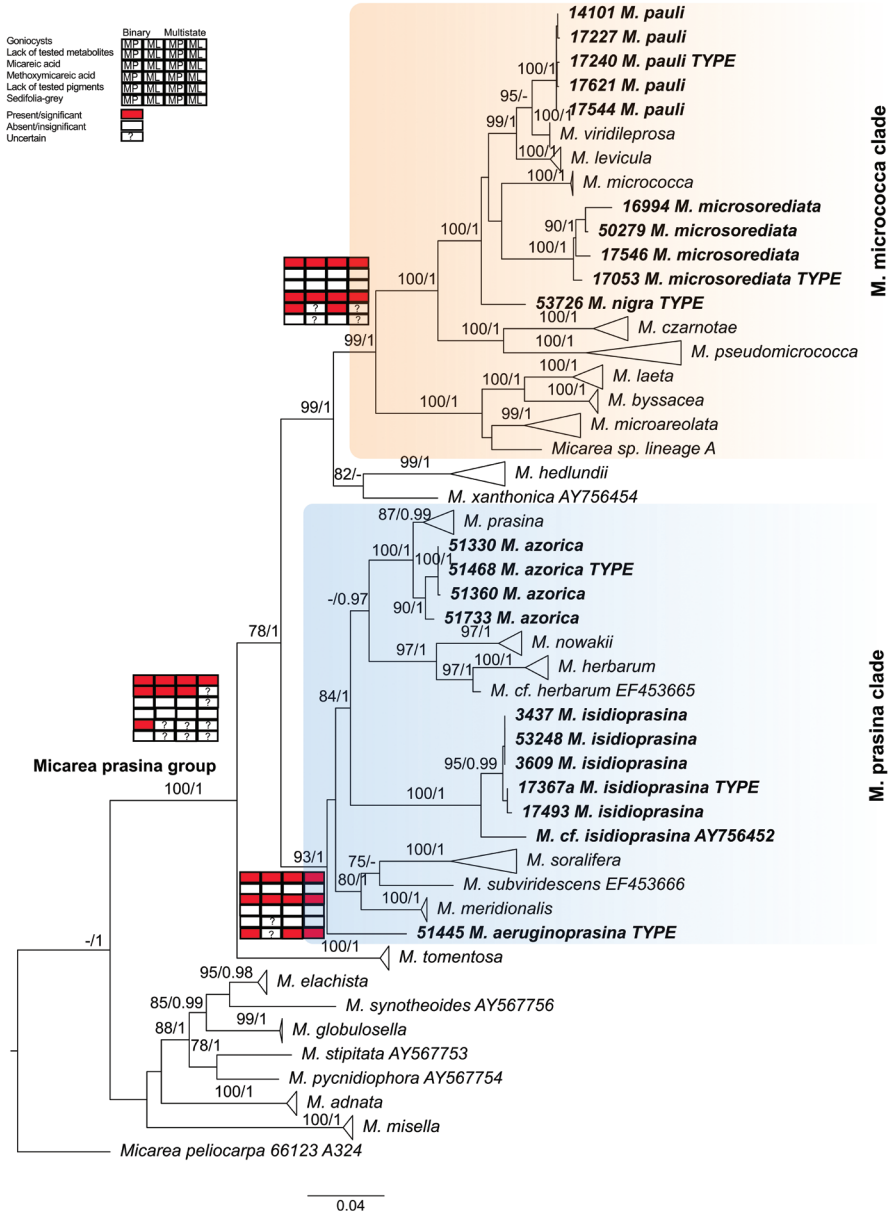

Figure 1. Maximum likelihood tree based on three-loci dataset. Bootstrap supports ≥ 70 for ML and posterior probabilities ≥ 0.95 (second value) for Bayesian methods are indicated near the branches. The highly supported clades with previously described species represented by numerous sequences are collapsed. Herbarium collection numbers for newly sequenced specimens precede the names of species and type specimens are marked. Newly described species are marked in **bold**. *Micarea micrococca* (orange) and *M. prasina* (blue) clades are indicated with shading. Ancestral states for selected characters reconstructed based on binary or multistate datasets using maximum parsimony (MP) or maximum likelihood methods (ML) are marked for the main clades: *M. prasina* group, *M. micrococca* clade and *M. prasina* clade using red (= present/significant) and white (= absent/insignificant) boxes or ? (= uncertain).

supported group with the type species of *M. prasina* s.str. (100 BS and 1 PP), whereas specimens of *M. prasina* form a well-supported group (87/0.99). Furthermore, they are sister to *M. nowakii* and *M. herbarum*, which are the only species within the *M. prasina* group developing almost entirely an endosubstratal thallus with only a few areoles. With the exception of *M. herbarum* and *M. nowakii*, this lineage (97 BS and 1 PP) also includes a sequence which seems to be different from both species (EF453665) and may indicate the existence of an undescribed taxon. Specimens of the newly described *M. isidioprasina* form a highly supported group (100 BS and 1 PP) with a single sequence from North America originally assigned to *M. prasina* (AY756452; see Andersen and Ekman 2005), but genetically more similar to *M. isidioprasina*. This sample is also morphologically similar to *M. isidioprasina* due to the isidioid thallus and pale apothecia (Czarnota and Guzow-Krzemińska 2010) and, therefore, is named here as *M.* cf. *isidioprasina* in Figure 1. *Micarea meridionalis*, *M. soralifera* and *M. subviridescens* form a highly supported group (80 BS and 1PP).

To investigate the diagnostic traits traditionally used for the taxonomic classification within the *M. prasina* group, we focused both on the *M. micrococca* and the *M. prasina* clades separately and the whole *M. prasina* together (Fig. 1) and employed both maximum parsimony and Mk1 models, based on the multistate and binary datasets (Suppl. material 2, Tables S2–S3 and Suppl. material 1, Figs S1–S15). The likelihoods for each set of characters are given in Suppl. material 2, Table S4. Our analyses found that the presence of methoxymicareic acid is restricted to the *M. micrococca* clade that accommodates several species containing this substance. However, *M. levicula* and *M. viridileprosa* are exceptions by producing gyrophoric acid (Suppl. material 1, Fig. S13). The ancestral state reconstructions show that the presence of methoxymicareic acid is the most parsimonious and the most likely ancestral state for the *M. micrococca* clade (Fig. 1, Tables 1–3 and Suppl. material 1, Figs S3, S13). On the other hand, micareic acid is the ancestral state for *M. prasina* clade in all analyses (Fig. 1, Tables 1–3, Suppl. material 1, Figs S2, S13). However, the reconstructions of ancestral state for the whole *M. prasina* group show the lack of any secondary metabolites in their ancestors in most of the analyses. However, the maximum likelihood analysis, based on the multistate dataset, suggests uncertainty as both the lack of any secondary metabolites and the presence of micareic acid are more likely than other states (Fig. 1, Tables 1–3 and Suppl. material 1, Figs S2, S13).

The evolution of pigments, present in the apothecia, was also analysed, but some of the results remain uncertain in our analyses. Parsimony reconstructions, based on the binary dataset, suggest the lack of any pigment in the apothecia, while other analyses do not exclude the possibility that Sedifolia-grey pigment was present in the ancestor of *M. prasina* group (Fig. 1, Tables 1–3, Suppl. material 1, Figs S9–S12, S14). Moreover, the results obtained for the *M. micrococca* clade, using two different methods, are not fully consistent. Maximum parsimony analyses suggest a lack of pigments in their ancestors therefore resulting in multiple gains of Sedifolia-grey pigment and a single gain of Cinereorufa-green pigments in this lineage. However, maximum likelihood analyses show that both the lack of pigments in apothecia and the presence of Sedifolia-grey pigment may have occurred in their ancestor (Fig. 1, Tables 1–3, Suppl.

Table 1. Most parsimonious ancestral character states for selected subclades of the *M. prasina* group. The results that differ between maximum likelihood and maximum parsimony methods for each dataset are marked with *.

Characters	*M. prasina* group	*M. micrococca* clade	*M. prasina* clade
Morphological characters	goniocysts	goniocysts	goniocysts
Secondary metabolites	lack of any substance*	methoxymicareic acid	micareic acid
Presence of apothecial pigments	uncertain (lack of pigments OR Sedifolia-grey)	lack of pigments or unknown*	Sedifolia-grey
Goniocysts	present	present	present
Isidia	absent	absent	absent
Soredia	absent	absent	absent
Gyrophoric acid	absent	absent	absent
Methoxymicareic acid	absent	present	absent
Micareic acid	absent	absent	present
Prasinic acid	absent	absent	absent
Thiophanic acid	absent	absent	absent
Cinereorufa-green	absent	absent	absent
Elachista-brown	absent	absent	absent
Sedifolia-grey	absent*	absent*	present*
Superba-brown	absent	absent	absent

Table 2. Most likely ancestral character states in multistate analysis and their likelihoods for selected subclades of *M. prasina* group. Values for the most likely states are given in **bold**. The results that differ between maximum likelihood and maximum parsimony methods are marked with *

Characters	State	*M. prasina* group	*M. micrococca* clade	*M. prasina* clade
Morphological characters	other or unknown	0.03672198	0.00009398	0.00056073
	goniocysts	**0.95494636**	**0.99972253**	**0.99844142**
	soredia	0.00411906	0.00009117	0.00008044
	isidia	0.00421261	0.00009232	0.00091742
Secondary metabolites	lack of any substances	**0.78962855**	0.05876201	0.00749498
	prasinic acid	0.01031084	0.00338938	0.00052042
	micareic acid	**0.117972***	0.01320396	**0.98892236**
	methoxymicareic acid	0.04762568	**0.90867382**	0.00176536
	gyrophoric acid	0.01528514	0.00349062	0.00050881
	thiophanic acid	0.01917779	0.01248021	0.00078808
Presence of apothecial pigments	lack of pigment or unknown	**0.39914052**	**0.73149364**	0.03357191
	Sedifolia-grey	**0.44528926**	**0.21519349***	**0.95640101**
	Cinereorufa-green	0.04803049	0.02251569	0.00293747
	Elachista-brown	0.05745307	0.01546335	0.00302814
	Superba-brown	0.05008665	0.01533383	0.00406148

material 1, Figs S9–S12, S14). In case of the *M. prasina* clade, maximum likelihood analyses, based on the binary dataset, give uncertain results as both presence and absence of Sedifolia-grey are equally likely; however parsimony analysis for the binary dataset and both analyses for the multistate dataset show the presence of Sedifolia-grey pigment in apothecia of their ancestor.

Morphological characters, i.e. the presence of goniocysts observed in many species of the *M. prasina* group, soredia observed in *M. microsorediata*, *M. soralifera* and *M. viridileprosa* and isidia present in *M. aeruginoprasina*, *M. isidioprasina*, *M. nigra* and *M. pauli* were also evaluated (Fig. 1, Tables 1–3, Suppl. material 1 Figs S9–S12, S14). It was found that the presence of goniocysts is the most parsimonious and the most likely state for the ancestor of the *M. prasina* group in all analyses (Fig. 1, Tables 1–3 and

Table 3. Most likely ancestral character states based on analysis of binary dataset and their likelihoods for selected subclades of *M. prasina* group. Values for the most likely states are given in **bold**. The results that differ between maximum likelihood and maximum parsimony methods are marked with *

Characters	State	*M. prasina* group	*M. micrococca* clade	*M. prasina* clade
Goniocysts	Present	**0.85180046**	**0.99078786**	**0.93297055**
	Absent	0.14819954	0.00921214	0.06702945
Isidia	Present	0.00354307	0.00079891	0.01513079
	Absent	**0.99645693**	**0.99920109**	**0.98486921**
Soredia	Present	0.00099039	0.00020816	0.00004518
	Absent	**0.99900961**	**0.99979184**	**0.99995482**
Gyrophoric acid	Present	0.00499412	0.00058456	0.00011577
	Absent	**0.99500588**	**0.99941544**	**0.99988423**
Methoxymicareic acid	Present	0.0023099	**0.85313833**	0.00010697
	Absent	**0.9986901**	0.14686167	**0.99989303**
Micareic acid	Present	0.02913989	0.00055219	**0.98044653**
	Absent	**0.97086011**	**0.99944781**	0.01955347
Prasinic acid	Present	0.00002438	0.0000051	0.00000103
	Absent	**0.99997562**	**0.9999949**	**0.99999897**
Thiophanic acid	Present	0.0000248	0.00000102	0.00001393
	Absent	**0.9999752**	**0.99999898**	**0.99998607**
Cinereorufa-green	Present	0.00002408	0.0000016	0.00000099
	Absent	**0.99997592**	**0.9999984**	**0.99999901**
Elachista-brown	Present	0.00002503	0.0000052	0.00000102
	Absent	**0.99997497**	**0.9999948**	**0.99999898**
Sedifolia-grey	Present	0.49999914*	0.49994168*	0.50492012
	Absent	0.50000086	0.50005832	0.49507988*
Superba-brown	Present	0.00050986	0.00004725	0.00000944
	Absent	**0.99949014**	**0.99995275**	**0.99999056**

Suppl. material 1, Figs S6, S15). However, this character has been lost in the lineage represented by *M. herbarum* and *M. nowakii* lacking goniocysts (Fig. 1, Tables 1–3 and Suppl. material 1, Figs S6, S15). Isidia and soredia evolved independently at multiple times in the *M. prasina* group resulting in the formation of isidiate thalli in the studied species, i.e. *M. aeruginoprasina*, *M. isidioprasina*, *M. nigra* and *M. pauli* or sorediate thalli in *M. microsorediata*, *M. soralifera* and *M. viridileprosa* (Fig. 1, Tables 1–3 and Suppl. material 1, Figs S7, S8, S15).

Discussion

Challenges in species delimitation within *M. prasina* group were already mentioned by Coppins (1983) and other authors (e.g. Czarnota 2007; Czarnota and Guzow-Krzemińska 2010; van den Boom et al. 2017; Launis et al. 2019a, b). Since Coppins (1983), who treated *M. prasina* in a wide sense with morphologically variable chemical races which were further recognised as distinct species, the introduction of molecular data revealed even greater variability within this group and numerous other species were described based on phenotypic and molecular data (e.g. Czarnota and Guzow-Krzemińska 2010; Guzow-Krzemińska et al. 2016; van den Boom et al. 2017; Launis et al. 2019a, b). Many species within this group have goniocystoid thallus, micareoid

photobiont and Sedifolia-grey pigment in the apothecia, however a high variation in secondary metabolites production, which are treated as diagnostic characters, is observed within the *M. prasina* group. In the phylogenetic tree (Fig. 1) two main clades were distinguished; *M. micrococca* clade which groups mainly taxa containing methoxymicareic acid and *M. prasina* clade which mainly comprises species containing micareic acid. However, there are some exceptions as other substances may be produced by selected representatives of the group, e.g. gyrophoric, prasinic or thiophanic acids or some taxa do not produce any secondary metabolites. Within this group, numerous phenotypic differences are applied to distinguish species, e.g. size and shape of apothecia, size and type of paraphyses, size of ascospores, thallus structure including the vegetative diaspores and presence of pigments. Recently introduced crystalline granules showed to be valuable traits in the taxonomy of the group (Launis et al. 2019a, b). However, the application of molecular data seems to be essential to support delimitation of species within this group (e.g. Launis et al. 2019a, b; this study).

The evolution of new morphological characters involves multiple subsequent evolutionary steps. In our study, ancestral state reconstructions showed that the presence of goniocysts is the most parsimonious and most likely state for the ancestor of the *M. prasina* group (Fig. 1, Tables 1–3 and Suppl. material 1, Figs S6, S15). However, the development of goniocysts was apparently lost in some lineages during evolution as several species within the group do not develop such structures but produce other vegetative diaspores (soredia and/or isidia). Whether the structures from which soredia and isidia develop are goniocysts or areoles is not easy to assign. Based on literature, goniocysts are more or less round vegetative diaspores (therefore similar to soredia) and are produced from the endosubstratal parts of thalli multiple times to form a layer as in *M. prasina* s.str. (Coppins 1983; Barton and Lendemer 2014). As the thallus parts developing isidioid or soredioid diaspores did not resemble goniocysts as defined in previous works, we determined all these structures as areoles, as already proposed by Guzow-Krzemińska et al. (2016). Although soredia in the newly described *M. microsorediata* and recently recognised *M. soralifera* (Guzow-Krzemińska et al. 2016) may resemble goniocysts, they are at least at the beginning produced in delimited soralia over the thallus and differ in the structure and colour from the non-sorediate parts of thalli.

In our study, ancestral state reconstructions suggest that isidia evolved independently multiple times in this group of lichens resulting in the formation of almost entirely isidiate thalli in four species, i.e. *M. aeruginoprasina*, *M. isidioprasina*, *M. nigra* and *M. pauli* (Suppl. material 1, Figs S6–S8, S15). Prieto et al. (2013) suggested that losing an existing character could be expected to occur much more rapidly and in fewer steps than gaining a new character. A similar case is represented by sorediate species and the production of soredia developed in unrelated lineages. Only one lineage lost the ability to produce goniocysts or any other lichenised vegetative diaspores (i.e. *M. herbarum* and *M. nowakii*). Species belonging to this clade develop thin episubstratal thalli with few areoles or merely an endosubstratal layer (Czarnota 2007; van den Boom et al. 2017). The acquisition of different thallus organisation may have resulted from adaptation to drier ecological niches. Many collections of the species from this clade were found in

drier and open habitats (Czarnota 2007; van den Boom et al. 2017). In comparison, taxa developing distinct episubstratal thalli seem to be confined to more humid and shaded localities (Czarnota 2007). However, this hypothesis needs further ecological studies.

Secondary metabolites have been extensively used in the chemotaxonomy of lichens. The *Micarea prasina* group shows a high variation in chemistry even in closely related species (e.g. Czarnota 2007; Czarnota and Guzow-Krzemińska 2010). Species belonging to this group produce gyrophoric, micareic, methoxymicareic and prasinic acids, as well as xanthones (Elix et al. 1984; Coppins and Tønsberg 2001; van den Boom and Coppins 2001). Gyrophoric acid is the simplest tridepside comprising three orsellinic units which originate from condensation of one acetyl-CoA and three malonyl-CoA units as shown by Mosbach (1964). Although gyrophoric acid is commonly produced in the genus *Micarea* (e.g. Coppins 1983; Czarnota 2007), in the *M. prasina* group, it is only present in *M. levicula* and *M. viridileprosa* and the still unsequenced *M. kartana* (Kantvilas 2018). Both *M. levicula* and *M. viridileprosa* belong to the *M. micrococca* clade which is otherwise characterised by the production of methoxymicareic acid.

Micareic and methoxymicareic acids are the most common secondary metabolites produced by species of the *M. prasina* group. They are structurally related diphenyl ethers ('pseudodepsidones') (Huneck and Yoshimura 1996), but they have a distincly different substitution pattern and probably also biosynthetic origin (Elix et al. 1984). As numerous diphenyl ethers co-occur with structurally related depsidones, it was hypothesised that they are biosynthesis precursors or catabolites of similarly substituted depsidones (Huneck and Yoshimura 1996). In the work on the secondary metabolites of chemical races of the *M. prasina* s.l., Elix et al. (1984) suggested that enzymatically induced Smiles rearrangement of *para*-depside prasinic acid might lead to the formation of micareic acid, a very likely biosynthetic pathway for this metabolite. They also pointed out that other rearrangements, such as nuclear hydroxylation followed by O-methylation, are necessary for the formation of methoxymicareic acid, but the actual order of those processes remain unknown. However, the chemical races of *M. prasina* s.l. they studied actually represent several species which were later distinguished as *M. micrococca* (methoxymicareic acid chemotype), *M. prasina* s.str. (micareic acid chemotype) and *M. subviridescens* (prasinic acid chemotype) (Coppins 2009); furthermore, other new species have also been recognised within the *M. prasina* group. Both micareic and methoxymicareic acids are produced by several species within the *M. prasina* group, while prasinic acid has only been reported from *M. subviridescens*. So far, no co-occurrence of any of those substances has been observed in any species within the *M. prasina* group.

Reconstructions of the ancestral state for the whole *M. prasina* group suggest that the most recent common ancestor did not produce any secondary metabolites. This may suggest that the production of a wide range of secondary metabolites in this group of lichens could have resulted from independent gains of ability to biosynthesise various substances during evolution. The scenario, in which the ability to produce micareic acid in the ancestor of *M. prasina* clade or methoxymicareic acid in the ancestor of *M. micrococca* clade being gained only once during evolution, seems to be reasonable since losing an existing character could be expected to occur more rapidly and in fewer

steps than gaining a new character (e.g. Prieto et al. 2013). Those evolutionary events could have been followed with the loss of those traits in some lineages and successive independent gains of ability to biosynthesise prasinic (*M. subviridescens*) or gyrophoric acids (*M. levicula* and *M. viridileprosa*) in some species.

To summarise, our study showed that phenotypical variation within the *Micarea prasina* group has been previously underestimated and, based on field work and laboratory studies, six new species within this group are described (see Taxonomy).

Taxonomy

Micarea aeruginoprasina **van den Boom, Guzow-Krzemińska, Brand & Sérus., sp. nov.**
MycoBank No.: MB 831821
Fig. 2A

Diagnosis. Species characterised by inconspicuous, pale brownish to moderately brownish, isidiate thallus, branched to coralloid isidia, emarginate, adnate to slightly convex apothecia measuring 0.1–0.5 mm in diam., which are pale cream to pale brown or aeruginose with pigment (Sedifolia-grey, K+ violet, C+ violet) present in hypothecium, (0–)1-septate ascospores measuring 9–14 × 4.5–5.5 µm and the production of micareic acid.

Type. PORTUGAL. Azores, Terceira, NW of Angra do Heroismo, W of Pico Gordo, Mistério dos Negros (N), trail from Lagoa do Negro to the West, 550 m alt., 38°44.15'N, 27°16.30'W, ± damp *Juniperus brevifolia* forest, with some young *Vaccinium cylindraceum*, on *Juniperus brevifolia*, 28 June 2014, P. & B. van den Boom 51445 (holotype LG; isotypes UGDA, hb v.d. Boom, mtSSU GenBank accession number: MK562024, *Mcm7* GenBank accession number: MN105888).

Description. Thallus indeterminate, inconspicuous, thin, endosubstratal to episubstratal in non-isidiate parts as a thin film over the substrate or minutely granular, pale to moderately brown, isidiate; prothallus not visible; granules vertically proliferating to form isidia; isidia branched to coralloid, crowded or separated, up to 250 µm tall and 25 µm wide, with a distinct and complete hyphal layer; apothecia abundant, adnate to slightly convex, emarginate, rounded to slightly irregular, pale cream to pale brown or aeruginose, often different colours in a single apothecium, 0.1–0.5 mm in diam.; excipulum sometimes paler, instinct; hymenium 40–50 µm high, hyaline; hypothecium hyaline to pale aeruginose brownish (Sedifolia-grey), K+ violet, C+ violet; paraphyses, sparse, branched, 1.0–1.2(–1.5) µm wide, tips not widened and not pigmented; asci cylindrical to clavate, 35–40 × 11–14 µm, 8–spored; ascospores ellipsoidal to ovoid, (0−)1-septate, 9–14 × 4.5–5.5 µm; pycnidia not observed; crystalline granules (studied in polarised light) visible in hypothecium and in thallus, soluble in K.

Photobiont micareoid, cells thin walled, 6–9 µm in diam., clustered in compact groups.

Chemistry. Micareic acid detected by TLC. Sedifolia-grey in apothecia (hypothecium), its presence sometimes indistinct.

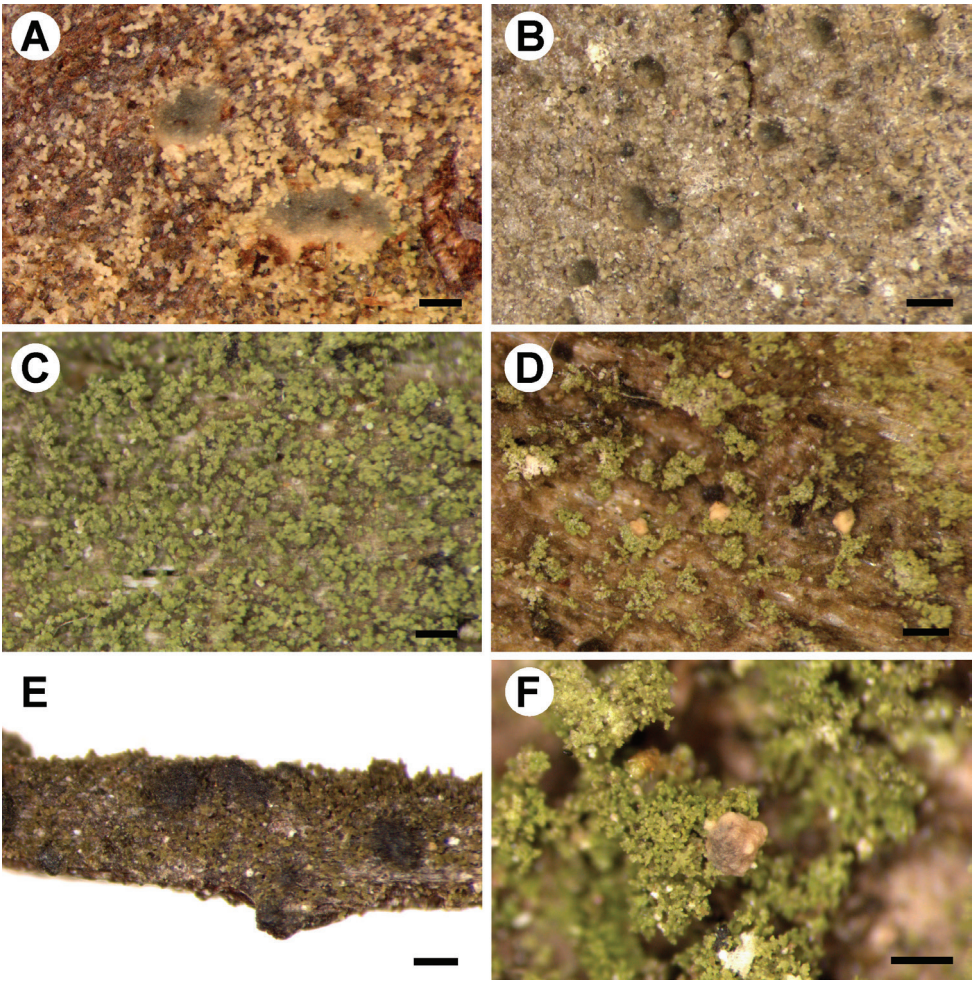

Figure 2. Morphology of newly described *Micarea* species **A** *M. aeruginoprasina* (holotype) **B** *M. azorica* (holotype) **C** *M. isidioprasina* (holotype) **D** *M. microsorediata* (holotype) **E** *M. nigra* (holotype) **F** *M. pauli* (holotype). Scale bars: 200 µm (**A–C, E**); 300 µm (**D, F**).

Habitat and distribution. In the type locality *Micarea aeruginoprasina* grows abundantly on trunks of *Juniperus brevifolia*, in a subnatural degradated forest, dominated by *J. brevifolia* shrubs and trees. In other localities, it was found on *Cryptomeria* and *Erica* trunks, also in forested areas.

The new species is only known from the island Terceira in the Azores, where it is known from several localities.

Etymology. The epithet refers to the often aeruginose colour of the apothecia and the resemblance in secondary chemistry to *M. prasina*.

Additional specimens examined. PORTUGAL. Azores, Terceira, NW of Angra do Heroismo, south edge of Reserva Florestal da Lagoa das Patas, area around a pond 'Lagoa das Patas', mature *Cryptomeria* trees and some *Camellia* shrubs, on *Cryptomeria*,

38°43.01'N, 27°17.32'W, 520 m alt., 28 June 2014, P. & B. van den Boom 51878 (hb v.d. Boom); NW of Angra do Heroismo, NNE of Santa Bárbara, Serra de Santa Bárbara, road to the summit, forests with mainly *Cryptomeria* trees, trees at edge of forest, on *Cryptomeria*, 38°43.49'N, 27°19.33'W, 800 m alt., 1 July 2014, P. & B. van den Boom 51622 (hb v.d. Boom); NE of Serreta, north trail to Lagoínha, forest with *Cryptomeria japonica*, *Myrica faya*, *Erica*, etc., on *Erica*, 38°45.28'N, 27°20.50'W, 500 m alt., 2 July 2014, P. & B. van den Boom 51691 (hb v.d. Boom).

Notes. This species is unique within the group due to the presence of the Sedifolia-grey pigment in hypothecium. It is similar to *M. prasina* because of its production of micareic acid, but the latter has Sedifolia-grey pigment in the epihymenium and its thallus consists of goniocysts (isidiate in *M. aeruginoprasina*). However, it is not closely related to *M. prasina*, being resolved as basal in the *M. prasina* clade and the sequences of their molecular markers are very different. In the Azores archipelago, the most widespread *prasina*-like species is *M. azorica*, newly described in this paper, which, however, is not isidiate and contains Superba-brown in the apothecia. *Micarea aeruginoprasina* resembles *M. byssacea*, which can have somewhat the same coloured and adnate apothecia; however, *M. byssacea* is not isidiate, contains methoxymicareic acid and the apothecial pigment is absent in hypothecium (Czarnota and Guzow-Krzemińska 2010). Morphologically, the new species is similar to *M. levicula*, especially due to the finely isidiose thallus and the adnate apothecia, which are, however, paler in *M. levicula* and that species contains gyrophoric acid (Coppins 1983; Brand et al. 2014).

Micarea isidioprasina, *M. nigra* and *M. pauli* also have isidiate thalli, but only *M. aeruginoprasina* has pale cream to pale brown or aeruginose apothecia. *Micarea isidioprasina* and *M. pauli* are often sterile and, to date, *M. aeruginoprasina* and *M. nigra* have always been found with apothecia, but, based only on the thallus characters, *M. nigra* and *M. pauli* can be distinguished due to the production of methoxymicareic acid and *M. isidioprasina* has green isidia (shades of brown in *M. aeruginoprasina*).

***Micarea azorica* van den Boom, Guzow-Krzemińska, Brand & Sérus., sp. nov.**
MycoBank No.: MB 831822
Fig. 2B

Diagnosis. Species characterised by pale to moderately brownish thallus consisting of goniocysts, convex to subglobose, emarginate, pale greyish-brown to dark brown (with Superba-brown pigment) apothecia measuring 0.1–0.3 mm in diam., (0–)1-septate, narrowly ellipsoidal to ovoid ascospores measuring 9–11 × (2.5–)3–4 µm, sessile to slightly stalked, pale to moderately brown mesopycnidia, bacillar mesoconidia measuring 6.5–8 × 0.9–1.1 µm and the production of micareic acid.

Type. PORTUGAL. Azores, Terceira, NW of Angra do Heroismo, south edge of Reserva Florestal da Lagoa das Patas, area around a pond 'Lagoa das Patas', 520 m alt., 38°43.01'N, 27°17.32'W, mature *Cryptomeria* trees and *Camellia* shrubs, on

Cryptomeria japonica, 28 June 2014, P. & B. van den Boom 51468 (holotype LG; isotypes UGDA, hb v.d.Boom, mtSSU GenBank accession number: MK562026, *Mcm7* GenBank accession number: MN105891).

Description. Thallus inconspicuous, thinly scurfy to somewhat farinose-granular, pale to moderately brownish and consisting of goniocysts; prothallus not seen; apothecia abundant, convex to subglobose, emarginate, pale greyish-brown to dark brown, often unevenly coloured in a single apothecium (partly dark, partly pale), 0.1−0.3 mm in diam.; hymenium ca. 32−40 µm tall; epihymenium with grey-brown pigment, K−, C− (Superba-brown); hypothecium hyaline; paraphyses, abundant, branched, ca. 1.0–1.5(–1.8) µm wide, tips not widened and not pigmented; asci 25–35 × 11–14 µm, 8-spored; ascospores narrowly ellipsoidal to ovoid, (0–)1-septate, 9–11 × (2.5–)3–4 µm; mesopycnidia occasionally abundant, sessile to slightly stalked, 40–60 µm in diam., pale to moderately brown, the ostiole sometimes gaping; mesoconidia bacillar, simple, 6.5−8 × 0.9−1.1 µm; crystalline granules (studied in polarised light) visible in epithecium and in thallus, soluble in K.

Photobiont micareoid, cells thin-walled, 4–10 µm in diam., clustered in compact groups.

Chemistry. Micareic acid detected by TLC. Superba-brown in apothecia (epihymenium).

Habitat and distribution. To date, known only from the Azores archipelago (Terceira island) from three localities where it was found on bark of trees.

Etymology. The name refers to the archipelago of the Azores, where the species occurs.

Additional specimens examined. PORTUGAL. Azores, Terceira, NW of Angra do Heroismo, Reserva Florestal Viveira da Falca, 460 m alt., 38°42.90'N, 27°16.78'W, picnic area with many mature *Cryptomeria* trees, some *Acer* trees and *Camellia*, on *Cryptomeria*, 28 June 2014, P. & B. van den Boom 51330 (hb. v.d. Boom); N of Serreta, Reserva Florestal da Serreta, 80 m alt., 38°46.27'N, 27°21.42'W, picnic area in open forest with mixed trees and shrubs, on tree, 2 July 2014, P. & B. van den Boom 51733 (hb. v.d. Boom).

Notes. The new species is resolved as sister to *M. prasina* s.str. with strong support, being morphologically and chemically similar to that species, but differing in the absence of the Sedifolia-grey pigment, responsible for the typical reaction K+ violet in *M. prasina* s.str (Coppins 1983; Czarnota 2007; Launis et al. 2019a). Instead of Sedifolia-grey pigment, Superba-brown is present in *M. azorica*.

The identity of *M. prasina* s.str. has been recently solved by Launis et al. (2019a, b) and its occurrence is confirmed from boreal and temperate Europe (Finland, Germany, Poland) and Eastern North America (Canada: New Brunswick and USA: Maine) (Launis et al. 2019b; this paper). Other records need confirmation as, previously, other species have been included in the variation of *M. prasina*.

Micarea azorica resembles *M. lithinella* (Nyl.) Hedl. due to its brownish, convex to subglobose small apothecia, but the latter is mainly a saxicolous species, has smaller conidia, 4−5.5 × 0.5−1 µm and does not contain secondary metabolites (Coppins 1983; Czarnota 2007).

Micarea isidioprasina **Brand, van den Boom, Guzow-Krzemińska, Sérus. & Kukwa, sp. nov.**
MycoBank No.: MB 831823
Fig. 2C

Diagnosis. Species characterised by granular-isidiate thallus, pale grey to grey-beige apothecia, 0–1-septate, ovoid, ellipsoidal or oblong ascospores measuring 7–13 × 3.5–4.5 µm and the presence of micareic acid.

Type. POLAND. Równina Bielska, Białowieża Primeval Forest, Białowieża National Park, forest section no 256, *Pino-Quercetum*, on wood of log, 21 Aug 2015, M. Kukwa 17367a, A. Łubek (holotype UGDA; isotype KTC, ITS GenBank accession number: MN095789, mtSSU GenBank accession number: MK562016, *Mcm7* GenBank accession number: MN105897).

Description. Thallus crustose, granular-isidiate, indeterminate, endosubstratal to rarely episubstratal in non-isidiate parts and then as a thin greenish film over the substrate or minutely areolate, isidiate; prothallus not seen; areoles up to 0.05 mm in diam., green, soon developing isidia; isidia abundantly branched and coralloid, crowded and forming an almost continuous layer locally over the substrate, but in younger parts of thalli separated, green to olive green (Sedifolia-grey, K+ violet), up to 250 µm tall and 25 µm wide, with a distinct and complete hyphal layer; apothecia rarely developed, white to beige, some patchily grey, up to 0.45 mm in diam., convex; excipulum poorly developed, as a narrow, hyaline zone, hyphae radiating, branched and anastomosing; hymenium up to 50 µm tall, hyaline; epihymenium and hypothecium hyaline; paraphyses of one type, 1–1.5 µm thick, sparse, mostly apically branched and anastomosed, hyaline throughout; asci cylindrical-clavate, 30–45 × 12–15 µm, 8-spored; ascospores, 0–1-septate, ovoid, ellipsoidal or oblong, 11–14 × 3.5–4.5 µm; pycnidia not seen; crystalline granules (studied in polarised light) present rather sparsely in hymenium (as strands between asci and paraphyses) and abundantly in isidia, soluble in K.

Photobiont chlorococcoid, micareoid, cells globose to ellipsoidal, 4–7 µm in diam.

Chemistry. Micareic acid detected by TLC. Sedifolia-grey pigment present in outermost parts of some isidia.

Habitat and distribution. The species grows on wood (decomposing logs) and acidic bark of trees in various forest communities in well preserved forest.

To date, it is known from Belgium, Germany, France, Poland and Romania.

Etymology. The name of the new species refers to the presence of isidia and the chemistry of *M. prasina*.

Additional specimens examined. BELGIUM. Herbeumont, forest by the Semois river, 265 m alt., 49°45'N, 05°13'E, on *Quercus* tree in forest, 2013, E. Sérusiaux 3609 (LG). FRANCE. Vosges, Dépt. Haut-Rhin, Hohneck, Frankenthal nature preserve, 48°02'N, 07°01'E, 1100 m alt., on dead *Fagus* in forest, 2013, E. Sérusiaux LG DNA 3437 (LG). GERMANY. Niedersachsen, S of Goslar, Rammelsberg, 360 m alt., 51°53.01'N, 10°25.23'E, trail along *Picea* forest and brooklet with *Acer*, *Alnus* and *Betula* trees, 12 May 2015, P. & B. van den Boom 53248 (hb. v.d. Boom). POLAND.

Roztocze Środkowe, Roztoczański National Park, S of Zwierzyniec village, Bukowa Góra nature reserve, 50°35'47"N, 22°57'48"E, ca. 280 m alt., beech forest, on wood of log, 15 Sept 2015, M. Kukwa 17493 (UGDA); Równina Bielska, Białowieża Primeval Forest, Białowieża National Park, forest section no 256, *Carici elongatae-Alnetum*, on wood of logs, bark *Picea abies* and *Alnus glutinosa*, Aug 2014, M. Kukwa 14030, 14038, 14107, 14112, A. Łubek (KTC, UGDA); ibidem, *Circaeo-Alnetum*, on wood of log, Aug 2014, M. Kukwa 13299, A. Łubek (KTC, UGDA); ibidem, *Tilio-Carpinetum*, on wood of log, Aug & Oct 2014, M. Kukwa 13418, 14358, A. Łubek (KTC, UGDA); ibidem, *Circaeo-Alnetum*, on wood of snag, Oct 2014, M. Kukwa 14243, A. Łubek (KTC, UGDA). ROMANIA. W of Brasov, S of Zarnesti, Praia Craiului National Park, 1350 m alt., 45°31'N, 25°16'E, on *Fagus* inside forest, 2016, E. Sérusiaux LG DNA 6260 & 6265 (LG).

Notes. *Micarea isidioprasina* is an isidiate species of the *M. prasina* group containing micareic acid as the main secondary metabolite. It is usually sterile and in Poland often grows in similar habitats with *M. pauli*, a species described in this paper, from which it can be separated with certainty by analyses of secondary metabolites, as the latter contains methoxymicareic acid.

Micarea aeruginoprasina and *M. nigra* also develop similar isidiate thalli, but *M. aeruginoprasina* has pale cream to pale brown or aeruginose apothecia (often mottled with all colours in the same apothecium) and *M. nigra* develops dark greyish to black apothecia. When sterile, all three species may be more difficult to separate, especially *M. aeruginoprasina* which also produces micareic acid (*M. nigra* contains methoxymicareic acid), but that species has pale brown isidia. Additionally, the so far known distributions of all three species do not overlap and *M. aeruginoprasina* and *M. nigra* are known from the Azores and continental Portugal, respectively.

Micareic acid is also the main secondary metabolite in the somewhat morphologically similar *M. prasina*, but the latter is not isidiate, often richly fertile and its thallus consists of goniocysts (Czarnota 2007; Launis et al. 2019a, b).

Micarea microsorediata **Brand, van den Boom, Guzow-Krzemińska, Sérus. & Kukwa, sp. nov.**
MycoBank No. MB 831824
Fig. 2D

Diagnosis. Species morphologically similar to *Micarea viridileprosa*, characterised by sorediate thallus, delimited or diffuse and confluent soralia with green or locally bluish soredia produced from the thallus areoles, white and immarginate when mature apothecia, 0.2–0.3 mm in diam., cylindrical to ellipsoidal (0–)1-septate ascospores measuring 9.5–13 × 2.8–3.5 µm and the presence of methoxymicareic acid.

Type. POLANd. Wysoczyzna Żarnowiecka, Pużyckie Łęgi nature reserve, 54°38'N 17°51'E, *Circaeo-Alnetum*, on wood of log, 12 Aug 2015, M. Kukwa 17053 (holotype UGDA, ITS GenBank accession number: MN095791, mtSSU GenBank accession number: MK562012, *Mcm7* GenBank accession number: MN105906).

Description. Thallus diffuse, up to 10 cm wide, consisting of finely granular soredia, often with a powdery appearance, vivid green or green, sometimes with bluish tinge; prothallus not seen; areoles up to 25 µm in diam., green, soon bursting to produce soredia; soralia at first delimited, produced from small, convex areoles, soon fused and confluent, sometimes forming a sorediate continuous layer; soredia simple, up to 20 µm in diam., sometimes slightly elongated or in more or less rounded consoredia up 35 µm in diam. apothecia rarely present, adnate, first with indistinct margin, then immarginate, 0.2–0.3 mm in diam., white or slightly brownish; excipulum in young apothecia present, 15–25 µm wide, of thin irregular hyphae; hymenium ca. 30−42 µm tall; epihymenium and hypothecium hyaline; paraphyses thick (in K), branched and anastomosing, ca. 1.2−1.5 µm wide; asci 29–35 × 7–10 µm, 8-spored; ascospores cylindrical to ellipsoidal, 9.5–13 × 2.8–3.5 µm, (0–)1-septate; micropycnidia present in some specimens, ca. 60 µm in diam., with dark brown tops (K–); microconidia narrow fusiform to bacilliform, 7 × 0.8 µm; mesopycnidia, mesoconidia 3.8 × 1.4 µm; crystalline granules (studied in polarised light) visible in hymenium and in thallus, soluble in K.

Photobiont micareoid, cells thin-walled, 4–8(–9) µm in diam.

Chemistry. Methoxymicareic acid detected by TLC. Soredia in exposed habitats with Sedifolia-grey pigment, K+ violet.

Habitat and distribution. The new species occurs on acidic bark of various trees such as *Alnus*, *Betula*, *Fagus* and *Quercus*, usually in humid forests, also on decaying wood (logs and stumps) and rarely on terrestrial decaying mosses in, for example, steep slopes in heath and dunes. It is a very common species in the south of the Netherlands and some areas in Poland and is mostly found on microhabitats where only few other lichens species co-occur. On several occasions, *Normandina pulchella* (Borrer) Nyl. and squamules of *Cladonia* spp. are the only accompanying lichens.

To date, the species has been found in Belgium, Germany, the Netherlands, Poland and Portugal.

One specimen of *Micarea microsorediata* was invaded by *Nectriopsis micareae* Diederich, van den Boom & Ernst (see below additional specimens examined).

Etymology. The epithet refers to the production of soredia and the similarity to *M. micrococca* due to the same secondary chemistry.

Additional specimens examined. BELGIUM. Limburg, N of Achel, Rozendaal, 51°17.0'N, 5°29.9'E, 35 m alt., *Pinus* forest with *Betula* and *Quercus* trees, on wood of fallen decaying trunk, 28 Dec. 2018, P. & B. van den Boom 58046 (hb v.d. Boom); NE of Achel, near Tomp, 51°16.10'N, 5°29.8'E, 35 m alt., along small road, *Pinus* forest with *Betula* and *Quercus* trees, on *Betula*, 28 Dec. 2018, P. & B. van den Boom 58052 (hb v.d. Boom); NE of Lommel, Kolonie, E of 'Afwateringskanaal', 51°14.40'N, 5°23.6'E, 50 m alt., *Pinus* forest, on *Prunus*, 28 Dec. 2018, P. & B. van den Boom 58054 (hb v.d. Boom); ENE of Lommel, E of Kolonie, 51°15.50'N, 5°24.35'E, 40 m alt., between edge of *Pinus* forest and edge of reserve Hageven, on *Betula* and *Quercus robur*, 28 Dec. 2018, P. & B. van den Boom 58055, 58056 (hb v.d. Boom). GERMANY. Nedersaksen, N of Bentheim, NE of Wengsel, Isterberg, 52°21.4'N, 7°9.0'E,

Pinus forest with some sandstone outcrops, on *Quercus rubra*, 26 Aug. 2015, M. & D. Brand, P. & B. van den Boom 53633 (hb v.d. Boom). POLAND. Bory Tucholskie, Kręgi Kamienne nature reserve, close to Wda river, NW from Odry, 53°53'59.50"N, 17°59'42.07"E, black alders close to river, on *Alnus glutinosa*, 19 June 2018, M. Kukwa 19991 (UGDA); Równina Bielska, Białowieża Forest, Białowieża National Park, forest section no 256, *Peucedano-Pinetum*, on twig of *Picea abies*, *Quercus robur* and wood of log, May 2014, M. Kukwa 13462, 13660, 13675, 13778, A. Łubek (KTC); ibidem, *Pino-Quercetum*, on *Quercus robur*, Aug. 2014, M. Kukwa, 13321, A. Łubek (KTC, UGDA); ibidem, *Tilio-Carpinetum*, on *Quercus robur*, Aug. 2014, M. Kukwa 13420a, 13392 (as admixture in a specimen of *Biatora ligni-mollis* T. Sprib. & Printzen), A. Łubek (KTC, UGDA); ibidem, *Carici elongatae-Alnetum*, on bark of log, *Alnus glutinosa* and *Picea abies*, Aug. 2014, M. Kukwa, 14000, 14002, 14012, 14045, 14109, A. Łubek (KTC, UGDA); ibidem, *Circaeo-Alnetum*, on wood of snag, Oct. 2014, M. Kukwa, 14139, A. Łubek (KTC); ibidem, *Tilio-Carpinetum*, on wood of branch of the log, Oct. 2014, M. Kukwa, 14350, A. Łubek (KTC, UGDA); ibidem, *Peucedano-Pinetum*, on *Alnus glutinosa*, March 2015, M. Kukwa, 13308, A. Łubek (KTC, UGDA); ibidem, *Carici elongatae-Alnetum*, on wood of stump, May 2015, M. Kukwa, 15789, A. Łubek (KTC, UGDA); ibidem, *Circaeo-Alnetum*, on *Alnus glutinosa*, 29 Sept. 2015, M. Kukwa, 17546, A Łubek (KTC, UGDA); ibidem, *Querco-Piceetum*, on *Carpinus betulus*, Aug 2015, M. Kukwa, 17379, 17436, A. Łubek (UGDA; KTC); ibidem, *Circaeo-Alnetum*, on *Alnus glutinosa*, 1 Oct. 2015, M. Kukwa, 17592, A Łubek (KTC, UGDA); ibidem, *Pino-Quercetum*, on wood of log, 4 Oct. 2015, M. Kukwa, 17641, A. Łubek (KTC, UGDA); Wybrzeże Słowińskie, Białogóra nature reserve, forest section no. 14, 54°49'29"N, 17°57'21"E, *Empetro nigri-Pinetum*, on *Pinus sylvestris*, 21 April 2010, M. Kukwa 7721 (UGDA); ibidem, forest section no. 22, 54°49'27"N, 17°57'52"E, open area with few trees and *Myrica gale*, on *Betula pendula*, 22 Sept. 2010, M. Kukwa, 8280, A. Jabłońska, M. Oset (UGDA); Wysoczyzna Polanowska, Skotawskie Łąki nature reserve, 54°16'03"N, 17°33'37"E, large group of black alders, on *Alnus glutinosa*, 11 April 2017, M. Kukwa, 19212, 19219 (UGDA); ibidem, by NE part of Lipieniec lake, 54°15'44"N, 17°33'26"E, group of black alder trees on meadow, on *Alnus glutinosa*, 27 June 2017, M. Kukwa, 19800a, 19801, 19806 (UGDA); ibidem, by unnamed lake (N of Lipieniec lake), 54°15'46"N, 17°33'03"E, black alder forest, by lake, on *Alnus glutinosa*, *Pinus sylvestris* and *Sambucus nigra*, 27 June 2017, M. Kukwa, 19839, 19845, 19849, 19850 (UGDA); Torfowisko Potoczek nature reserve, 54°09'49"N, 16°57'11"E, *Vaccinio uliginosi-Betuletum pubescentis*, on wood of log and *Picea abies*, 11 Aug. 2015, M. Kukwa, 16994, 17001a (UGDA); Wysoczyzna Żarnowiecka, Pużyckie Łęgi nature reserve, 54°38'N 17°51'E, *Circaeo-Alnetum*, on *Alnus glutinosa* and wood of log, 12 Aug. 2015, M. Kukwa, 17032, 17040, 17053 (UGDA). PORTUGAL. Estremadura, W of Lisbon, WSW of Sintra, WSW of Linhó, along road to Malveira da Serra, nature park Quinta do Pisão, trail in forest with mainly *Pinus* trees, on *Pinus*, 38°45.50'N, 9°24.60'W, 160 m alt., 18 Oct. 2015, P. & B. van den Boom 53789 (hb v.d. Boom); W of Lisbon, S of Sintra, garden of Na-

tional Palace de la Pena, mixed (mature) trees and shrubs, on tree-fern, 38°47.23'N, 9°23.42'W, 490 m alt., 20 Oct. 2015, P. & B. van den Boom 53907 (hb v.d. Boom). THE NETHERLANDS. Noord-Brabant, NE of Oirschot, Woekensesteeg, grid-ref. 51.23.23, trail in mixed forest, on wood of fallen trunk, 4 Oct. 2014, P. & B. van den Boom 51991 (hb v.d. Boom, hb Brand 67113); N of Oirschot, De Mortelen, grid-ref. 51.23.12, trail in damp mixed forest, on *Fagus sylvatica*, 5 June 2017, P. & B. van den Boom 56372 (hb v.d. Boom); E of Best, S side of Wilhelmina channel, grid-ref. 51.24.53, trail in *Pinus* forest, on *Quercus rubra*, 22 July 2018, P. & B. van den Boom 57647 (hb v.d. Boom); ENE of Oostelbeers, Oostelbeerse Heide, grid-ref. 51.32.34, forest, on *Pseudotsuga*, 26 May 2016, P. & B. van den Boom 55028 (hb v.d. Boom); NNW of Wintelre, S side of Straatsche Heide, grid-ref. 51.33.51, *Pinus* forest at edge of *Calluna* heathland with some *Quercus robur* trees, on *Quercus robur*, 14 April 2016, P. & B. van den Boom 54996 (hb v.d. Boom); W of Son, E of Nieuwe Heide, grid-ref. 51.24.45, E side of trail in *Pinus* forest, on *Betula*, 22 June 2014, P. & B. van den Boom 51315 (hb v.d. Boom); S of Best, Aarlesche Heide, S of high-way, grid-ref. 51.33.25, in *Pinus* forest, on *Quercus rubra*, 1 Nov. 2014, P. & B. van den Boom 52515 (hb v.d. Boom); S of Best, Aarlesche Heide, S of highway, grid ref. 51.34.21, grassy *Calluna* heathland, with scattered trees, on *Quercus robur*, 24 Jan. 2014, P. & B. van den Boom 50279 (hb v.d. Boom).

Specimen of *Nectriopsis micareae*. ThE NETHERLANDS. Noord-Brabant, S of Best, Aarlesche Heide, S of highway, grid ref. 51.34.21, grassy *Calluna* heathland, with scattered trees, on *Micarea microsorediata* growing on *Quercus robur*, 24 Jan. 2014, P. & B. van den Boom 50278 (hb v.d. Boom).

Notes. The new species is morphologically similar to *M. viridileprosa* and *M. soralifera*, but those species differ in their contents of secondary lichen metabolites: *M. viridileprosa* contains gyrophoric acid, whereas *M. soralifera* produces micareic acid (van den Boom and Coppins 2001; Guzow-Krzemińska et al. 2016).

Micarea microsorediata produces methoxymicareic acid, a substance present in *M. byssacea*, *M. nigra*, *M. pauli* and other species of the *M. micrococca* clade (Fig. 1), but these species are not sorediate and some of them also have darker apothecia containing the Sedifolia-grey pigment (Czarnota 2007; Czarnota and Guzow-Krzemińska 2010; Launis et al. 2019a; this paper).

***Micarea nigra* van den Boom, Guzow-Krzemińska, Brand & Sérus., sp. nov.**
MycoBank No.: MB 831825
Fig. 2E

Diagnosis. Species characterised by the production of branched isidia, dark greyish to almost black apothecia containing Cinereorufa-green pigment and measuring 0.15–0.5 mm in diam., (0–)1-septate, narrowly ellipsoidal to clavate ascospores measuring 7.5–12 × (2.5–)3–4.5 µm and the production of methoxymicareic acid.

Type. PORTUGAL. Estremadura, W of Lisbon, W of Sintra, Park de la Monserrate, 200 m alt., 38°47.30'N, 9°25.07'W, parkland with mixed (mature) trees and shrubs, on fern tree, 15 Oct. 2015, P. & B. van den Boom 53726 (holotype LG; isotypes UGDA, hb v.d. Boom, mtSSU GenBank accession number: MK562029).

Description. Thallus inconspicuous, thin, consisting of often branched and vertically proliferating fine isidia; prothallus not seen; areoles up to 0.1 mm in diam.; isidia developing from small areoles, vertically branched and coralloid, in some parts crowded and forming almost a continuous layer, but separated in younger parts of thalli, brownish-green, up to 500 µm tall and 30 µm wide, with a distinct and complete hyphal layer; apothecia abundant, adnate, flat to moderately convex, emarginate, 0.15–0.5 mm in diam., dark greyish to almost black, sometimes with a pale greyish rim; hymenium greenish, with pale brownish streaks, K–, C−, 30–40 µm tall; epihymenium aeruginose greenish, with Cinereorufa-green pigment, K+ green intensifying; hypothecium hyaline; paraphyses sparse, branched, tips not widened and not pigmented, ca. 1.0−1.5 µm wide; asci cylindrical to clavate, 24–28 × 9–12 µm, 8-spored; ascospores narrowly ellipsoid to clavate, 7.5–12 × (2.5–)3–4.5 µm, (0–)1-septate; micropycnidia inconspicuous, rare, 30–60 µm in diam., with dark brown top (K–, C−); microconidia bacilliform, sometimes slightly curved, aseptate, 7–10 × 0.5–0.9 µm; crystalline granules (studied in polarised light) not visible in apothecium, but detected in isidia (sometimes isidia very abundant and sometimes very few), insoluble in K.

Photobiont micareoid, cells thin-walled, 4–8 µm in diam., clustered in compact masses.

Chemistry. Methoxymicareic acid detected by TLC. Cinereorufa-green in apothecia (epihymenium).

Habitat and distribution. Abundantly present on a trunk of a fern tree in a parkland where many tropical and exotic fern and tree species have been introduced.

To date, it is only known from the type locality in Portugal (Sintra).

Etymology. The epithet chosen for this species refers to its very dark appearance, the thallus being dark greenish and the apothecia mostly blackish.

Notes. This species is resolved in the *M. micrococca* group (Fig. 1) and is unique because of its dark grey to almost black apothecia and the presence of Cinereorufa-green pigment in epihymenium.

Micarea nigra resembles *M. aeruginoprasina*, *M. isidioprasina* and *M. pauli*. *Micarea aeruginoprasina* and *M. isidioprasina* differ in the presence of micareic acid instead of methoxymicareic acid and paler apothecia. In addition, *M. aeruginoprasina* produces different pigment in the apothecia (Sedifolia-grey). *Micarea pauli* differs in the production of methoxymicareic acid, Sedifolia-grey pigment in the apothecia and different distribution (see under that species).

Some morphs of *M. prasina* can also have dark apothecia, but this species contains micareic acid and Sedifolia-grey in the apothecia (Coppins 1983; Czarnota 2007; Launis et al. 2019a, b). *Micarea subviridescens* can have blackish apothecia and is sometimes epiphytic, but it produces prasinic acid (Coppins 1983).

***Micarea pauli* Guzow-Krzemińska, Łubek & Kukwa, sp. nov.**
MycoBank No.: MB 831826
Fig. 2F

Diagnosis. Species characterised by isidiate thallus, pale grey to grey beige apothecia with Sedifolia-grey pigment, 0–1-septate, ovoid, ellipsoidal or oblong ascospores measuring 7–13 × 3.5–4.5 µm and the presence of methoxymicareic acid.

Type. POLANd. Równina Bielska, Białowieża Forest, Białowieża National Park, forest section no 256, *Carici elongatae-Alnetum*, on *Alnus glutinosa*, 17 Aug 2015, M. Kukwa & 17240, A. Łubek (holotype UGDA; isotype KTC, mtSSU GenBank accession number: MK562014, *Mcm7* GenBank accession number: MN105912).

Description. Thallus crustose, indeterminate, endosubstratal to rarely episubstratal in non-isidiate parts and then as a thin greenish film over the substrate or minutely areolate, isidiate; prothallus not evident; areoles up to 0.1 mm in diam., green, soon developing isidia; isidia branched and coralloid, crowded and forming almost a continuous layer over the substrate, but separated in younger parts of thalli, green to olive green, up to 0.5 mm tall and 30 µm wide, with a distinct and complete hyphal layer; apothecia rarely developed (in 2 specimens only), beige with spots of grey pigment, pale grey to grey-beige, up to 0.5 mm in diam., irregular in shape, convex, with a white rim; excipulum as a narrow, hyaline zone, hyphae radiating, branched and anastomosing; hymenium up to 45 µm tall; epihymenium partly olive-grey due to the presence of Sedifolia-grey pigment (K+ violet, C+ violet) confined to the gel matrix; hypothecium hyaline to pale straw coloured in upper part; paraphyses 1–1.5 µm thick, sparse, mostly apically branched and anastomosing, hyaline throughout; asci cylindrical-clavate, 30–35 × 9–12 µm, 8-spored; ascospores, 0–1-septate, ovoid, ellipsoidal or oblong, 7–13 × 3.5–4.5 µm; pycnidia not seen; crystalline granules (studied in polarised light) abundant in hymenium and isidia, soluble in K.

Photobiont chlorococcoid, micareoid, cells globose to ellipsoidal, 4–7 µm in diam.

Chemistry. Methoxymicareic acid detected by TLC. Sedifolia-grey in apothecia (epihymenium).

Habitat and distribution. This species is so far known only in Poland from Białowieża Forest, where it grows in deciduous forests on bark of *Alnus glutinosa* (5 specimens), *Tilia cordata* (1 specimen) and on wood (2 specimens).

Etymology. The species is named after our friend, Paweł Czarnota, specialist in the genus who monographed it in Poland.

Additional specimens examined. POLAND. Równina Bielska, Białowieża Forest; Białowieża National Park, forest section no 256, *Carici elongatae-Alnetum*, on *Alnus glutinosa* and *Picea abies*, Aug. 2014, M. Kukwa 13194, 13330, 13345, A. Łubek (KTC, UGDA); ibidem, *Tilio-Carpinetum*, on *Tilia cordata*, Aug. 2014, M. Kukwa 14101, A. Łubek (KTC, UGDA); ibidem, *Carici elongatae-Alnetum*, on *Alnus glutinosa*, 17 Aug. 2015, M. Kukwa, 17227, A. Łubek (KTC, UGDA, hb v.d. Boom); ibidem, *Querco-Piceetum*, on *Alnus glutinosa*, 29 Sept. 2015, M. Kukwa 17544, A. Łubek (KTC, UGDA); ibidem, *Peucedano-Pinetum*, on *Alnus glutinosa*, March 2015,

M. Kukwa 13308 (KTC, UGDA); *Pino-Quercetum*, on wood of snag, 1 Oct. 2015, M. Kukwa 17582a, A. Łubek (KTC); *Pino-Quercetum*, on wood of log, 2 Oct. 2015, M. Kukwa 17619, A. Łubek (KTC, UGDA); *Carici elongatae-Alnetum*, on *Alnus glutinosa*, 3 Oct. 2015, M. Kukwa 17621, A. Łubek (KTC, UGDA).

Notes. *Micarea pauli* is an isidiate species with Sedifolia-grey pigment in its apothecia. It can be separated from the similar *M. isidioprasina*, with which it grows in Białowieża Forest, by the presence of methoxymicareic acid.

Micarea aeruginoprasina and *M. nigra* are also similar in thallus morphology, but they differ in the pigmentation of apothecia. *Micarea aeruginoprasina* develops pale cream to pale brown or aeruginose apothecia, which are often mottled in colour in one apothecium, whereas in *M. nigra* the apothecia are dark greyish to black. Without apothecia, they can be difficult to separate from *M. pauli*, especially *M. nigra* which also contains methoxymicareic acid (*M. aeruginoprasina* produces micareic acid), but so far, *M. aeruginoprasina* and *M. nigra* are only known from the Azores and continental Portugal, respectively.

Methoxymicareic acid is the main secondary metabolite, also found in *M. byssacea*, *M. micrococca* and other species in the *M. micrococca* clade (Fig. 1), but those species are never isidiate (Czarnota 2007; Czarnota and Guzow-Krzemińska 2010; Launis et al. 2019a).

Acknowledgements

We thank Dr Jacek Pokrzywnicki (University of Gdańsk) for the help with the Latin name of *Micarea pauli*. Prof. Mark R.D. Seaward is acknowledged for language correction of the final version of the manuscript. We are grateful to Heidi Lee Andersen and the anonymous reviewer for their constructive comments that improved the manuscript. Martin Kukwa and Anna Łubek received funding for the research from the Polish-Norwegian Research Programme operated by the National Centre for Research and Development under the Norwegian Financial Mechanism 2009–2014 in the frame of Project Contract No Pol-Nor/196829/87/2013.

Conflict of interest: The authors declare that they have no conflict of interest.

References

Altschul SF, Gish W, Miller W, Myers EW, Lipman DJ (1990) Basic local alignment search tool. Journal of Molecular Biology 215(3): 403–410. https://doi.org/10.1016/S0022-2836(05)80360-2

Andersen HL, Ekman S (2004) Phylogeny of the Micareaceae inferred from nrSSU DNA sequences. Lichenologist 36(1): 27–35. https://doi.org/10.1017/S0024282904013507

Andersen HL, Ekman S (2005) Disintegration of the Micareaceae (lichenized Ascomycota): a molecular phylogeny based on mitochondrial rDNA sequences. Mycological Research 109(1): 21–30. https://doi.org/10.1017/S0953756204001625

Andersen HL (2004) Phylogeny and classification of *Micarea*. PhD Thesis, University of Bergen, Norway.

Aptroot A, Cáceres MED (2014) New lichen species from termite nests in rainforest in Brazilian Rondonia and adjacent Amazonas. Lichenologist 46(3): 365–372. https://doi.org/10.1017/S0024282913000340

Barton J, Lendemer JC (2014) *Micarea micrococca* and *Micarea prasina*, the first assessment of two very similar species in eastern North America. Bryologist 117(3): 223–231. https://doi.org/10.1639/0007-2745-117.3.223

Brand AM, Van Den Boom PPG, Sérusiaux E (2014) Unveiling a surprising diversity in the lichen genus *Micarea* (Pilocarpaceae) in Réunion (Mascarenes archipelago, Indian Ocean). Lichenologist 46(3): 413–439. https://doi.org/10.1017/S0024282913000911

Brodo IM (1978) Changing concepts regarding chemical diversity in lichens. Lichenologist 10(1): 1–111. https://doi.org/10.1017/S0024282978000031

Brodo IM (1986) Interpreting chemical variation in lichens for systematic purposes. Bryologist 89(2): 132–138. https://doi.org/10.2307/3242753

Buschbom J, Mueller GM (2006) Testing "species pair" hypotheses: Evolutionary processes in the lichen-forming species complex *Porpidia flavocoerulescens* and *Porpidia melinodes*. Molecular Biology and Evolution 23(3): 574–586. https://doi.org/10.1093/molbev/msj063

Cáceres MED, Mota DA, de Jesus LS, Aptroot A (2013) The new lichen species *Micarea corallothallina* from Serra da Jiboia, an Atlantic rainforest enclave in Bahia, NE Brazil. Lichenologist 45(3): 371–373. https://doi.org/10.1017/S0024282912000886

Coppins BJ (1983) A taxonomic study of the lichen genus *Micarea* in Europe. Bulletin of the British Museum (Natural History), Botany series 11(2): 17–214.

Coppins BJ (2009) *Micarea*. In: Smith CW, Aptroot A, Coppins BJ, Fletcher A, Gilbert OL, James PW, Wolseley PA (Eds) The Lichens of Great Britain and Ireland. British Lichen Society, London, 583–606.

Coppins BJ, Tønsberg T (2001) A new xanthone-containing *Micarea* from Northwest Europe and the Pacific Northwest of North America. Lichenologist 33(2): 93–96. https://doi.org/10.1006/lich.2000.0311

Czarnota P. (2007) The lichen genus *Micarea* (Lecanorales, Ascomycota) in Poland. Polish Botanical Studies 23: 1–199.

Czarnota P, Guzow-Krzemińska B (2010) A phylogenetic study of the *Micarea prasina* group shows that *Micarea micrococca* includes three distinct lineages. Lichenologist 42(1): 7–21. https://doi.org/10.1017/S0024282909990211

Divakar PK, Molina MC, Lumbsch HT, Crespo A (2005) *Parmelia barrenoae*, a new lichen species related to *Parmelia sulcata* (Parmeliaceae) based on molecular and morphological data. Lichenologist 37(1): 37–46. https://doi.org/10.1017/S0024282904014641

Divakar PK, Crespo A, Blanco O, Lumbsch HT (2006) Phylogenetic significance of morphological characters in the tropical *Hypotrachyna* clade of parmelioid lichens (Parmeliaceae, Ascomycota). Molecular Phylogenetics and Evolution 40(2): 448–458. https://doi.org/10.1016/j.ympev.2006.03.024

Döring H, Clerc P, Grube M, Wedin M (2000) Mycobiont-specific PCR primers for the amplification of nuclear ITS and LSU rDNA from lichenized ascomycetes. Lichenologist 32(2): 200–204. https://doi.org/10.1006/lich.1999.0250

Elix JA, Jones AJ, Lajide L, Coppins BJ, James PW (1984) 2 new diphenyl ethers and a new depside from the lichen *Micarea prasina* Fr. Australian Journal of Chemistry 37(11): 2349–2364. https://doi.org/10.1071/CH9842349

Elix JA, Corush J, Lumbsch HT (2009) Triterpene chemosyndromes and subtle morphological characters characterise lineages in the *Physcia aipolia* group in Australia (Ascomycota). Systematics and Biodiversity 7(4): 479–487. https://doi.org/10.1017/S1477200009990223

Galtier N, Gouy M, Gautier C (1996) SEAVIEW and PHYLO_WIN: Two graphic tools for sequence alignment and molecular phylogeny. Computer Applications in the Biosciences 12(6): 543–548. https://doi.org/10.1093/bioinformatics/12.6.543

Gardes M, Bruns TD (1993) ITS primers with enhanced specificity for basidiomycetes – application to the identification of mycorrhizae and rusts. Molecular Ecology 2(2): 113–118. https://doi.org/10.1111/j.1365-294X.1993.tb00005.x

Gargas A, DePriest PT (1996) A nomenclature for PCR primers with examples from intron-containing SSU rDNA. Mycologia 88(5): 745–748. https://doi.org/10.1080/00275514.1996.12026712

Goffinet B, Miadlikowska J (1999) *Peltigera phyllidiosa* (Peltigeraceae, Ascomycotina), a new species from the Southern Appalachians corroborated by its sequences. Lichenologist 31(3): 247–256. https://doi.org/10.1006/lich.1998.0201

Gouy M, Guindon S, Gascuel O (2010) SeaView version 4: a multiplatform graphical user interface for sequence alignment and phylogenetic tree building. Molecular Biology and Evolution 27(2): 221–224. https://doi.org/10.1093/molbev/msp259

Guzow-Krzemińska B, Węgrzyn G (2000) Potential use of restriction analysis of PCR-amplified DNA fragments in construction of molecular data-based identification keys of lichens. Mycotaxon 76: 305–313.

Guzow-Krzemińska B, Czarnota P, Łubek A, Kukwa M (2016) *Micarea soralifera* sp. nov., a new sorediate species in the *M. prasina* group. Lichenologist 48(3): 161–169. https://doi.org/10.1017/S0024282916000050

Guzow-Krzemińska B, Flakus A, Kosecka M, Jabłońska M, Rodriguez-Flakus P, Kukwa M (2019) New species and new records of lichens from Bolivia. Phytotaxa 397(4): 257–279. https://doi.org/10.11646/phytotaxa.397.4.1

Huelsenbeck JP, Ronquist F (2001) MRBAYES: Bayesian inference of phylogenetic trees. Bioinformatics 17(8): 754–755. https://doi.org/10.1093/bioinformatics/17.8.754

Huneck S, Yoshimura Y (1996) Identification of lichen substances. Springer, Berlin Heidelberg New York, 1–493. https://doi.org/10.1007/978-3-642-85243-5_1

Kantvilas G (2018) *Micarea kartana* sp. nov. (lichenized Ascomycetes) from Kangaroo Island, South Australia. Swainsona 31: 55–58.

Kroken S, Taylor JW (2001) A gene genealogical approach to recognize phylogenetic species boundaries in the lichenized fungus *Letharia*. Mycologia 93(1): 38–53. https://doi.org/10.2307/3761604

Lanfear R, Calcott B, Ho SY, Guindon S (2012) PartitionFinder: combined selection of partitioning schemes and substitution models for phylogenetic analyses. Molecular Biology and Evolution, 29(6): 1695–1701. https://doi.org/10.1093/molbev/mss020

Lanfear R, Frandsen PB, Wright AM, Senfeld T, Calcott B (2016) PartitionFinder 2: new methods for selecting partitioned models of evolution for molecular and morphological

phylogenetic analyses. Molecular Biology and Evolution 34(3): 772–773. https://doi.org/10.1093/molbev/msw260

Launis A, Pykälä J, van den Boom P, Sérusiaux E, Myllys L (2019a) Four new epiphytic species in the *Micarea prasina* group from Europe. Lichenologist 51(1): 7–25. https://doi.org/10.1017/S0024282918000555

Launis A, Malícek J, Sérusiaux E, Svensson M, Tsurykau A, Myllys L (2019b) Sharpening species boundaries in the *Micarea prasina* group with notes on the type species *M. prasina*. Mycologia https://doi.org/10.1080/00275514.2019.1603044

Leavitt SD, Johnson LA, Goward T, St. Clair LL (2011) Species delimitation in taxonomically difficult lichen-forming fungi: an example from morphologically and chemically diverse *Xanthoparmelia* (Parmeliaceae) in North America. Molecular Phylogenetics and Evolution 60(3): 317–332. https://doi.org/10.1016/j.ympev.2011.05.012

Lendemer JC, Allen JL, Noell N (2015) The *Parmotrema* acid test: a look at species delineation in the *P. perforatum* group 40 y later. Mycologia 107(6): 1120–1129. https://doi.org/10.3852/14-263

Lumbsch HT (1998) The use of metabolic data in the lichenology at the species and subspecific levels. Lichenologist 30(4–5): 357–367. https://doi.org/10.1006/lich.1998.0147

Lumbsch HT, Schmitt I, Barker D, Pagel M (2006) Evolution of micromorphological and chemical characters in the lichen-forming fungal family Pertusariaceae. Biological Journal of the Linnean Society 89(4): 615–626. https://doi.org/10.1111/j.1095-8312.2006.00696.x

Lutsak T, Fernandez-Mendoza F, Nadyeina O, Senkardesler A, Printzen C (2017) Testing the correlation between norstictic acid content and species evolution in the *Cetraria aculeata* group in Europe. Lichenologist 49(1): 39–56. https://doi.org/10.1017/S0024282916000566

Maddison WP, Maddison DR (2018) Mesquite: a modular system for evolutionary analysis. Version 3.5 http://www.mesquiteproject.org.

McCarthy PM, Elix JA (2016) A new species of *Micarea* (lichenized Ascomycota, Pilocarpaceae) from alpine Australia. Telopea 19: 31–35. https://doi.org/10.7751/telopea10360

Meyer B, Printzen C (2000). Proposal for a standardized nomenclature and characterization of insoluble lichen pigments. Lichenologist 32(6): 571–583. https://doi.org/10.1006/lich.2000.0294

Miller MA, Pfeiffer W, Schwartz T (2010) Creating the CIPRES Science Gateway for inference of large phylogenetic trees. Proceedings of the Gateway Computing Environments Workshop (GCE), 14 November 2010, New Orleans, 1–8. https://doi.org/10.1109/GCE.2010.5676129

Molina MD, Crespo A, Blanco O, Lumbsch HT, Hawksworth DL (2004) Phylogenetic relationships and species concepts in *Parmelia* s.str. (Parmeliaceae) inferred from nuclear ITS rDNA and beta-tubulin sequences. Lichenologist 36(1): 37–54. https://doi.org/10.1017/S0024282904013933

Mosbach K (1964) On the biosynthesis of lichen substances. Part 1. The depside gyrophoric acid. Acta Chemica Scandinavica 18: 329–334. https://doi.org/10.3891/acta.chem.scand.18-0329

Nelsen MP, Gargas A (2008). Phylogenetic distribution and evolution of secondary metabolites in the lichenized fungal genus *Lepraria* (Lecanorales: Stereocaulaceae). Nova Hedwigia 86(1–2): 115–131. https://doi.org/10.1127/0029-5035/2008/0086-0115

Nelsen MP, Lumbsch HT, Lücking R, Elix JA (2008) Further evidence for the polyphyly of *Lepraria* (Lecanorales: Stereocaulaceae). Nova Hedwigia 87(3–4): 361–371. https://doi.org/10.1127/0029-5035/2008/0087-0361

Orange A, James PW, White FJ (2001) Microchemical Methods for the Identification of Lichens. British Lichen Society, London, 101 pp.

Ossowska E, Guzow-Krzemińska B, Dudek M, Oset M, Kukwa M (2018) Evaluation of diagnostic chemical and morphological characters in five *Parmelia* species (Parmeliaceae, lichenized Ascomycota) with special emphasis on the thallus pruinosity. Phytotaxa 383(2): 165–180. https://doi.org/10.11646/phytotaxa.383.2.3

Prieto M, Baloch E, Tehler A, Wedin M (2013) Mazaedium evolution in the Ascomycota (Fungi) and the classification of mazaediate groups of formerly unclear relationship. Cladistics 29(3): 296–308. https://doi.org/10.1111/j.1096-0031.2012.00429.x

Rambaut A (2012) FigTree v1.4.2. http://tree.bio.ed.ac.uk/software/figtree

Rambaut A, Drummond AJ (2007) Tracer v1.6. http://beast.bio.ed.ac.uk

Ronquist F, Huelsenbeck JP (2003) MrBayes 3: Bayesian phylogenetic inference under mixed models. Bioinformatics 19(12): 1572–1574. https://doi.org/10.1093/bioinformatics/btg180

Spribille T, Tuovinen V, Resl P, Vanderpool D, Wolinski H, Aime MC, Schneider K, Stabentheiner E, Toome-Heller M, Thor G, Mayrhofer H, Johannesson H, McCutcheon JP (2016) Basidiomycete yeasts in the cortex of ascomycete macrolichens. Science 353(6298): 488–492. https://doi.org/10.1126/science.aaf8287

Stamatakis A (2014) RAxML Version 8: A tool for phylogenetic analysis and post-analysis of large phylogenies. Bioinformatics 30(9): 1312–1313. https://doi.org/10.1093/bioinformatics/btu033

Svensson M, Thor G (2011) *Micarea capitata*, a new bryophilous lichen from Sweden. Lichenologist 43(5): 401–405. https://doi.org/10.1017/S0024282911000338

van den Boom PPG, Coppins BJ (2001) *Micarea viridileprosa* sp. nov., an overlooked lichen species from Western Europe. Lichenologist 33(2): 87–91. https://doi.org/10.1006/lich.2000.0310

van den Boom PPG, Ertz D (2014) A new species of *Micarea* (Pilocarpaceae) from Madeira growing on *Usnea*. Lichenologist 46(3): 295–301. https://doi.org/10.1017/S0024282913000698

van den Boom PPG, Brand AM, Coppins BJ, Sérusiaux E (2017). Two new species in the *Micarea prasina* group from Western Europe. Lichenologist 49(1): 13–25. https://doi.org/10.1017/S0024282916000633

White TJ, Bruns T, Lee S, Taylor JW (1990) Amplification and direct sequencing of fungal ribosomal RNA genes for phylogenetics. In: Innes MA, Gelfand DH, Sninsky JJ, White TJ (Eds) PCR Protocols: a Guide to Methods and Applications. Academic Press, New York, 315–322. https://doi.org/10.1016/B978-0-12-372180-8.50042-1

Zoller S, Scheidegger C, Sperisen C (1999) PCR primers for the amplification of mitochondrial small subunit ribosomal DNA of lichen-forming ascomycetes. Lichenologist 31(5): 511–516. https://doi.org/10.1006/lich.1999.0220

Supplementary material 1

Figures S1–S15 presenting ancestral character state reconstructions

Authors: Beata Guzow-Krzemińska, Emmanuël Sérusiaux, Pieter P. G. van den Boom, A. Maarten Brand, Annina Launis, Anna Łubek, Martin Kukwa

Data type: PDF file

Link: https://doi.org/10.3897/mycokeys.57.33267.suppl1

Supplementary material 2

Tables S1–S4

Authors: Beata Guzow-Krzemińska, Emmanuël Sérusiaux, Pieter P. G. van den Boom, A. Maarten Brand, Annina Launis, Anna Łubek, Martin Kukwa

Data type: PDF file

Explanation note: Additional tables with list of specimens used in this study, data matrices for ancestral character state reconstructions and probabilities of reconstructions with model Mk1.

Link: https://doi.org/10.3897/mycokeys.57.33267.suppl2

MycoKeys 57: 31–46 (2019)
doi: 10.3897/mycokeys.57.34501
http://mycokeys.pensoft.net

RESEARCH ARTICLE

A peer-reviewed open-access journal
MycoKeys
Launched to accelerate biodiversity research

Neotypification of *Protoparmeliopsis garovaglii* and molecular evidence of its occurrence in Poland and South America

Katarzyna Szczepańska[1], Pamela Rodriguez-Flakus[2], Jacek Urbaniak[1], Lucyna Śliwa[3]

1 *Department of Botany and Plant Ecology, Wroclaw University of Environmental and Life Sciences, pl. Grunwaldzki 24a, PL-50–363 Wrocław, Poland* **2** *Laboratory of Molecular Analyses, W. Szafer Institute of Botany, Polish Academy of Sciences, Lubicz 46, PL-31–512 Kraków, Poland* **3** *Department of Lichenology, W. Szafer Institute of Botany, Polish Academy of Sciences, Lubicz 46, PL-31–512 Kraków, Poland*

Corresponding author: *Katarzyna Szczepańska* (katarzyna.szczepanska@upwr.edu.pl)

Academic editor: *Garima Singh* | Received 13 March 2019 | Accepted 25 June 2019 | Published 1 August 2019

Citation: Szczepańska K, Rodriguez-Flakus P, Urbaniak J, Śliwa L (2019) Neotypification of *Protoparmeliopsis garovaglii* and molecular evidence of its occurrence in Poland and South America. MycoKeys 57: 31–46. https://doi.org/10.3897/mycokeys.57.34501

Abstract

Protoparmeliopsis garovaglii is a widely distributed placodioid lichen, which develops a distinctly rosette thallus, composed of elongated and strongly inflated to sinuous-plicate lobes. The taxon is characterised by high morphological plasticity and varied composition of secondary metabolites. However, the epithet was never typified. As such, the identity of *P. garovaglii,* in its strict sense, was unknown for a long time. Our phylogenetic ITS rDNA analyses, including newly generated sequences, show that European (Austria, Poland), North American (USA) and South American (Bolivia, Peru) specimens of *P. garovaglii* are placed in a strongly supported monophyletic clade, sister to *P. muralis*. We provide the first molecular evidence of the occurrence of *P. garovaglii* in South America (Bolivia and Peru) and the second record in Central Europe (Poland) was also provided. Furthermore, we neotypify *P. garovaglii* and it is reported here for the first time from Poland.

Keywords

Geographical distribution, ITS rDNA, lichenised fungi, phylogeny, taxonomy, typification

Introduction

The genus, *Protoparmeliopsis* Choisy, belongs to the large family of lichenised fungi Lecanoraceae. It includes species with a placodioid or umbilicate type of thallus, growing on siliceous rocks or on soil (Zhao et al. 2016). They produce lecanorine apothecia and *Lecanora*-type asci, specifically containing hyaline, simple ascospores. Their centre of distribution is concentrated in semi-arid regions of the northern Hemisphere. Although well established at present, owing to their treatment by Zhao et al. (2016), the history of the genus taxonomy and nomenclature is very complicated.

The *Protoparmeliopsis* genus was proposed by Choisy in 1929 with *Protoparmeliopsis muralis* indicated as a type species. However, the generic concept was not followed and, consequently, the majority of the lecanoroid species with characteristic placodioid thallus morphology were, for decades, included into the *Lecanora* subg. *Placodium* sect. *Placodium* group. This section was proposed by Ryan and Nash (1993) for the *Lecanora* species characterised by an areolate-squamulose, lobate or subfoliose thallus, usually with a true cortex and loose medulla. Modern insights into the genus taxonomy afforded by molecular studies, however, revealed that thallus morphology in lecanoroid lichens does not reflect phylogenetic relationships. Moreover, the genus, *Lecanora* sensu lato, as well as subgenus, *Placodium,* turned out to be highly heterogeneous and polyphyletic (Poelt and Grube 1993; Arup and Grube 1998; Pérez-Ortega et al. 2010; Kondratyuk et al. 2014b; Leavitt et al. 2016). Still, the *Protoparmeliopsis* genus was not accepted as a separate genus in the family, Lecanoraceae, for a long time, based on the molecular data (Lumbsch and Huhndorf 2007, 2010). Recent studies have identified it as a well-supported, monophyletic clade nested within *Lecanora* s.l. and it has been subsequently posited to be accepted at the generic level (Kondratyuk et al. 2014b; Miadlikowska et al. 2014; Zhao et al. 2016).

During independent research, concentrated on the biodiversity of saxicolous lichens in Bolivia and Peru, as well as southern Poland, an interesting placodioid representative of Lecanoraceae has been found. Morphology and chemistry of the species suggested that it belongs to the *Protoparmeliopsis* genus. However, establishing its epithet turned out to be challenging. The scope of our study was to explain the systematic position of the lichen with application of integrated taxonomy tools. The survey revealed that the collection represents *P. garovaglii* and the status of the species is briefly discussed. As the epithet was never typified, a herbarium query was performed and, as a result, the species is neotypified herein.

Material and methods

Morphology and chemistry

This study is based on collections from the following herbaria: ASU, KRAM, L, MIN and WRSL, as well as the first author's private material (hb. Szczepańska). The mor-

phology and anatomy of the specimens were studied with a dissecting and light microscope according to routine techniques. For light microscopy, vertical, free-hand sections of apothecia were cut by a razor blade and mounted in water. Hymenium measurements were made in water and ascospores measurements in 10% potassium hydroxide – KOH (K). The structure and conglutination of paraphyses were also studied in K. The solubility of granules in epihymenium was tested with K and N (50% nitric acid). At least 10 measurements of the morphological variables were made for each sample and 20 spores from different specimens were assessed, as well as their minimum and maximum values being calculated.

Chemical examination included colour reactions and thin-layer chromatography (TLC). Spot test reactions of thalli, apothecial margins and discs were made with K, sodium hypochlorite [commercial laundry bleach] (C) and paraphenylenediamine [solution in 95% ethyl alcohol] (PD). The TLC analyses were undertaken in solvent system A, B' and C using the standardised method of Culberson (1972) and following Orange et al. (2001).

Descriptions of the species are based on our own observations, measurements and TLC analyses made while examining the specimens cited in this paper. All specimens presented in the manuscript as in "Specimens examined" and included in the molecular analysis were studied; however, the morphological description of *Protoparmeliopsis garovaglii* is primarily based on the proposed neotype specimen. The terminology used in the descriptions of the species is based on Ryan et al. (2004).

DNA extraction, amplification and sequencing

Genomic DNA was extracted from lichen thalli using the CTab method (Cubero and Crespo 2002). Dried tissues were frozen using liquid nitrogen and disrupted using Mixer Mill MM400 (Retsch; Haan, Germany). The isolated DNA was visualised on 1% TBE agarose gel. The fungal Internal Transcribed Spacer (ITS) rDNA region, which is a commonly used universal barcode marker in studies of non-lichenised and lichenised fungi, has been used in our study. ITS rDNA regions were amplified using primers ITS1F (Gardes and Bruns 1993) and ITS4 (White et al. 1990). The PCR reaction mix included (in the total volume of 20 µl): 1U Taq recombinant polymerase (Thermo-Fisher Scientific, USA), 10X Taq Buffer, 1 mM $MgCl_2$, 0.5 µM of each primer, 0.4 mM dNTP and 1 µl DNA template. The PCR cycle was undertaken with a Veriti Thermal Cycler (Life Technologies; Carlsbad, CA, USA) with the following parameters: 8 min at 95 °C, followed by 32 cycles: 45 s at 95 °C, 45 s at 52 °C (annealing), 1 min at 72 °C, with a final extension step of 10 min at 72 °C. Prior to sequencing, PCR products were purified using GeneMATRIX PCR/DNA Clean Up Purification Kit (Eurx; Gdańsk, Poland). Sequencing, post-reaction purification and readings were undertaken by the sequencing service Genomed (Genomed S.A.; Warsaw, Poland), using an ABI 377XL Automated DNA Sequencer (Applied Biosystems; Carlsbad, CA, USA).

Phylogenetic analysis

The obtained ITS rDNA sequences were assembled and manually edited using Geneious Pro, version 8.0. (Biomatters Ltd) and we also compared our fragments against the BLAST database in order to avoid potential contamination of other fungi (Altschul et al. 1990). We selected ITS sequences of *Protoparmeliopsis garovaglii*, *P. achariana*, *P. macrocyclos*, *P. muralis*, *P. peltata*, *P. zareii* and related genera (*Myriolecis*, *Protoparmelia* and *Rhizoplaca*), newly obtained in this study or downloaded from GenBank. Detailed information regarding sequences including GenBank accession numbers and specimen localities are found in Table 1. Subsequently, the final alignment was performed on the GUIDANCE 2 webserver (Sela et al. 2015) using the MAFFT algorithm (Katoh et al. 2005). The unreliable sites were removed (ca. 90% of sites remain in the alignment) in order to reduce errors caused by ambiguous sites (Penn et al. 2010). The nucleotide substitution models were separately searched for each subset of the partition of the ITS region (ITS1, 5.8S, ITS2) to find the best-fitting model using the corrected Akaike information criterion (AICc) as an optimality model criterion for a greedy algorithm search, as implemented in PartitionFinder version 1.0.1 (Lanfear et al. 2012).

The phylogenetic construction was generated using the Maximum Likelihood (ML) bootstrap tree with simultaneous heuristic search, as implemented in RaxmlGUI version 0.9 beta 2 (Stamatakis 2006; Silvestro and Michalak 2012) under the GTRGAMMA substitution model and 200 bootstrap re-samples. Bayesian Inference was carried out with Markov Chain Monte Carlo (MCMC) implemented in MrBayes

Table 1. The species and specimens studied; newly generated sequences for this study are in bold.

Species	Isolate	Locality	Collector (-s)	Voucher specimens (herbarium)	GenBank no. (ITS)
Myriolecis contractula	AFTOL-ID 877	USA, Washington country	Brodo	Brodo 31501 (DUKE)	HQ650604
Myriolecis dispersa		USA, Illinois	Leavitt	Leavitt 12-002 (BRY-C)	KT453733
		Unitet Kingdom	Hill *s.n.*		KT453734
Protoparmeliopsis achariana				U155	AF070019
Protoparmeliopsis garovaglii		Austria			AF189718
	78	USA, Idaho	Leavitt	Leavitt 078 (BRY-C)	KU934540
	88	USA, Idaho	Leavitt	Leavitt 078 (BRY-C)	KU934541
	89	USA, Idaho	Leavitt	Leavitt 079 (BRY-C)	KT453728
	95	USA, Idaho	Leavitt	Leavitt 095 (BRY-C)	KU934542
	104	USA, Idaho	Leavitt	Leavitt 104 (BRY-C)	KU934544
	105	USA, Idaho	Leavitt	Leavitt 105 (BRY-C)	KU934545
	106	USA, Idaho	Leavitt	Leavitt 106 (BRY-C)	KU934546
	107	USA, Idaho	Leavitt	Leavitt 107 (BRY-C)	KU934547
	108	USA, Idaho	Leavitt	Leavitt 108 (BRY-C)	KU934548
	109	USA, Idaho	Leavitt	Leavitt 109 (BRY-C)	KU934549
	110	USA, Idaho	Leavitt	Leavitt 110 (BRY-C)	KU934543
	116	USA, Idaho	Leavitt	Leavitt 116 (BRY-C)	KU934550
	139	USA, Utah	Leavitt	Leavitt 139 (BRY-C)	KU934551
	140	USA, Utah	Leavitt	Leavitt 140 (BRY-C)	KU934535
	142	USA, Utah	Leavitt	Leavitt 142 (BRY-C)	KT453729
	142	USA, Utah	Leavitt	Leavitt 142 (BRY-C)	KU934536
	145	USA, Utah	Leavitt	Leavitt 145 (BRY-C)	KT453727
	199	USA, Utah	Leavitt	Leavitt 199 (BRY-C)	KU934537

Species	Isolate	Locality	Collector (-s)	Voucher specimens (herbarium)	GenBank no. (ITS)
Protoparmeliopsis garovaglii	**L21**	**Poland**	**Szczepańska**	**Szczepańska 1240 (WRSL)**	**MK084624**
	L88	**Bolivia**	**Flakus**	**Flakus 17529 (KRAM)**	**MK084625**
	L89	**Bolivia**	**Flakus**	**Flakus 21175 (KRAM)**	**MK084626**
	L90	**Bolivia**	**Flakus**	**Flakus 21118 (KRAM)**	**MK084627**
	L91	**Peru**	**Flakus**	**Flakus 9540 (KRAM)**	**MK084629**
	L92	**Peru**	**Flakus**	**Flakus 9603 (KRAM)**	**MK084628**
Protoparmeliopsis macrocyclos		Sweden		U273	AF159933
Protoparmeliopsis muralis				M122	AF070015
	DNA 9890	Germany, Saxony	Scholz	Scholz 0275697 (M)	KT818623
	SK 765	Romania	J.-S. Hur	J.-S. Hur (RO11-130) KOLRI	KP059048
		Russia	Vondrak	Vondrak 106a (PRA)	KU934559
		Russia	Vondrak	Vondrak 106b (PRA)	KU934560
		Russia	Vondrak	Vondrak 9405 (PRA)	KU934556
		Russia	Vondrak	Vondrak 9417 (PRA)	KU934557
		Russia	Vondrak	Vondrak 9417 (PRA)	KT453724
	77	USA, Utah	Leavitt	Leavitt 077 (BRY-C)	KU934552
	141	USA, Utah	Leavitt	Leavitt 141 (BRY-C)	KT453725
	143	USA, Utah	Leavitt	Leavitt 143 (BRY-C)	KU934554
Protoparmeliopsis peltata		Iran	Sohrabi	MS014622	KT453723
		Iran	Sohrabi	MS014620 (personal herbarium)	KU934739
		Iran	Sohrabi	MS014621pelt (personal herbarium)	KU934721
		Iran	Sohrabi	MS014623 (personal herbarium)	KU934722
		Iran	Sohrabi	MS014624pelt (personal herbarium)	KU934723
		Iran	Sohrabi	MS014630 (personal herbarium)	KU934731
		Iran	Sohrabi	MS014637 (personal herbarium)	KU934732
		Iran	Sohrabi	MS014638 (personal herbarium)	KU934733
		Kazakhstan		Kaz 12921c	KU934745
		Kazakhstan		Kaz 13085pelt	KU934746
		Kazakhstan		Kaz 12943	KU934747
		Kazakhstan		Kaz 12948	KU934748
		Kazakhstan		Kaz 13082	KU934749
		Kyrgyzstan	?Lommi, Sampsa	H920340	KU934720
		Kyrgyzstan		H9203329	KU934719
		Kyrgyzstan		H9203118	KU934735
		Kyrgyzstan		H9203304	KU934736
		Kyrgyzstan		H9203334	KU934737
		Kyrgyzstan		H9203194	KU934738
		Russia	Vondrak	Vondrak 9987 (PRA)	KU934725
		Russia	Vondrak	Vondrak 9997 (PRA)	KU934726
		Russia	Vondrak	Vondrak 10016 (PRA)	KU934727
		Russia	Vondrak	Vondrak 10022 (PRA)	KU934728
		Russia	Vondrak	Vondrak 10041 (PRA)	KU934729
		Russia	Vondrak	Vondrak 10130 (PRA)	KU934730
		Russia	Vondrak	Vondrak 9423 (PRA)	KU934740
		Russia	Vondrak	Vondrak V127 (PRA)	KU934751
		Russia	AsLap	951	KU934742
		Russia	AitLap	876	KU934744
		Russia	Sar	937	KU934743
		Turkey	Vondrak	Vondrak 9783 (PRA)	KU934724
		USA	Leavitt	Leavitt 601 (BRY-C)	KU934734
		USA	Leavitt	Leavitt 663 (BRY-C)	KU934741
	U198	USA, Arizona		cf. ASU	AF159925
		USA, Utah			KT453722
Protoparmeliopsis zareii	480	Iran	B. Zarei-Darki	Zarei-Darki 1111 (SK)	KP059049
	480	Iran	B. Zarei-Darki	Zarei-Darki 1111 (SK)	KP059049

v3.2.3 (Ronquist et al. 2011). MrBayes was set to three independent parallel runs, each with four incrementally heated chains started, the run length was settled to 40M generations and, to infer convergence, the average standard deviation of the split frequencies was printed every 1000th generation, discarding the first 50% of the trees sampled as a burn-in fraction. The analyses were stopped after 1M generations when the standard deviation had dropped below 0.01. The resulting phylogenetic trees were visualised in Figtree software (Rambaut 2014).

Results

Phylogeny

A total of 77 sequences were analysed in this study. The final alignment matrix contained eight OTUs and 545 unambiguously aligned nucleotides positions. The phylogeny shows highly supported clades [bootstrap support (BS) = 75%, posterior probability (PP) = 1] inferred from a single locus phylogeny, clearly delimiting the Lecanoraceae as separate from *Myriolecis* (outgroup) (Fig. 1). *P. garovaglii* forms a monophyletic clade highly supported (BS = 95%, PP = 1) within *Protoparmeliopsis*. The newly generated sequence from Poland is placed in a monophyletic clade [BS = 100%, PP = 1] together with the Austrian sequence. South American (Bolivian and Peru; for the first time molecularly confirmed in this study) and USA populations are placed in different clades but lack statistical support.

Taxonomy

***Protoparmeliopsis garovaglii* (Körb.) Arup, Zhao Xin & Lumbsch; Fungal Diversity 78: 301 (2016) [2015].**
Mycobank: 387928
Figs 2a–b

Basionym. *Placodium garovaglii* Körb., Parerga Lichenol. (Breslau) 1:54 (1859) ≡ *Squamaria garovaglii* (Körb.) Anzi, Cat. Lich. Sondr. 46 (1860) ≡ *Lecanora garovaglii* (Körb.) Zahlbr., Ann. Naturhist. Hofmus. 15:208 (1900) ≡ *Placolecanora garovaglii* (Körb.) Räsänen, Hedwigia 81:230 (1944).

Type. Hungary. Szent-György-hegy Mt, 'Ad saxa basaltica montis "Szentgyörgyhegy" prope pagum Kisapáti, comit. Zala. Altit. ca. 400 m. s. m. Mens. Jun. 1920, G.Timkó' [*Flora Hungarici exsiccata* 617, as *Lecanora garovaglii*] (neotype: WRSL-5777, designated here).

Description. Thallus lichenised, placodioid, thick, usually distinctly circular, up to 12 cm diam., not very closely attached to the substrate, prothallus not present. Marginal lobes elongated, distinctly convex, swollen, sinuous, smooth 0.4–1.8 mm wide and 3–10 mm long, broadened and rounded at the ends (Figs. 2c–d). Thallus centre

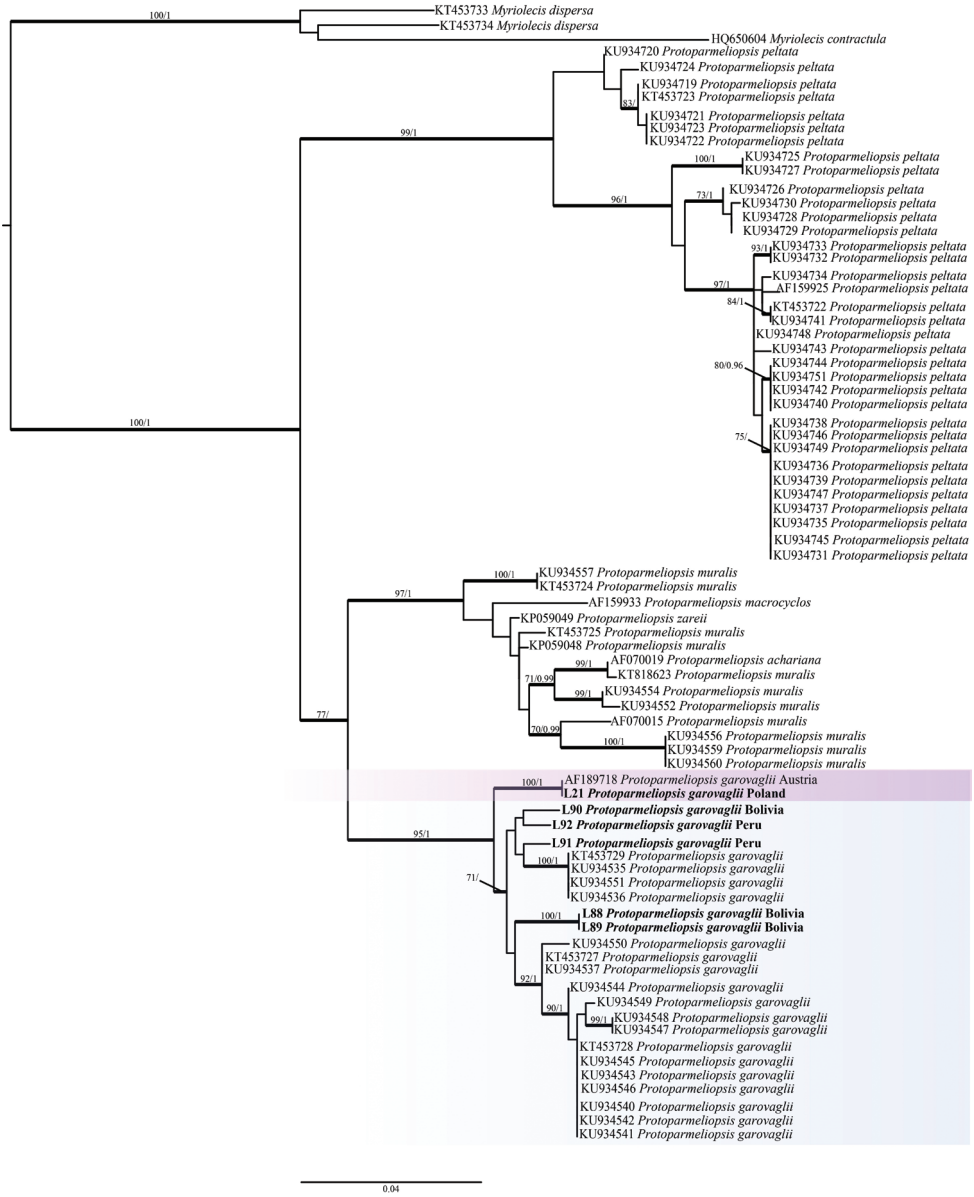

Figure 1. Bayesian Inference of the phylogenetic relationship within *Protoparmeliopsis* species, based on ITS rDNA sequences. High bootstrap support values are shown above thickened branches and bold numbers representing clades (ML – BP ≥ 70%, Bayesian analysis – PP ≥ 0.9). Highlighted squares represent *P. garovaglii* populations in Europe, South and North America. Parmeliaceae species were selected as the outgroup.

more or less areolate. Areoles convex, irregular, overlapping, 0.25–1.0 mm diam. Upper surface mat, pale yellowish-green to greyish-green, tending to be darker in the central part of the thallus, sometimes shining and darker also at the edges of the marginal lobes. Lower surface pale brown. Medulla white, in older lobes distinctly hollow in

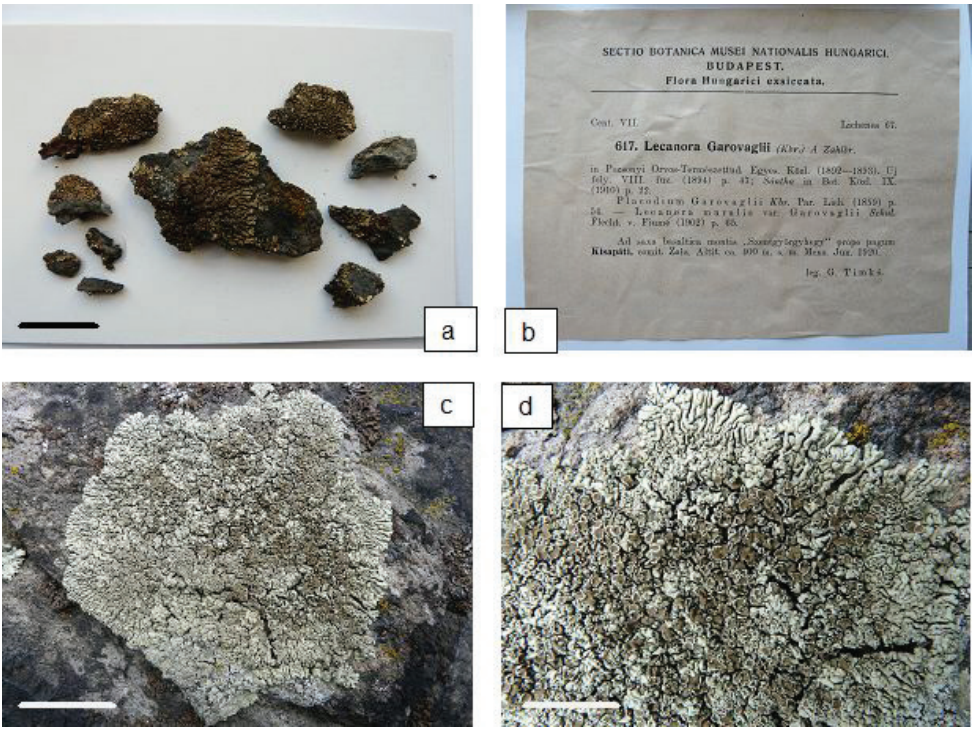

Figure 2. a, b Neotype for *Protoparmeliopsis garovaglii* designated in WRSL herbarium **c, d** Thallus of *Protoparmeliopsis garovaglii* in natural habitat. Scales: 2 cm (**a**); 4 cm (**c**); 2 cm (**d**).

the middle part. Apothecia sessile to constricted at base, dispersed to clustered towards thallus centre, 0.5–2.0 mm diam., circular, older angular, proper margin persistent, paler or concolorous with thallus, matte, slightly radially cracked, flexuose in older and disappearing in mature apothecia. Disc pale brown to yellowish-brown, becoming darker in the centre of thallus, epruinose, flat. Hymenium colourless, 50–60 µm high, hypothecium colourless, epihymenium orange-brown with small granules soluble in K and insoluble in N. Asci clavate, eight-spored. Paraphyses simple or weakly branched with swollen apices. Ascospores hyaline, simple, ellipsoid to oblong-elipsoid, 10–12 × 6–7 µm. Pycnidia not seen.

Chemistry. thallus K+ pale yellow, C–, KC+ yellow, P–; medulla K+ pale yellow, C–, KC+ yellow, P–. Secondary metabolites detected by TLC: ± isousnic, +usnic and ±placodiolic acids (cortex); +zeorin and ± unidentified terpenoides (medulla).

Distribution. the species is widely distributed in the world. It occurs in Europe, Asia, Africa (Morocco; Egea 1996), North America (Canada; Freebury 2014 and USA; Ryan et al. 2004) and South America (Feuerer et al. 1998; Feuerer and Sipman 2005). In Asia, it has been noted in Afghanistan (Poelt and Wirth 1968), India (Upreti and Chatterjee 1998; Singh and Sinha 2010), Iran (Sohrabi et al. 2010), Mongolia (Schubert and Klement 1971), Pakistan (Poelt 1961), Russia (Vondráková and Vondrák 2015), Tajikistan (Kudratov and Mayrhofer 2002) and Turkey (Halici and Candan 2007). In Europe, its records are derived so far from Armenia (Gasparyan et al. 2016),

Austria (Hafellner and Türk 2001), the Czech Republic (Vězda and Liška 1999), Germany (Wirth 1995), Greece (Grube et al. 2001), Italy (Nimis 2016), Netherlands (Aptroot 2011), Portugal and Spain (Llimona and Hladun 2001), as well as Ukraine (Kondratyuk et al. 1996). Here, the species is reported for the first time from Poland.

Ecology. *Protoparmeliopsis garovaglii* is widespread, occurring mostly in dry and warm Mediterranean to mountain areas, foothills and submontane sites (Ryan et al. 2004). It prefers slightly calcareous or basic silicate rocks (limestone, basalt, rhyolite, schist, pumice, volcanic ash, sandstone) and usually occupies sunny habitats, especially steep surfaces (Wirth 1995; Ryan et al. 2004). However, it is noteworthy that, on its northernmost locality in the Netherlands, the species was recorded on a tombstone (Aptroot 2011). In Poland, it was found in mountain areas with outcrops of basalt rocks in the form of a volcanic chimney, surrounded by granite casing. It occupied a lit, warm and dry place on the horizontal surface of the basalt rock with a southern exposure and was accompanied by other lichens such as *Acarospora fuscata*, *Candelariella coralliza*, *Protoparmeliopsis muralis*, *Lecanora rupicola* and *Rhizocarpon geographicum*. During the present study in Bolivia and Peru, *P. garovaglii* was recorded in high Andean open-vegetative regions and in open semi-desert montane areas.

Exiccates examined. Pišut, *Lichenes Slovakiae exsiccati* 36, as *Lecanora garovaglii* (KRAM); Suza, *Lichenes Bohemoslovakiae exiccati* 233, as *Lecanora garovaglii* (KRAM); Weber, *Lichenes exsiccati* 118, as *Lecanora garovaglii* (KRAM).

Specimens examined. Poland. Przedgórze Sudeckie foreland: Wzgórza Strzegomskie hills, Góra Świętego Jerzego Mt, 50°58'25"N, 16°20'10"E, on basalt rocks, 354 m alt., 4 Oct. 2013, K.Szczepańska 1240 (WRSL). Bolivia. Dept. La Paz, Prov. Bautista Saavedra: Anmin Apolobamba, near Taypi Cañuma village, 15°03'20"S, 69°09'07"W, 4506 m alt., 5 July 2010, A.Flakus 17529 & P.Rodriguez-Flakus (KRAM, LPB); on the road from Apolo to Charazani villages (162 km), la Cruz Charazani-Pelechuco, 15°15'00"S, 69°02'51"W, 4545 m alt., 19 May 2011, A.Flakus 21118, 21175, 21176 & O.Plata (KRAM, LPB). Peru. Cañon del Colca, Dept. Arequipa, Prov. Caylloma: near Cabanaconde village, 15°37'56"S, 71°57'49"W, 3462 m alt., 4 July 2006, A.Flakus 9540 (KRAM); *ibid.* 15°38'18"S, 71°57'43"W, 3480 m alt., 5 July 2006, A.Flakus 9603 (KRAM).

Additional specimens examined. Austria. Lower Austria: sunny slate rocks near Krems on the Danube River, 250 m alt., 3 Jan. 1897, Baumgarten (L). USA. Arizona. *Coconino Co*.: Grand Canyon National Forest, top of Hermit Trail, pinyon-juniper woodland, on limestone, 1950 m alt., 11 July 1994, T.H.Nash III 35474 (ASU); *ibid.*, South Kaibab Trail, on sandstone, 1950 m alt., 29 June 1991, M.Boykin 2053 (ASU); *Greenlee Co*.: Apache National Forest, Juan Miller Canyon camp-ground, along the Blue River, ponderosa pine forest with riparian sp., on acid rock, 1740 m alt., 6 June 1998, T.H.Nash III 41809 (ASU); *Maricopa Co*.: Crater Range, along AZ 85, 42 km S of Gila Bend Sonoran Desert, on granite, 425 m alt., 27 Feb. 1998, T.H.Nash III 40608 (ASU); *Santa Cruz Co*.: Coronado National Forest, hillsides to S of Pena Blanca Lake (ca. 15 km WNW of Nogales) and just S of Ruby-Nogales Rd., oak woodland steep slope with rhyolite, on rhyolite, 1200 m alt., 2 June 1998, T.H.Nash III 41656 (ASU). Idaho. *Twin Falls Co*.: E side of U.S. Hwy 30, 6.8 km S of Bills, on

basalt, 915 m alt., 11 Sept. 1998, B.D.Ryan 32953 (ASU). Nevada. *Churchill* Co.: US Hwy 50, N end of Desatoga Mountains, 84 m E of Fallon, 1830 m alt., July 1984, B.D.Ryan 11554 (MIN). North Dakota. *Billings Co*.: Theodore Rooselvelt Nat. Park, S. Unit One mile S of Paddock Creek along park road, on ridge E of road on scoria rock, 2500 ft. alt., 25 July 1982, C.Wetmore 45128 (MIN). Montana. *Park Co*.: Yellowstone National Park, Grazing enclosure 1 mile W of Gardiner at northern edge of park, open grassland on knoll with sagebrush and rock outcrop, 5300 ft. alt., 21 July 1998, C.Wetmore 80972 (MIN).

Discussion

Protoparmeliopsis garovaglii was traditionally characterised by its typically elongate and strongly inflated-plicate lobes of the thalli. For most details, the species was studied by Ryan and Nash (1993), who treated it as a single frequent widespread and extremely variable taxon – *Lecanora garovaglii* s.l., including *L. cascadensis* H. Magn., *L. nevadensis* H. Magn. and *L. peruviana* (Müll. Arg.) Zahlbr. By examining hundreds of specimens, the authors were deeply involved in discussions about the species' variety concerning colour of apothecial discs and associated epihymenial features. They finally concluded that the set of mentioned phenotypic traits is often not clearly expressed and does not exhibit clear correlations with other characters, such as secondary chemistry. Moreover, both disc colour and cortical chemistry correlate with habitat and distribution, respectively, rather than directly with each other. According to us, this serves as evidence of possible phenotypic plasticity, not taxon speciation. The cortical chemistry variation throughout the geographical range of *L. garovaglii* with three cortical substances (isousnic, usnic and placodiolic acids) in different combinations is a separate, interesting problem, discussed in the paper by Ryan and Nash (1993) and ending with the statement that the name cannot be unambiguously assigned to any of the known chemotypes as it is not typified. In this situation, the authors referred to the only specimen under the name, *Placodium garovaglii*, available at that time in the Körber "Typenherbar" in L, originating from "Vel Furva" (Valfurva city, Italy) and containing isousnic and usnic acids in the cortex. However, Körber's collection is kept in the Leiden Herbarium as two different parts. Specimens from the first (Hauptsammlung) are labelled as "Koerber Stammherbar" and those from the second (Typensammlung) as "Koerber Typenherbar" (Liška 2013). It is not clear if Ryan and Nash (1993) searched for original material in both collections or only in the "Typenherbar".

During our study, we tried to trace the original collection of the species. Type citation in the protologue is: 'An basaltigem Gestein "in monte supra Varzi" von Garovaglio gesammelt (Herb. Heufl.)' [Italy, Prov. Pavia, Region of Lombardy, the mountain above Varzi city, on basalt rock, leg. Garovaglio] (Körber, 1859–1865). Heufler's herbarium was sold after his death and currently the final destination of the samples is unknown. We started our enquiries at IBF where Haufler deposited much of his herbarium material during his lifetime. This did not bring any resolution as our double request did not elicit a response. We also requested the specimens of *P. garovaglii*

from L herbarium. Subsequent to the request, we received the historical collection of *P. garovaglii* from the locality: Lower Austria, sunny slate rocks near Krems on the Danube River, alt. 250 m, 3 Jan. 1897, leg. Baumgarten. Obviously, the species cannot be lectotypified, as there is only one locality cited in the protologue and the original collection of the species from *locus classicus* could not be located at any herbaria and may have been lost. For name typification, we considered the collection available at L, however, its lowland origin and cortical chemistry (usnic and placodiolic acids) indicate that it would not be the best choice. We have also made a request at WRSL herbarium knowing that some small part of Körber's collection is also located there. However, none of Körber's specimens representing *P. garovaglii* was available. The most appropriate material for the neotype of the historical collections seen by us is apparently the exsiccate from WRSL, collected in the mountain area of Hungary and it was designated there. This specimen is well preserved, was collected from the basalt rock, has typical morphology suitable to the description given in the protologue and the following cortical chemistry: isousnic, usnic and placodiolic acids (the most frequent chemotype in Europe, according to Ryan and Nash (1993)).

The species most closely related and likely to be confused with *P. garovaglii* is *P. muralis*. In contrast to *P. garovaglii*, the thallus of *P. muralis* is smaller and much more strongly attached to the substrate. Furthermore, thallus lobes of the latter species are distinctly shorter, flattened and thinner and not swollen or sinuous-plicate as they are in the case of *P. garovaglii*. Both species can also be distinguished by their chemistry. *Protoparmeliopsis muralis* contains usnic acid and zeorin but also atranorin, leucotylin, murolic and psoromic acids; the latter are not produced by *P. garovaglii* (Wirth 1995; Ryan et al. 2004; Edwards et al. 2009). To some extent, *P. garovaglii* may also be mistaken with *Rhizoplaca subdiscrepans* (Nyl.) R. Sant., especially as both species have similar colour of the upper surface of the thallus and prefer similar, warm and dry habitats (Wirth 1995; Hafellner and Türk 2001). However, in contrast to *P. garovaglii*, the thallus of *R. subdiscrepans* is usually verrucose-squamulose, polyphyllous, without distinct lobes at the margin and pruinose apothecial discs (Ryan 2001). Both species also have similar cortical chemistry with isousnic, usnic and placodiolic acids in the upper cortex, but *P. garovaglii* additionally contains zeorin in the medulla.

Protoparmeliopsis garovaglii was included in previous phylogenetic frameworks focused on European, North American and Asian populations (Arup and Grube 1998, 2000; Leavitt et al. 2016; Kondratyuk et al. 2014a, b). In this study, we included new sequences from South America and they are placed in a single, highly supported, species-level lineage (BS = 100%, PP = 1). There is a geographical differentiation tendency based on our molecular output. The Polish specimen is placed in a monophyletic clade with a highly supported group (BS = 100%, PP = 1) together with the Austrian sequence. Bolivian, Peruvian and North American populations are placed in different clades but, in most cases, the internal node lacks statistical support. This tendency may follow a population geographical disjunction of different organisms, including lichens, in which the morphological and chemical characters are highly variable in a single species, making a real challenge for species delimitation and, in most cases, these species are treated as a 'complex'. In the case of lichenised fungi, some previous extensive

studies on molecular population or/and phylogeography analyses on species recognition boundaries, such as *Usnea perpusilla* (Wirtz et al. 2008), *Leptogium furfuraceum* (Otálora et al. 2010) *Xanthoparmelia pulla* (Amo de Paz et al. 2012), were performed.

In our study, we analysed differences in morphology, anatomy and chemistry of specimens representing different clades. European material is characterised by a pale green colour of the thallus with elongated, distinctly convex and swollen marginal lobes, which is not very closely attached to the substrate. The apothecial discs are epruinose, bright to dark brown in colour. Within material originating from Bolivia and Peru, we found very similar morphology of the apothecia and thallus, however the thallus colour of Bolivian specimens is more pale yellow than green. In North American, the thallus in many cases is smaller and more closely attached to the substrate, with flat, shorter and narrower marginal lobes (0.3–1.2 mm wide and 2–6 mm long) and is additionally pruinose at the ends. The colour of the discs is usually brown but also yellow-green or yellow-orange, when the upper surface of the thallus has more orange tint. No significant differences were found in the colour or height of the hymenium and epihymenium, nor the paraphyses or shape and size of spores in the specimens representing different clades. Furthermore, we have not found any correlation between secondary chemistry of the thallus and species distribution. Both specimens from Europe, South and North America (Bolivia, Peru and USA) contain zeorin and usnic acids as solid components, when isousnic and placodiolic acids, as well as unidentified terpenoides may be present or absent; however, no sample from South America contained isousnic acid.

Based on these observations, we may confirm great phenotypic variation of specimens representing *P. garovaglii* s.l., also observed by Ryan and Nash (1993). However, we cannot unambiguously correlate perceivable morphotypes with appropriate clades. In particular, morphological differentiation may also greatly reflect responses of individuals to diversity of habitat conditions. Moreover, any far-reaching conclusions must be based on a larger sampling size and should be statistically supported.

We do not claim to assign any taxonomic resolutions concerning *P. garovaglii* s.l. until further molecular population studies provide evidence for species delimitation within the species-complex. The intention of the current study was to genetically support the identification of *P. garovaglii* in collections from areas of research interest to the authors. As a result, molecular evidence of the species occurrences in Poland and South America (Bolivia and Peru) was supplied. Typification of the epithet *P. garovaglii*, via this work, should be useful for further circumscription of related taxa.

Acknowledgements

The curators of ASU, L, MIN and WRSL are gratefully acknowledged for loan of specimens. PRF is greatly indebted to the Director of Herbario Nacional de Bolivia, Instituto de Ecología, Universidad Mayor de San Andrés, La Paz, for generous cooperation. We are grateful to Adam Flakus (Kraków) and Martin Kukwa (Gdańsk) for

helpful assistance with TLC analyses. This work was supported by statutory funds of Wroclaw University of Environmental and Life Sciences and the W. Szafer Institute of Botany, Polish Academy of Sciences as well as by National Science Centre, Poland, project 2016/21/B/NZ8/02463.

References

Altschul SF, Gish W, Miller W, Myers EW, Lipman DJ (1990) Basic local alignment search tool. Journal of Molecular Biology 215: 403–410. https://doi.org/10.1016/S0022-2836(05)80360-2

Amo de Paz G, Cubas P, Crespo A, Elix JA, Lumbsch HT (2012) Transoceanic dispersal and subsequent diversification on separate continents shaped diversity of the *Xanthoparmelia pulla* group (Ascomycota). PLoS ONE 7(6): e39683. https://doi.org/10.1371/journal.pone.0039683

Aptroot A (2011) De Warme schotelkorst (*Lecanora garovaglii*): een submediterraan korstmos nieuw voor Nederland. Buxbaumiella 89: 46–48.

Arup U, Grube M (1998) Molecular systematics of Lecanora subgenus Placodium. Lichenologist 30: 415–425. https://doi.org/10.1006/lich.1998.0149

Arup U, Grube M (2000) Is *Rhizoplaca* (Lecanorales, lichenized Ascomycota) a monophyletic genus? Canadian Journal of Botany 78: 318–327. https://doi.org/10.1139/b00-006

Choisy M (1929) Genres nouveaux pour la lichénologie dans le groupe des Lécanoracées. Bulletin de la societe botanique de France 76: 521–527. https://doi.org/10.1080/00378941.1929.10837179

Cubero OF, Crespo A (2002) Isolation of nucleic acids from lichens. In: Kranner IC, Beckett RP, Varma AK (Eds) Protocols in Lichenology. Springer Lab Manuals. Springer, Berlin, Heidelberg, 381–391. https://doi.org/10.1007/978-3-642-56359-1_23

Culberson CF (1972) Improved conditions and new data for identification of lichen products by standardized thin-layer chromatographic method. Journal of Chromatography 72: 113–125. https://doi.org/10.1016/0021-9673(72)80013-X

Edwards B, Aptroot A, Hawksworth DL, James PW (2009) *Lecanora* Ach. in Luyken (1809). In: Smith CW, Aptroot A, Coppins BJ, Fletcher A, Gilbert OL, James PW, Wolseley PA (Eds) The Lichens of Great Britain and Ireland. British Lichen Society, London, 465–502.

Egea JM (1996) Catalogue of lichenized and lichenicolous fungi of Morocco. Bocconea 6: 19–114.

Feuerer T, Sipman HJM (2005) Additions to the lichenized and lichenicolous fungi of Bolivia. Herzogia 18: 139–144.

Feuerer T, Ahti T, Vitikainen O (1998) Lichenological investigations in Bolivia. In: Marcelli MP, Seaward MRD (Eds) Lichenology in Latin America: history, current knowledge and applications. CETESB, São Paulo, 71–86.

Freebury CE (2014) Lichens and lichenicolous fungi of Grasslands National Park (Saskatchewan, Canada). Opuscula Philolichenum 13: 102–121.

Gardes M, Bruns TD (1993) ITS primers with enhanced specificity for basidiomycetes-application to the identification of mycorrhizae and rusts. Molecular Ecology 2: 113–118. https://doi.org/10.1111/j.1365-294X.1993.tb00005.x

Gasparyan A, Aptroot A, Burgaz AR, Otte V, Zakeri Z, Rico VJ, Arauja E, Crespo A, Divakar PK, Lumbsch HT (2016) Additions to the lichenized and lichenicolous mycobiota of Armenia. Herzogia 29: 692–705. https://doi.org/10.13158/heia.29.2.2016.692

Grube M, Lindblom L, Mayrhofer H (2001) Contributions to the lichen flora of Crete: A compilation of references and some new records. Studia Geobotanica 20: 41–59.

Hafellner J, Türk R (2001) Die liechenisierten Pilze Österreichs – eine Checkliste der bisher nachgewiesenen Arten mit Verbreitungsangaben. Stapfia 76: 3–167.

Halici MG, Candan M (2007) Notes on some lichenicolous fungi species from Turkey. Turkish Journal of Botany 31: 353–356. https://doi.org/10.3906/bot-0811-1

Katoh K, Kuma K, Toh H, Miyata T (2005) MAFFT version 5: improvement in accuracy of multiple sequence alignment. Nucleic Acids Research 33: 511–518. https://doi.org/10.1093/nar/gki198

Körber GW (1859–1865) Parerga Lichenologica. Ergänzungen zum Systema Lichenum Germaniae. E. Trewendt, Breslau, 1–501. https://doi.org/10.5962/bhl.title.87905

Kondratyuk S, Navrotskaya I, Khodosovtsev A, Solonina O (1996) Checklist of Ukrainian lichens. Bocconea 6: 217–294.

Kondratyuk S, Jeong MH, Galanina IA, Yakovchenko LS, Yatsyna AP, Hur JS (2014a) Molecular phylogeny of placodioid lichen-forming fungi reveal a new genus, *Sedelnikovaea*. Mycotaxon 129: 269–282. https://doi.org/10.5248/129.269

Kondratyuk S, Kim J, Kondratiuk AS, Jeong M, Jang S, Pirogov MV, Hur J (2014b) First data on molecular phylogeny of the genus *Protoparmeliopsis* M. Choisy (Lecanoraceae, Ascomycota). Modern Phytomorphology 5: 63–68.

Kudratov I, Mayrhofer H (2002) Catalogue of the lichenized and lichenicolous fungi of Tajikistan. Herzogia 15: 91–128.

Lanfear R, Calcott B, Ho SYW, Guidon S (2012) PartitionFinder: combined selection of partitioning schemes and substitution models for phylogenetic analyses. Molecular Biology and Evolution 29: 1695–1701. https://doi.org/10.1093/molbev/mss020

Leavitt SD, Kraichak E, Vondrak J, Nelsen MP, Sohrabi M, Pérez-Ortega S, St Clair LL, Lumbsch HT (2016) Cryptic diversity and symbiont interactions in rock-posy lichens. Molecular Phylogenetics and Evolution 99: 261–274. https://doi.org/10.1016/j.ympev.2016.03.030

Liška J (2013) The significance of Körber's "Typenherbar", with an explanation of the locality abbreviations on his labels. Lichenologist 45: 25–33. https://doi.org/10.1017/S0024282912000552

Llimona X, Hladun NL (2001) Checklist of the lichens and lichenicolous fungi of the Iberian Peninsula and Balearic Islands. Bocconea 14: 1–581.

Lumbsch HT, Huhndorf SH (2007) Outline of Ascomycota. Myconet 13: 1–58.

Lumbsch HT, Huhndorf SH (2010) Myconet. Volume 14. Part One. Outline of Ascomycota – 2009. Fieldiana Life and Earth Sciences 1: 1–42. https://doi.org/10.3158/1557.1

Miadlikowska J, Frank Kauff F, Högnabba F, Oliver JC, Molnár K, Fraker E, Gaya E, Hafellner J, Hofstetter V, Cécile Gueidan C, Otálora MAG, Hodkinson B, Kukwa M, Lücking R, Björk C, Sipman HJM, Burgaz AR, Thell A, Passo A, Myllys L, Goward T, Fernández-Brime S, Hestmark G, Lendemer J, Lumbsch HT, Schmull M, Schoch CL, Sérusiaux E, Maddison DR, Arnold AE, Lutzoni F, Stenroos S (2014) A multigene phylogenetic synthesis for the class Lecanoromycetes (Ascomycota): 1307 fungi representing 1139 infrageneric taxa, 317 genera and 66 families. Molecular Phylogenetics and Evolution 79: 132–168. https://doi.org/10.1016/j.ympev.2014.04.003

Nimis PL (2016) The Lichens of Italy. A Second Annotated Catalogue. EUT Edizioni Università di Trieste, Trieste, 740 pp.

Orange A, James PW, White FJ (2001) Microchemical methods for the identification of lichens. British Lichen Society, London, 91 pp.

Otálora MAG, Martínez I, Aragón G, Molina MC (2010) Phylogeography and divergence date estimates of a lichen species complex with a disjunct distribution pattern. American Journal of Botany 97: 216–23. https://doi.org/10.3732/ajb.0900064

Penn O, Privman E, Landan G, Graur D, Pupko T (2010) An alignment confidence score capturing robustness to guide-tree uncertainty. Molecular Biology and Evolution 27: 1759–1767. https://doi.org/10.1093/molbev/msq066

Pérez-Ortega S, Spribille T, Palice Z, Elix JA, Printzen C (2010) A molecular phylogeny of the Lecanora varia group, including a new species from western North America. Mycological Progress 9: 523–535. https://doi.org/10.1007/s11557-010-0660-y

Poelt J (1961) Flechten auf dem NW-Karokaram im Rahmen der Deutschen Karakoram-Expedition 1959 von F. Lobbichler und Dr. J. Schneider gesammelt. Mitteilungen der Botanischen Staatssammlung München 4: 83–94.

Poelt J, Grube M (1993) Beiträge zur Kenntnis der Flechtenflora des Himalaya VIII. –Lecanora subgen. Placodium. Nova Hedwigia 57: 305–352.

Poelt J, Wirth V (1968) Flechten aus dem nordbstlichen Afghanistan, gesammelt von H. Roemer im Rahmen der Deutschen Wakhan-Expedition 1964. Mitt. Bot. Staatssammlung München. 7: 219–261.

Rambaut A (2014) Figtree v.1.4.2. Retrieved from http://tree.bio.ed.ac.uk/software/figtree/.

Ronquist F, Teslenko M, van der Mark P, Ayres D, Darling A, Höhna S, Larget B, Liu L, Suchard MA, Huelsenbeck JP (2011) MrBayes 3.2: efficient Bayesian phylogenetic inference and model choice across a large model space. Systematic Biology 61: 539–542. https://doi.org/10.1093/sysbio/sys029

Ryan BD (2001) *Rhizoplaca*. In: Nash III TH, Ryan BD, Gries C, Bungartz F (Eds) Lichen Flora of the Greater Sonoran Desert Region, Vol. 1. Lichens Unlimited, Tempe, 442–448.

Ryan BD, Nash III TH (1993) *Lecanora* Section *Placodium* (Lichenized Ascomycotina) in North America: New Taxa in the *L. garovaglii* Group. Bryologist 96: 288–298. https://doi.org/10.2307/3243856

Ryan BD, Lumbsch HT, Messuti MI, Printzen C, Śliwa L, Nash III TH (2004) *Lecanora*. In: Nash III TH, Ryan BD, Gries C, Bungartz F (Eds) Lichen Flora of the Greater Sonoran Desert Region, Vol. 2. Lichens Unlimited, Tempe, 176–286.

Schubert R, Klement O (1971) Beitrag zur Flechtenflora der Mongolischen Volksrepublik. Feddes Repertorium 82: 187–262. https://doi.org/10.1002/fedr.19710820302

Sela I, Ashkenazy H, Katoh K, Pupko T (2015) GUIDANCE2: accurate detection of unreliable alignment regions accounting for the uncertainty of multiple parameters. Nucleic Acids Research 43 (Web Server issue), W7–W14. https://doi.org/10.1093/nar/gkv318

Silvestro D, Michalak I (2012) RaxmlGUI: A graphical front-end for RAxML. Organisms Diversity and Evolution 12: 335–337. https://doi.org/10.1007/s13127-011-0056-0

Stamatakis A (2006) RAxML-VI-HPC: maximum likelihood-based phylogenetic analyses with thousands of taxa and mixed models. Bioinformatics 22: 2688–2690. https://doi.org/10.1093/bioinformatics/btl446

Singh KP, Sinha GP (2010) Indian Lichens. An Annotated Checklist. Botanical Survey of India, Ministry of Environment and Forests, M/S Bishen Singh Mahendra pal Singh, Uttarakhand.

Sohrabi M, Sipman H, Toghranegar Z, Nezhadsatari T (2010) A contribution to the lichenized mycota of Zanjan province, Iran. Iranian Journal of Botany 16: 125–129.

Upreti DK, Chatterjee S (1998) Lichen genus *Lecanora* subgenus *Placodium* in India. Feddes Repertorium 109: 279–289. https://doi.org/10.1002/fedr.19981090310

Vězda A, Liška J (1999) A catalogue of lichens of the Czech Republic. Institute of Botany, Academy of Sciences of the Czech Republic, Průhonice, 283 pp.

Vondráková OS, Vondrák J (2015) Some new lichen records from the Orenburg Region. Novitates Systematicae Plantarum Non Vascularium 49: 231–238.

White TJ, Bruns TD, Lee S, Taylor J (1990) Amplification and direct sequencing of fungal ribosomal RNA genes for phylogenetics. In: Innis M, Gelfand D, Sninsky J, White T (Eds) PCR Protocols: a Guide to Methods and Applications. Academic Press, New York, 315–322. https://doi.org/10.1016/B978-0-12-372180-8.50042-1

Wirth V (1995) Die Flechten Baden-Württembergs (2nd edn), Vol. 1. Eugen Ulmer, Stuttgart, 1006 pp.

Wirtz N, Printzen C, Lumbsch HT (2008). The delimitation of Antarctic and bipolar species of neuropogonoid *Usnea* (Ascomycota, Lecanorales): a cohesion approach of species recognition for the *Usnea perpusilla* complex. Mycological Research 112: 472–484. https://doi.org/10.1016/j.mycres.2007.05.006

Zhao X, Leavitt SD, Zhao ZT, Zhang LL, Arup U, Grube M, Pérez-Ortega S, Printzen C, Śliwa L, Kraichak E, Divakar PK, Crespo A, Lumbsch TH (2016) Towards a revised generic classification of lecanoroid lichens (Lecanoraceae, Ascomycota) based on molecular, morphological and chemical evidence. Fungal Diversity 78: 293–304. https://doi.org/10.1007/s13225-015-0354-5

MycoKeys 57: 47–60 (2019)
doi: 10.3897/mycokeys.57.36628
http://mycokeys.pensoft.net

RESEARCH ARTICLE

A peer-reviewed open-access journal
MycoKeys
Launched to accelerate biodiversity research

Phylogeny and taxonomy of two new *Plectosphaerella* (Plectosphaerellaceae, Glomerellales) species from China

Zhi-Yuan Zhang[1], Wan-Hao Chen[2], Xiao Zou[1], Yan-Feng Han[1], Jian-Zhong Huang[3], Zong-Qi Liang[1], Sunil K. Deshmukh[4]

1 *Institute of Fungus Resources, Department of Ecology, College of Life Sciences, Guizhou University, Guiyang 550025, Guizhou, China* **2** *Department of Microbiology, Guiyang College of Traditional Chinese Medicine, Guiyang 550025, Guizhou, China* **3** *Engineering Research Center of Industrial Microbiology, Ministry of Education, Fujian Normal University, Fuzhou 350108, Fujian, China* **4** *TERI-Deakin Nano Biotechnology Centre, The Energy and Resources Institute, Darbari Seth Block, IHC Complex, Lodhi Road 110003, New Delhi, India*

Corresponding author: *Yan-Feng Han* (swallow1128@126.com)

Academic editor: *Danny Haelewaters* | Received 30 May 2019 | Accepted 28 July 2019 | Published 7 August 2019

Citation: Zhang Z-Y, Chen W-H, Zou X, Han Y-H, Huang J-Z, Liang Z-Q, Deshmukh SK (2019) Phylogeny and taxonomy of two new *Plectosphaerella* (Plectosphaerellaceae, Glomerellales) species from China. MycoKeys 57: 47–60. https://doi.org/10.3897/mycokeys.57.36628

Abstract

The genus *Plectosphaerella* is the largest genus in the family Plectosphaerellaceae. Some species are plant pathogens, whereas others are soil-borne. Seven *Plectosphaerella* isolates were collected from various locations in the southwest of China. Using multi-locus phylogenetic (LSU, ITS, EF1α, RPB2) analyses combined with morphological characteristics, two new species, *Plectosphaerella guizhouensis* **sp. nov.** and *Plectosphaerella nauculaspora* **sp. nov.** are described, illustrated and compared with related species.

Keywords

Filamentous fungi, Plectosphaerellaceae, Multi-locus, Morphology, Taxonomy

Introduction

The genus *Plectosphaerella* Kleb., established in 1929, is the largest genus in the family Plectosphaerellaceae (Sordariomycetes, Glomerellales) (Giraldo and Crous 2019), consisting of some plant pathogen and soil-borne species. Previously, *Plectosphaerella* was

proposed as a member of Hypocreaceae (Sordariomycetes, Hypocreales) (Gams and Gerlagh 1968, Barr 1990) or Sordariaceae (Sordariomycetes, Sordariales) (Uecker 1993). Zare et al. (2007) established the family Plectosphaerellaceae to accommodate *Acrostalagmus* Corda, *Gibellulopsis* Bat. & G. Maia, *Plectosphaerella* and *Verticillium* Nees. At that time, there were only five species in the genus *Plectosphaerella*, i.e. *P. cucumerina* (Lindf.) W. Gams, *P. cucumeris* Kleb., *P. himantia* (Pers.) Kirschst., *P. melaena* (Fr.) Kirschst. and *P. silenes* (Niessl) Kirschst. Carlucci et al. (2012) transferred all species of the anamorphic genus *Plectosporium* M.E. Palm, W. Gams & Nirenberg to *Plectosphaerella*. Subsequently, several new species and new combinations were introduced and transferred to the genus. To date, the genus *Plectosphaerella* contains 14 accepted species (Carlucci et al. 2012, Liu et al. 2013, Crous et al. 2015, Su et al. 2017, Wijayawardene et al. 2017, Giraldo and Crous 2019, Phookamsak et al. 2019).

Members of the genus *Plectosphaerella* are isolated from different habitats throughout the world, including plants, animals and soil. For example, *P. tabacinum* (J.F.H. Beyma) M.E. Palm, W. Gams & Nirenberg (the anamorph of *P. cucumerina*) has a cosmopolitan distribution with reports in Canada and the USA (North America), Belgium, England, Italy, The Netherlands and Switzerland (Europe), Egypt (Africa) etc. (Raimondo and Carlucci 2018, Giraldo and Crous 2019). It has been isolated from 11 species in 9 different plant genera: *Arabidopsis thaliana*, *Arabidopsis* sp., *Cucumis melo*, *Galium spurium*, *Hydrilla verticillate*, *Nicotiana tabacum*, *Pyrus malus*, *Solanum lycospersicon*, *Viola odorata*, *Viola tricolor*, *Austropotamobius pallipes* etc. (Alderman and Polglase 1985, Palm et al. 1995, Smith-Kopperl et al. 1999, Domsch et al. 2007, Giraldo and Crous 2019). Another common species, *P. plurivora* A.J.F. Phillips, Carlucci & M.L. Raimondo, has been reported from Australia, Belgium, Germany, Italy, The Netherlands, New Zealand, UK, the USA etc. and is isolated from soil, *Lolium perenne*, *Nicotiana tabacum*, *Solanum lycopersicum*, *Solanum tuberosum* etc. (Giraldo and Crous 2019). Raimondo and Carlucci (2018) reported that *Plectosphaerella* spp. could result in root and collar rot, plus vascular and leaf symptoms. Only two species, *P. oligotrophica* T.T. Liu, D.M. Hu & L. Cai and *P. humicola* Giraldo López & Crous, have been isolated from soils (Liu et al. 2013, Giraldo and Crous 2019).

During the investigation of keratinolytic fungi from different soils in China, seven isolates in the genus *Plectosphaerella* were obtained in Guizhou Province, China. The aim of our project was to identify these isolates, based on combined molecular phylogeny and morphological characteristics.

Materials and methods

Isolates and Morphology

Soil samples were collected from Qianlingshan Park (26°60'N, 106°69'E), Guiyang city and the affiliated hospital of Zunyi Medical University (27°70'N, 106°94'E), Zunyi city, Guizhou Province, China by Zhi-Yuan Zhang on 10 Sept. 2016. Samples were collected 3–10 cm below the soil surface and placed in Ziploc plastic bags. Isola-

tion and purification of strains were undertaken according to methods described by Zhang et al. (2019). Sterile chicken feathers and human hairs were combined with the soil samples. Samples were placed in sterile Petri dishes, which were moistened with ddH_2O. The baited soil sample Petri dishes were incubated at 25 °C for 1 month and remoistened as necessary. Two grams of sample were added to test tubes containing 9 ml of ddH_2O. The mixture was then diluted to $1:10^4$ and 1 ml of suspension was evenly spread on plates containing Sabouraud's dextrose agar (SDA, 10 g of peptone, 40 g of dextrose, 20 g of Agar, 1 litre of ddH_2O) with anti-bacterial chloramphenicol and cycloheximide medium. Plates were incubated at 25 °C for 5 d. The axenic strains were then transferred to potato dextrose agar (PDA, Bio-way, China) plates for purification and to test-tube slants for storage at 4 °C.

Type collections of the novel species are deposited in the Mycological Herbarium of the Institute of Microbiology, Chinese Academy of Sciences, Beijing, China (**HMAS**). The ex-type living cultures and other strains of our study are deposited in the China General Microbiological Culture Collection Center (**CGMCC**) and the Institute of Fungus Resources, Guizhou University (**GZAC**). The axenic strains were incubated on PDA and Czapek agar (CA, Bio-way, China) at 25 °C in darkness. Macroscopic characterisation was undertaken after 14 d of incubation and the colony colours (surface and reverse) were observed. Preparations were mounted in ddH_2O to study the mycelial morphology, conidiogenous cells, conidial structures and other microstructures from PDA cultures. Photomicrographs of diagnostic structures were made using an OLYMPUS BX53 microscope equipped with differential interference contrast (DIC) optics, an OLYMPUS DP73 high-definition colour camera and cellSens software v.1.18.

DNA extraction, PCR amplification and Sequencing

Total genomic DNA was extracted from fresh fungal mycelia using the BioTeke Fungus Genomic DNA Extraction Kit (DP2032, BioTeke, China), following the manufacturer's instructions. The internal transcribed spacer (ITS) regions and the 5' end of the 28S nrRNA locus (LSU) were amplified and sequenced with the primer pairs ITS1/ITS4 (White et al. 1990) and LR0R/LR7 (Vilgalys and Hester 1990, Vilgalys and Sun 1994), respectively. Fragments of the translation elongation factor 1-alpha (EF1α) and the RNA polymerase II (RPB2) genes were amplified with primer sets EF1-983F/EF-2218R (Rehner and Buckley 2005) and RPB2-5F/RPB2-7cR (Liu et al. 1999), respectively. Polymerase chain reaction (PCR) was performed in 25 µl reactions containing 1.0 µl DNA template, 1.0 µl of each forward and reverse primers (10 µmol/l), 12.5 µl 2× MasterMix (Aidlab Biotechnologies Co. Ltd., Beijing, China) and 8.5 µl ddH_2O. Cycling conditions were as follows: initial denaturation at 94 °C for 5 min; followed by 35 cycles at 94 °C for 45 s, annealing depending on the locus (54 °C for ITS, LSU and EF1α, 56 °C for RPB2) for 45 s and extension at 72 °C for 60 s; and a final extension at 72 °C for 10 min. Sequencing was performed by TSINGKE Biological Technology (Kunming, China), using the corresponding primers.

Phylogenetic Analyses

The DNA sequences, generated in this study, were assembled using Lasergene software (version 6.0, DNASTAR). Sequence data, mostly from Giraldo and Crous (2019), were downloaded from NCBI GenBank for molecular phylogenetic analyses (Table 1). Two sequences of *Brunneochlamydosporium nepalense* (isolates CBS 277.89 and CBS 971.72) were chosen as outgroup taxa. Sequences of each locus were aligned through MAFFT v.7.407 (Katoh and Standley 2013), using the default parameters and manually corrected in MEGA 6.06 (Tamura et al. 2013). The aligned sequences of multiple loci were concatenated by SequenceMatrix v.1.7.8 (Vaidya et al. 2011).

Maximum likelihood (ML) analyses were constructed with IQ-TREE v. 1.6.11 (Nguyen et al. 2015). The best-fit model of substitution for each locus was estimated using IQ-TREE's ModelFinder function (Kalyaanamoorthy et al. 2017) under the Bayesian Information Criterion (BIC). The selected models were TIMe+R2 for LSU, TNe+R2 for ITS, TIM2+F+R3 for EF1α and TN+I+G4 for RPB2. Bootstrap analyses was performed using the ultrafast bootstrap approximation (Minh et al. 2013) with 1,000 replicates and a bootstrap support (BS) ≥ 95% was considered as statistically significant.

For Bayesian Inference (BI), a Markov Chain Monte Carlo (MCMC) algorithm was used to generate phylogenetic trees with Bayesian probabilities using MrBayes v.3.2 (Ronquist et al. 2012) for the combined sequence datasets. The selection of the best-fit nucleotide substitution model for each locus was calculated by the Akaike Information Criterion (AIC) with Modeltest v.3.7 (Posada and Crandall 1988). The GTR+I+G model was selected for all datasets (LSU, ITS, EF1α, RPB2). Two runs were executed simultaneously for 5,000,000 generations and sampled every 500 generations. After the BI analyses, both runs were examined with Tracer v.1.5 (Drummond and Rambaut 2007) to determine burn-in and check for convergence. The final tree was submitted to TreeBASE, submission ID: 24412 (http://www.treebase.org).

Results

Phylogenetic analyses

Fifty-five strains (including the seven with new sequence data) were included in our multi-locus dataset (Table 1), which comprised 2536 positions, of which 322 were phylogenetically informative (35 of LSU, 54 ITS, 76 EF1α, and 157 RPB2). Tree topology of the Bayesian analyses was similar to that of the Maximum likelihood analyses.

The analyses of concatenated dataset (Figure 1) showed that our isolates CGMCC 3.19658, CGMCC 3.19659 and CGMCC 3.19660 clustered in a single clade with maximum support (BI pp = posterior probability 1, ML BS 100). Similarly, the isolates CGMCC 3.19656 and CGMCC 3.19657 clustered in another single clade with high support (BI pp 1, ML BS 100). Furthermore, our isolates CGMCC 3.19654 and CGMCC 3.19655 clustered with other *Plectosphaerella plurivora* isolates from CBS in a single subclade supported by BI pp = 0.92.

Table 1. Strains included in the phylogenetic analyses.

Species	Strain No.	GenBank Accession Number			
		LSU	ITS	EF1α	RPB2
Brunneochlamydosporium nepalense	CBS 277.89	LR025812	LR026683	LR026385	LR026111
	CBS 971.72 **T**	LR025813	LR026684	LR026386	LR026112
Plectosphaerella alismatis	CBS 113362 **T**	LR025932	LR026794	LR026489	LR026196
P. citrullae	CBS 131740	LR025933	LR026795	LR026490	–
	CBS 131741 **T**	LR025934	LR026796	LR026491	LR026197
P. cucumerina	CBS 137.33	LR025935	LR026797	LR026492	LR026198
	CBS 137.37 **T**	LR025936	LR026798	LR026493	LR026199
	CBS 139.60	LR025937	LR026799	LR026494	LR026200
	CBS 286.64	LR025938	LR026800	LR026495	LR026201
	CBS 355.36	LR025939	LR026801	LR026496	–
	CBS 367.73	LR025940	LR026802	LR026497	LR026202
	CBS 400.58	LR025941	LR026803	LR026498	LR026203
	CBS 567.78	LR025942	LR026804	LR026499	LR026204
	CBS 619.74	LR025943	LR026805	LR026500	LR026205
	CBS 632.94	LR025944	LR026806	LR026501	LR026206
	CBS 101014	LR025945	LR026807	LR026502	LR026207
	CBS 101958	LR025946	LR026808	LR026503	LR026208
	CBS 131739	LR025947	LR026809	LR026504	–
P. delsorboi	CBS 116708 **T**	LR025948	LR026810	LR026505	LR026209
P. guizhouensis	**CGMCC 3.19658 = GZUIFR-QL9.9.1 T**	**MK880431**	**MK880441**	**MK930453**	**MK930460**
	CGMCC 3.19659 = GZUIFR-QL9.9.2	**MK880432**	**MK880442**	**MK930454**	**MK930461**
	CGMCC 3.19660 = GZUIFR-QL9.9.3	**MK880433**	**MK880443**	**MK930455**	**MK930462**
P. humicola	CBS 423.66 **T**	LR025949	LR026811	LR026506	LR026210
P. melonis	CBS 489.96 **T**	LR025950	LR026812	LR026507	–
	CBS 525.93	LR025951	LR026813	LR026508	–
P. oligotrophica	CBS 440.90	LR025952	LR026814	LR026509	LR026211
P. oratosquillae	NJM 0662 **T**	–	AB425974	–	–
	NJM 0665	–	AB425975	–	–
P. pauciseptata	CBS 131744	LR025953	LR026815	LR026510	–
	CBS 131745 **T**	LR025954	LR026816	LR026511	LR026212
P. plurivora	CBS 101.87	LR025955	LR026817	LR026512	–
	CBS 215.84	LR025956	LR026818	LR026513	–
	CBS 260.89	LR025957	LR026819	LR026514	LR026213
	CBS 261.89	LR025958	LR026820	LR026515	–
	CBS 291.38	LR025959	LR026821	LR026516	–
	CBS 292.66	LR025960	LR026822	LR026517	LR026214
	CBS 386.68	LR025961	LR026823	LR026518	LR026215
	CBS 406.85	LR025962	LR026824	LR026519	–
	CBS 417.81	LR025963	LR026825	LR026520	–
	CBS 642.63	LR025964	LR026826	LR026521	LR026216
	CBS 757.68	LR025965	LR026827	LR026522	LR026217
	CBS 101607	LR025966	LR026828	LR026523	LR026218
	CBS 131742 **T**	LR025967	LR026829	LR026524	LR026219
	CBS 131860	LR025968	LR026830	LR026525	LR026220
	CBS 143233 **T**	MG386133	MG386080	LR026526	LR026221
	CGMCC 3.19654 = GZUIFR-H26.5.1	**MK880436**	**MK880444**	**MK930456**	**MK930463**
	CGMCC 3.19655 = GZUIFR-H26.5.2	**MK880437**	**MK880445**	**MK930457**	**MK930464**
	CBS 139623 **T**	KR476783	KR476750	LR026527	LR026222
	CBS 139624	MH878144	KR476751	LR026528	LR026223
P. ramiseptata	CBS 131743	LR025969	LR026831	LR026529	LR026224
	CBS 131861 **T**	LR025970	LR026832	LR026530	LR026225
P. sinensis	ACCC 39144	KX527892	KX527889	–	–
	ACCC 39145 **T**	KX527891	KX527888	–	–
P. nauculaspora	**CGMCC 3.19656 = GZUIFR-QL8.12.1 T**	**MK880424**	**MK880439**	**MK930451**	**MK930458**
	CGMCC 3.19657 = GZUIFR-QL8.12.2	**MK880425**	**MK880440**	**MK930452**	**MK930459**

T= type strain, strains and sequences generated in this study are shown in **bold. ACCC:** Agricultural Culture Collection of China, Beijing, China; **CBS:** Westerdijk Fungal Biodiversity Institute, Utrecht, The Netherlands; **CGMCC:** China General Microbiological Culture Collection Center; **GZAC:** Guizhou University, Institute of Fungus Resources; "–" represents the absence of GenBank accession.

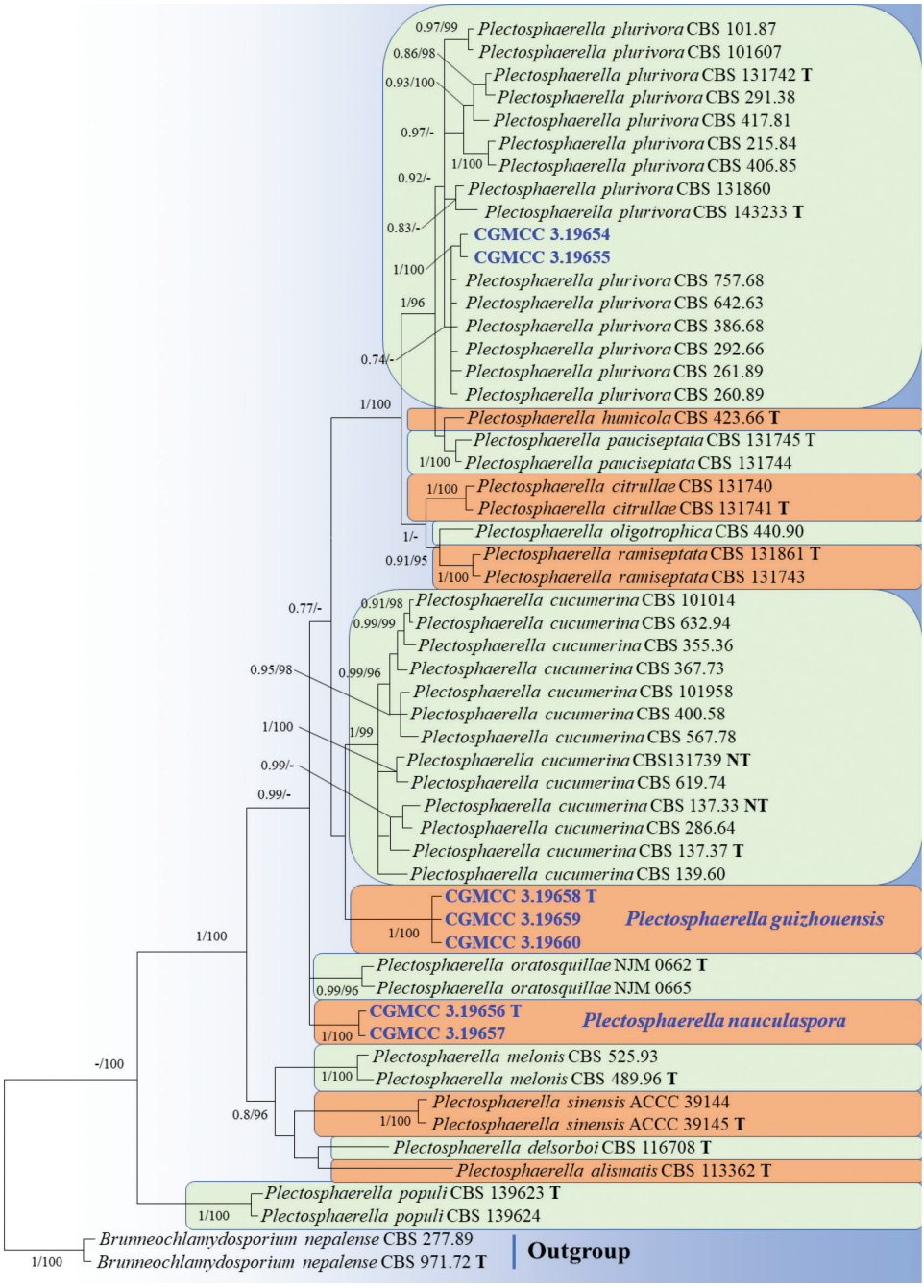

Figure 1. Phylogenetic tree of *Plectosphaerella* species derived from Bayesian analyses and Maximum Likelihood analyses, based on the combined sequences dataset of LSU+ITS+EF1α+RPB2. Bayesian posterior probabilities (BI pp) greater than 0.7 and Maximum Likelihood bootstrap support values (ML BS) greater than 95% are shown above branches. New isolates are in bold and blue. The tree used *Brunneochlamydosporium nepalense* (CBS 277.89 and CBS 971.72) as outgroup.

Taxonomy

Plectosphaerella guizhouensis **Zhi.Y. Zhang, Y.F. Han & Z.Q. Liang, sp. nov.**
MycoBank: MB 830971
Figure 2

Etymology. Referring to Guizhou, the province where the isolate was collected.

Description. *Sexual morph* not observed. *Asexual morph* on CA. *Mycelium* hyaline, smooth, septate, branched and thin-walled, 1–2 µm ($\bar{x}$=1.5 µm) wide. *Conidiophores* solitary, unbranched or rarely branched, hyaline, smooth, thin-walled, sometimes radiating out from hyphal coils. *Conidiogenous cells* growing from a short branch or directly from mycelia, phialides, discrete, polymorphic, cylindrical, sub-cylindrical or ampulliform; terminal or lateral, hyaline, smooth, solitary, straight at the apex, sometimes bent or helicoid, gradually tapering to the apex, 3.5–17 × 0.5–2 µm ($\bar{x}$ = 9.5 × 1.5 µm, n = 20), collarette cylindrical, 0.5–1 µm deep. *Conidia* aggregating in slimy heads, non-septate or 1-septate, fusiform or cylindrical, sometimes rounded at both ends, hyaline, smooth, thin-walled; 2–6.5 × 1.5–5 µm ($\bar{x}$ = 5.5 × 2 µm, n = 10) (1-septate), 3–5 × 1–1.5 µm ($\bar{x}$ = 4 × 1.5 µm, n = 10) (non-septate). *Chlamydospores* absent.

Culture characteristics. Colonies on PDA reaching 74–75 mm diam. in 14 d at 25 °C, milk white, flat, aerial hyphae sparse, floccose at periphery, sub-rounded, margin regular, reverse milk white. Colonies on CA reaching 65–67 mm diam. in 14 d at 25 °C, white to milk white, flat, floccose, margin weakly undulate to faintly fimbriate, reverse milk white.

Typification. CHINA, Guizhou, Guiyang, Qianlingshan Park, 26°60'N, 106°69'E, 1210 m a.s.l., on soil, 10 Sep. 2016, collected and isolated by Zhi-Yuan Zhang, HMAS 255618 (holotype), ex-type CGMCC 3.19658 (= GZUIFR-QL9.9.1); ex-isotype CGMCC 3.19659 (= GZUIFR-QL9.9.2) and CGMCC 3.19660 (= GZUIFR-QL9.9.3).

Notes. Based on multi-locus phylogenetic analyses (Figure 1, see Results) and similar morphological characteristics, the three strains are regarded as the same species, which cluster together very well and form a single clade separated from other species of *Plectosphaerella* (Figure 1). Morphologically, *Plectosphaerella guizhouensis* differs from others species by the fusiform or cylindrical conidia, non-septate conidia (average 4 × 1.5 µm) and separate conidia (5.5 × 2 µm) (see Key). Therefore, based on combined phylogenetic and morphological evidence, *P. guizhouensis* is identified as a new species of *Plectosphaerella*.

Plectosphaerella nauculaspora **Zhi.Y. Zhang, Y.F. Han & Z.Q. Liang, sp. nov.**
MycoBank: MB 830972
Figure 3

Etymology. From "naucula", referring to the navicular conidia.

Description. *Sexual morph* not observed. *Asexual morph* on CA. *Mycelium* hyaline, smooth, septate, branched and thin-walled, 1–1.2 µm ($\bar{x}$=1.5 µm) wide. *Conidiophores*

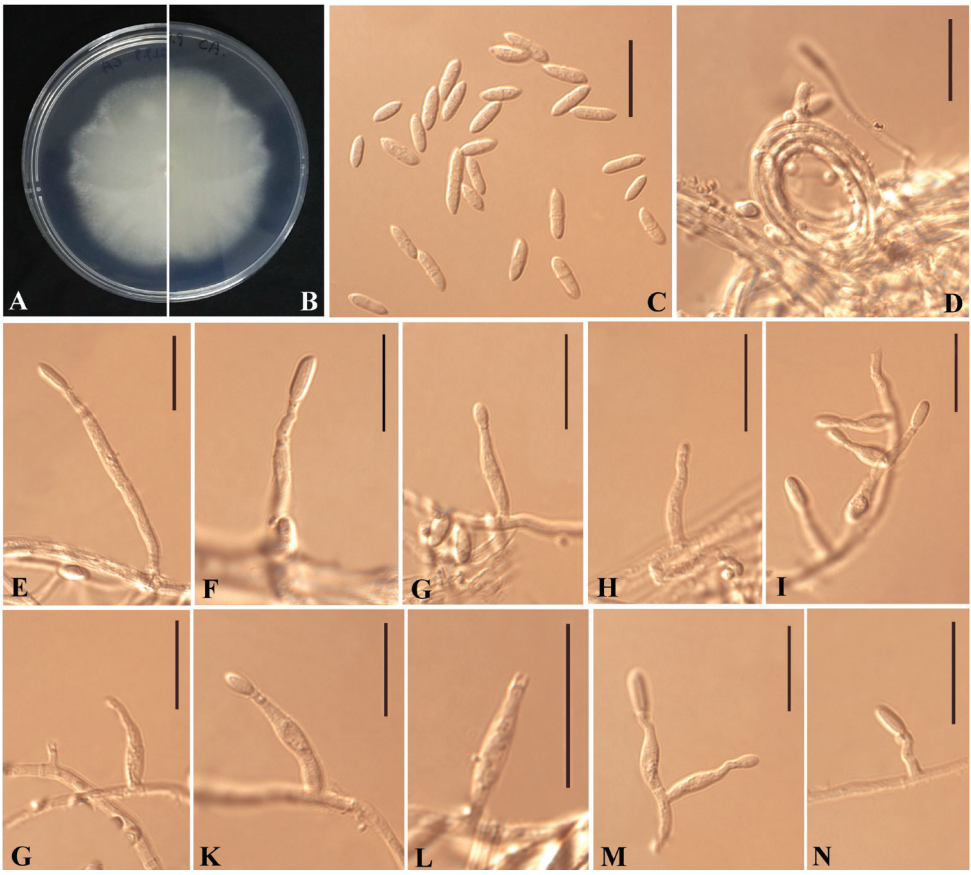

Figure 2. *Plectosphaerella guizhouensis* (HMAS 255618, holotype). **A–B** The front and reverse of colony on CA after 14 d at 25 °C **C** Septate and aseptate conidia **D** Hyphal coils **E–N** Phialides. Scale bars: 10 μm (**C–N**).

solitary, unbranched or rarely branched, hyaline, smooth, thin-walled, hyphal coils not observed. *Conidiogenous cells* growing from short branch or directly from mycelia, phialides, discrete, polymorphic, cylindrical, sub-cylindrical or ampulliform; terminal or lateral, hyaline, smooth, gradually tapering to the apex, straight at the apex, sometimes bent or helicoid, 3–37 × 0.5–2 μm ($\bar{x}$ = 11 × 1 μm, n = 10), collarette minute, cylindrical, 0.5–1 μm deep. *Conidia* aggregating in slimy heads, 1- or 2–celled, mostly navicular, rarely fusiform or cylindrical, sometimes swollen at both ends, hyaline, smooth, thin-walled, 4–7 × 1–2 μm ($\bar{x}$ = 5 × 1.5 μm, n = 10) (1-septate), 3–5 × 1–1.5 μm ($\bar{x}$ = 4 × 1.5 μm, n = 6) (non-septate). *Chlamydospores* not observed.

Culture characteristics. Colonies on PDA reaching 75–76 mm diam. in 14 d at 25 °C, milk white, flat, sub-rounded, margin regular, reverse milk white. Colonies on CA reaching 63–65 mm diam. in 14 d at 25 °C, milk white, aerial hyphae sparse, flat, margin weakly undulate to faintly fimbriate, reverse milk white.

Typification. CHINA, Guizhou, Guiyang, Qianlingshan Park, 26°60'N, 106°69'E, 1220 m a.s.l., on soil, 10 Sep. 2016, collected and isolated by Zhi-Yuan Zhang, HMAS

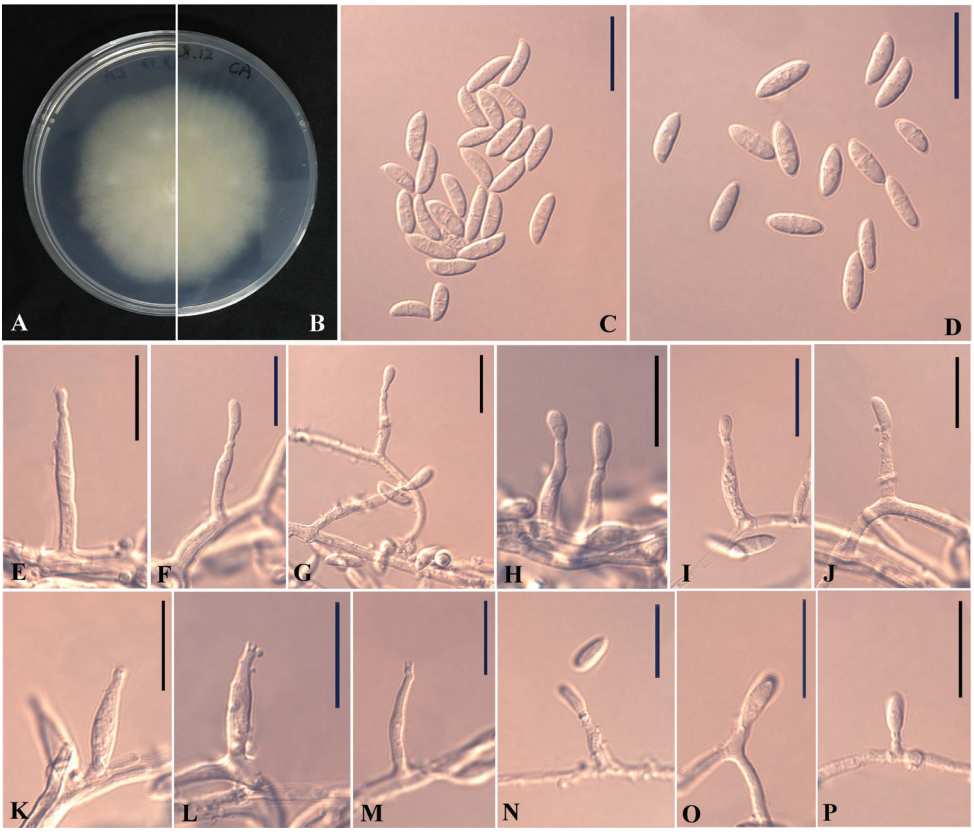

Figure 3. *Plectosphaerella nauculaspora* (HMAS 248154, holotype). **A–B** The front and reverse of colony on CA after 14 d at 25 °C **C–D** Conidia **E–P** Phialides. Scale bars: 10 μm (**C–P**).

248154 (holotype), ex-type CGMCC 3.19656 (= GZUIFR-QL8.12.1); ex-isotypes CGMCC 3.19657 (= GZUIFR-QL8.12.2).

Notes. Phylogenetically, our two isolates CGMCC 3.19656 and CGMCC 3.19657 cluster together very well and form a single clade separated from the other species of *Plectosphaerella* (Figure 1). Morphologically, *Plectosphaerella nauculaspora* is the only species that produces navicular conidia in this genus. Therefore, based on both morphological and phylogenetic evidence, *P. nauculaspora* is proposed as a novel species.

Discussion

In the present study, seven strains of *Plectosphaerella* fungi were isolated from soil in the Guizhou Province, China. Multi-locus phylogenetic analyses in combination with morphological data were used for identification. Our study resulted in the description of two new species, *P. guizhouensis* (3 isolates) and *P. nauculaspora* (2 isolates). In addition, our two isolates CGMCC 3.19654 and CGMCC 3.19655 closely clustered with

P. plurivora and their morphological characters are similar to the original description *P. plurivora* (Carlucci et al. 2012).

Plectosphaerella spp. have diverse life styles and habitat sources – including pathogens of several plants, endophytes of plants, pathogens of animals (mainly involving *Austropotamobius pallipes* and *Oratosquilla oratoria*) and saprophytes on soil (Alderman and Polglase 1985, Palm et al. 1995, Domsch et al. 2007, Duc et al. 2009, Carlucci et al. 2012, Liu et al. 2013, Su et al. 2017, Liang et al. 2017, Raimondo and Carlucci 2018, Giraldo and Crous 2019). Although *Plectosphaerella* spp. were initially isolated from plants (from healthy or symptomatic tissue), subsequent studies found that they also widely distributed on soils and do not necessarily exhibit host specificity (Carlucci et al. 2012, Raimondo and Carlucci 2018, Giraldo and Crous 2019). However, *P. oratosquillae* can only be isolated from animals and it exhibits host specificity (Duc et al. 2009). Likewise, some species (mainly *P. oligotrophica* and *P. humicola*) have so far only been isolated from soils. In comparison with these previous studies, our two new species and one known species of *Plectosphaerella* were obtained from the soil beside a park road by the baiting technique (a method specifically designed for isolating keratinophilic fungi, Zhang et al. 2019). More studies are needed to assess whether our new species could be isolated from other habitats.

At present, more and more studies use combined data from morphological characteristics and molecular phylogeny for identifying new species (e.g. Carlucci et al. 2012, Liu et al. 2013, Su et al. 2017, Giraldo and Crous 2019, Phookamsak et al. 2019). Throughout the years, several loci have been used in the phylogenetic analyses of *Plectosphaerella* and its allies, containing ITS, LSU, EF1α, β-tubulin, CaM and RPB2 (Zare et al. 2007, Duc et al. 2009, Carlucci et al. 2012, Liu et al. 2013, Su et al. 2017). Giraldo and Crous (2019) revised the Plectosphaerellaceae and their results suggested that the phylogeny based on LSU+ITS+EF1α+RPB2 can be used for resolving intergeneric and interspecific relationships within the family Plectosphaerellaceae. As a result, we also used the LSU+ITS+EF1α+RPB2 dataset for phylogenetic analyses of *Plectosphaerella*.

Key to the species of *Plectosphaerella*

1 Growing on crustaceans ..... ***P. oratosquillae***
– On other substrates **2**
2 Teleomorph known **3**
– Teleomorph unknown **5**
3 Ascomata globose or subglobose to pyriform **4**
– Ascomata subglobose to ovoid, or obpyriform ..... ***P. kunmingensis***
4 Asci 50–80 × 6–9 μm ..... ***P. cucumerina***
– Asci 31.4–43 × 6.2–8.2 μm ..... ***P. plurivora***
5 Chlamydospores present **6**
– Chlamydospores absent **8**

6 Conidia mostly septate **7**
– Conidia mostly aseptate ..... ***P. melonis***
7 Conidia 13–19.5 × 2.5–3 µm ..... ***P. alismatis***
– Conidia 6–10 × 1.5–4 µm ..... ***P. sinensis***
8 Phialides branched at tip **9**
– Phialides not branched at tip **11**
9 Phialides 0–3-septate ..... ***P. ramiseptata***
– Phialides 0–1-septate **10**
10 Oligotrophic, polyphialides infrequently seen, collarette 1–2.5 µm ..... ***P. oligotrophica***
– Non-oligotrophic, polyphialides frequently seen, collarette minute ..... ***P. pauciseptata***
11 Conidia ellipsoidal **12**
– Conidia cylindrical, ellipsoidal, fusiform, navicular **14**
12 Conidia mostly septate ..... ***P. delsorboi***
– Conidia aseptate **13**
13 Conidia av. 4 × 2 µm ..... ***P. populi***
– Conidia av. 7.9 × 3.5 µm ..... ***P. citrullae***
14 Conidia mostly navicular ..... ***P. nauculaspora***
– Conidia mostly cylindrical or fusiform **15**
15 Septate conidia 2–6.5 × 1.5–5 µm, aseptate conidia 3–5 × 1–1.5 µm ..... ***P. guizhouensis***
– Septate conidia 7.5–11 × 2.5–3.5 µm, aseptate conidia 5–8 × 2.1–3.3 µm ..... ***P. humicola***

Acknowledgements

We are grateful to the editor Danny Haelewaters (Purdue University, Indiana, USA) and the reviewers – Martina Réblová (Czech Academy of Sciences, Průhonice, Czech Republic) and Yong-Chun Niu (Chinese Academy of Agricultural Sciences, Beijing, China) for comments on the manuscript. This work was financially supported by the Ministry of Science and Technology of China (2013FY110400), Guangdong Technological Innovation Strategy of Special Funds (key areas of research and development programme) (2018B020205003), the National Natural Science Foundation of China (31460010, 31860002) and Construction Program of Biology First-class Discipline in Guizhou (GNYL[2017]009).

References

Alderman DJ, Polglase JL (1985) *Fusarium tabacinum* (Beyma) Gams as a gill parasite in the crayfish, *Austropotamobius pallipes* Lereboullet. Journal of fish disease 8: 249–252 https://doi.org/10.1111/j.1365-2761.1985.tb01222.x

Barr ME (1990) Prodromus to nonlichenized, pyrenomycetous members of class Hymenoascomycetes. Mycotaxon 39: 43–184.

Carlucci A, Raimondo ML, Santos J, Phillips AJL (2012) *Plectosphaerella* species associated with root and collar rots of horticultural crops in southern Italy. Persoonia 28: 34–48. http://dx.doi.org/10.3767/003158512X638251

Crous PW, Wingfield MJ, Guarro J, Hernández-Restrepo M, Sutton DA, Acharya K, Barber PA, Boekhout T, Dimitrov RA, Mueñas M, Dutta AK, Gené J, Gouliamova DE, Groenewald M, Lombard L, Morozova OV, Sarkar J, Smith MTh, Stchigel AM, Wiederhold NP, Alexandrova AV, Antelmi I, Armengol J, Barnes I, Cano-Lira JF, Castañeda Ruiz RF, Contu M, Courtecuisse PrR, da Silveira AL, Decock CA, de Goes A, Edathodu J, Ercole E, Firmino AC, Fourie A, Founier J, Furtado EL, Geering ADW, Gershenzon J, Giraldo A, Gramaje D, Hammerbacher A, He XL, Haryadi D, Khemmuk W, Kovalenko AE, Krawczynski R, Laich F, Lechat C, Lopes UP, Madrid H, Malysheva EF, Marín-Felix Y, Martín MP, Mostert L, Nigro F, Pereira OL, Picillo B, Pinho DB, Popov ES, Rodas Peláez CA, Rooney-Latham S, Sandoval-Denis M, Shivas RG, Silva V, Stoilova-Disheva MM, Telleria MT, Ullah C, Unsicker SB, van der Merwe NA, Vizzini A, Wagner HG, Wong PTW, Wood AR, Groenewald JZ (2015) Fungal planet description sheets: 320–370. Persoonia 34: 167–266 http://dx.doi.org/10.3767/003158515X688433

Domsch KH, Gams W, Anderson TH (2007) Compendium of Soil Fungi (2nd edn). IHW Verlag, Eching.

Drummond A, Rambaut A (2007) BEAST: Bayesian evolutionary analysis by sampling trees. BMC evolutionary biology 7: 214–221. https://doi.org/10.1186/1471-2148-7-214

Duc PM, Hatai K, Kurata O, Tensha K, Yoshitaka U, Yaguchi T, Udagawa SI (2009) Fungal infection of mantis shrimp (*Oratosquilla oratoria*) caused by two anamorphic fungi found in Japan. Mycopathologia 167: 229–247. https://doi.org/10.1007/s11046-008-9174-4

Gams W, Gerlagh M (1968) Beiträge zur Systematik und Biologie von *Plectosphaerella cucumeris* und der zugehörigen Konidienform. Persoonia 5: 177–188.

Giraldo A, Crous PW (2019) Inside Plectosphaerellaceae. Studies in mycology 92: 227–286. https://doi.org/10.1016/j.simyco.2018.10.005

Kalyaanamoorthy S, Minh BQ, Wong TK, von Haeseler A, Jermiin LS (2017) ModelFinder: fast model selection for accurate phylogenetic estimates. Nature Methods 14: 587–589. https://doi.org/10.1038/nmeth.4285

Katoh K, Standley DM (2013) MAFFT Multiple sequence alignment software version 7: improvements in performance and usability. Molecular Biology and Evolution 30: 772–780. https://doi.org/10.1093/molbev/mst010

Li PL, Chai AL, Shi YX, Xie XW, Li Bj (2017) First report of root rot caused by *Plectosphaerella cucumerina* on cabbage in China. Mycobiology 45: 110–113. https://doi.org/10.5941/myco.2017.45.2.110

Liu TT, Hu DM, Liu F, Cai L (2013) Polyphasic characterization of *Plectosphaerella oligotrophica*, a new oligotrophic species from China. Mycoscience 54: 387–393. http://dx.doi.org/10.1016/j.myc.2013.01.003

Liu YJ, Whelen S, Hall BD (1999) Phylogenetic relationships among Ascomycetes: evidence from an RNA polymerase II subunit. Molecular Biology Evolutionary 16: 1799–1808. https://doi.org/10.1093/oxfordjournals.molbev.a026092

Minh Q, Nguyen M, von Haeseler AA (2013) Ultrafast approximation for phylogenetic bootstrap. Molecular Biology and Evolution 30: 1188–1195. https://doi.org/10.1093/molbev/mst024

Nguyen LT, Schmidt HA, von Haeseler A, Minh BQ (2015) IQ-TREE: a fast and effective stochastic algorithm for estimating maximum-likelihood phylogenies. Molecular Biology and Evolution 32: 268–274. https://doi.org/10.1093/molbev/msu300

Palm ME, Gams W, Nirenberg HI (1995) *Plectosporium*, a new genus for *Fusarium tabacinum*, the anamorph of *Plectosphaerella cucumerina*. Mycologia 87: 397–406. https://doi.org/10.2307/3760837

Phookamsak R, Hyde KD, Jeewon R, Bhat DJ, Jones EBG, Maharachchikumbura SSN, Raspé O, Karunarathna SC, Wanasinghe DN, Hongsanan S, Doilom M, Tennakoon DS, Machado AR, Firmino AL, Ghosh A, Karunarathna A, Mešić A, Dutta AK, Thongbai B, Devadatha B, Norphanphoun C, Senwanna C, Wei DP, Pem D, Ackah FW, Wang GN, Jiang HB, Madrid H, Lee HB, Goonasekara ID, Manawasinghe IS, Kušan I, Cano J, Gené J, Li JF, Das K, Acharya K, Anil Raj KN, Latha KPD, Chethana KWT, He MQ, Dueñas M, Jadan M, Martín MP, Samarakoon MC, Dayarathne MC, Raza M, Park MS, Telleria MT, Chaiwan N, Matočec N, de Silva NI, Pereira OL, Singh PN, Manimohan P, Uniyal P, Shang QJ, Bhatt RP, Perera RH, Alvarenga RLM, Nogal-Prata S, Singh SK, Vadthanarat S, Oh SY, Huang SK, Rana S, Konta S, Paloi S, Jayasiri SC, Jeon SJ, Mehmood T, Gibertoni TB, Nguyen TTT, Singh U, Thiyagaraja V, Sarma VV, Dong W, Yu XD, Lu YZ, Lim YW, Chen Y, Tkalčec Z, Zhang YF, Luo ZL, Daranagama DA, Thambugala KM, Tibpromma S, Camporesi E, Bulgakov TS, Dissanayake AJ, Senanayake IC, Dai DQ, Tang LZ, Khan S, Zhang H, Promputtha I, Cai L, Chomnunit P, Zhao RL, Lumyong S, Boonmee S, Wen TC, Mortomer PE, Xu JC (2019) Fungal diversity notes 929–1035: taxonomic and phylogenetic contributions on genera and species of fungi. Fungal diversity 95: 1–273 https://doi.org/10.1007/s13225-019-00421-w

Posada D, Crandall KA (1998) Modeltest: testing the model of DNA substitution. Bioinformatics 14: 817–818. https://doi.org/10.1093/bioinformatics/14.9.817

Raimondo ML, Carlucci A (2018) Characterization and pathogenicity assessment of *Plectosphaerella* species associated with stunting disease on tomato and pepper crops in Italy. Plant pathology 67: 626–641. https://doi.org/10.1111/ppa.12766

Rehner SA, Buckley E (2005). A *Beauveria* phylogeny inferred from nuclear ITS and EF1–alpha sequences: evidence for cryptic diversification and links to *Cordyceps* teleomorphs. Mycologia 97: 84–98. https://doi.org/10.3852/mycologia.97.1.84

Ronquist F, Teslenko M, van der Mark P, Ayres DL, Darling A, Höhna S, Larget B, Liu L, Suchard MA, Huelsenbeck JP (2012) MrBayes 3.2: efficient Bayesian phylogenetic inference and model choice across a large model space. Systematic biology 61: 539–542. https://doi.org/10.1093/sysbio/sys029

Smith-Kopperl ML, Charudattan R, Berher RD (1999) *Plectosporium tabacinum*, a pathogen of the invasive aquatic weed *Hydrilla verticillate* in Flordia. Plant disease 83: 24–28 https://doi.org/10.1094/pdis.1999.83.1.24

Su L, Deng H, Niu YC (2017) Phylogenetic analysis of *Plectosphaerella* species based on multi-locus DNA sequences and description of *P. sinensis* sp. nov. Mycological progress 16: 823–829. https://doi.org/10.1007/s11557-017-1319-8

Tamura K, Stecher G, Peterson D, Filipski A, Kumar S (2013) MEGA6: molecular evolutionary genetics analysis version 6.0. Molecular Biology and Evolution 30: 2725–2729. https://doi.org/10.1093/molbev/mst197

Uecker FA (1993) Development and cytology of *Plectosphaerella cucumerina*. Mycologia 85: 470–479. https://doi.org/10.2307/3760707

Vaidya G, Lohman DJ, Meier R (2011) Sequence Matrix: concatenation software for the fast assembly of multi-gene datasets with character set and codon information. Cladistics 27: 171–180. https://doi.org/10.1111/j.1096-0031.2010.00329.x

Vilgalys R, Hester M (1990). Rapid genetic identification and mapping of enzymatically amplified ribosomal DNA from several *Cryptococcus* species. Journal of Bacteriology 172: 4238–4246. https://doi.org/10.1128/jb.172.8.4238-4246.1990

Vilgalys R, Sun BL (1994). Ancient and recent patterns of geographic speciation in the oyster mushroom *Pleurotus* revealed by phylogenetic analysis of ribosomal DNA sequences. Proceedings of the National Academy of Sciences of the United States of America 91: 4599–4603. https://doi.org/10.1073/pnas.91.10.4599

White TJ, Bruns T, Lee S, Taylor J (1990) Amplification and direct sequencing of fungal ribosomal RNA genes for phylogenetics. In: Innis MA, Gelfand D, Sninsky JJ, White TJ (Eds) PCR Protocols: a guide to methods and amplications. Academic Press, San Diego, 315–322. https://doi.org/10.1016/B978-0-12-372180-8.50042-1

Wijayawardene NN, Hyde KD, Rajeshkumar KC, Hawksworth DL, Madrid H, Kirk PM, Braun U, Singh RV, Crous PW, Kukwa M, Lücking R, Kurtzman CP, Yurkov A, Haelewaters D, Aptroot A, Lumbsch HT, Timdal, E, Ertz D, Etayo J, Phillips AJL, Groenewald JZ, Papizadeh M, Selbmann L, Dayarathne MC, Weerakoon G, Jones EBG, Suetrong S, Tian Q, Castañeda-Ruiz RF, Bahkali AH, Pang KL, Tanaka K, Dai DQ, Sakayaroj J, Hujslová M, Lombard L, Shenoy BD, Suija A, Maharachchikumbura SSN, Thambugala KM, Wanasinghe DN, Sharma BO, Gaikwad S, Pandit G, Zucconi L, Onofri S, Egidi E, Raja HA, Kodsueb R, Cáceres MES, Pérez-Ortega S, Fiuza PO, Monteiro JS, Vasilyeva LN, Shivas RG, Prieto M, Wedin M, Olariaga I, Lateef AA, Agrawal Y, Fazeli SAS, Amoozegar MA, Zhao GZ, Pfliegler WP, Sharma G, Oset M, Abdel-Wahab MA, Takamatsu S, Bensch K, De Silva NI, De Kesel A, Karunarathna A, Boonmee S, Pfister DH, Lu YZ, Luo ZL, Boonyuen N, Daranagama DA, Senanayake IC, Jayasiri SC, Samarakoon MC, Zeng XY, Doilom M, Quijada L, Rampadarath S, Heredia G, Dissanayake AJ, Jayawardana RS, Perera PH, Tang LZ, Phukhamsakda C, Hernández-Restrepo M, Ma XY, Tibpromma S, Gusmao LFP, Weerahewa D, Karunarathna SC (2017) Notes for genera: Ascomycota. Fungal Diversity 86: 1–594. https://doi.org/10.1007/s13225-017-0386-0

Zare R, Gams W, Starink-Willemse M, Summerbell RC (2007) *Gibellulopsis*, a suitable genus for *Verticillium nigrescens*, and *Musicillium*, a new genus for *V. theobromae*. Nova Hedwigia 85: 463–489.https://doi.org/10.1127/0029-5035/2007/0085-0463

Zhang ZY, Han YF, Chen WH, Liang ZQ (2019) Phylogeny and taxonomy of three new *Ctenomyces* (Arthrodermataceae, Onygenales) species from China. Mycokeys 47: 1–16. https://doi.org/10.3897/mycokeys.47.30740

MycoKeys 57: 61–84 (2019)
doi: 10.3897/mycokeys.57.38035
http://mycokeys.pensoft.net

RESEARCH ARTICLE

A peer-reviewed open-access journal
MycoKeys
Launched to accelerate biodiversity research

Crassisporus gen. nov. (Polyporaceae, Basidiomycota) evidenced by morphological characters and phylogenetic analyses with descriptions of four new species

Xing Ji[1], Dong-Mei Wu[2], Shun Liu[1], Jing Si[1], Bao-Kai Cui[1]

1 *Institute of Microbiology, School of Ecology and Nature Conservation, Beijing Forestry University, Beijing 100083, China* **2** *Biotechnology Research Institute, Xinjiang Academy of Agricultural and Reclamation Sciences / Xinjiang Production & Construction Group Key Laboratory of Crop Germplasm Enhancement and Gene Resources Utilization, Shihezi, Xinjiang 832000, China*

Corresponding author: *Bao-Kai Cui* (cuibaokai@yahoo.com)

Academic editor: *María P. Martín* | Received 6 July 2019 | Accepted 9 August 2019 | Published 21 August 2019

Citation: Ji X, Wu D-M, Liu S, Si J, Cui B-K (2019) *Crassisporus* gen. nov. (Polyporaceae, Basidiomycota) evidenced by morphological characters and phylogenetic analyses with descriptions of four new species. MycoKeys 57: 61–84. https://doi.org/10.3897/mycokeys.57.38035

Abstract

A new poroid wood-inhabiting fungal genus, *Crassisporus* gen. nov., is proposed on the basis of morphological characters and molecular evidence. The genus is characterized by an annual growth habit, effused-reflexed to pileate basidiocarps with pale yellowish brown to yellowish brown, concentrically zonate or sulcate, and velutinate pileal surface, a trimitic hyphal system with clamped generative hyphae, tissues turning to dark in KOH, oblong to broadly ellipsoid, hyaline, smooth, and slightly thick-walled basidiospores. Phylogenetic analysis based on ITS+nLSU sequences indicate that *Crassisporus* belongs to the core polyporoid clade. The combined ITS+nLSU+mtSSU+EF1-α+RPB2 sequences dataset of representative taxa in the Polyporaceae demonstrate that *Crassisporus* is grouped with *Haploporus* but forms a monophyletic lineage. In addition, four new species of *Crassisporus*, *C. imbricatus*, *C. leucoporus*, *C. macroporus*, and *C. microsporus* are described.

Keywords

core polyporoid clade, molecular phylogeny, polypore, taxonomy, wood-decaying fungi

Introduction

Polyporales is one of the most diverse orders of Basidiomycota including more than 1800 described species in 216 genera and 13 families (Kirk et al. 2008). In the last 10 years, many new genera in Polyporales have been established, such as *Datroniella* B.K.

Cui, Hai J. Li & Y.C. Dai (Li et al. 2014a), *Fragifomes* B.K. Cui, M.L. Han & Y.C. Dai (Han et al. 2016), *Megasporia* B.K. Cui, Y.C. Dai & Hai J. Li (Li and Cui 2013), *Pseudofibroporia* Yuan Y. Chen & B.K. Cui (Chen et al. 2017), and *Pseudomegasporoporia* X.H.Ji & F.Wu (Ji and Wu 2017).

During the investigations of species diversity and phylogeny of Polyporales, four new species were found that did not belong to any known genus, for which reason, a new genus is established to accommodate them. Morphologically, these four taxa do not fit any of the known polypore taxa. To confirm the position of the new genus, phylogenetic analyses of the new genus and related taxa within Polyporales were carried out based on the internal transcribed spacer (ITS) regions, the large subunit nuclear ribosomal RNA gene (nLSU), the small subunit mitochondrial rRNA gene sequences (mtSSU), the translation elongation factor 1-α gene (EF1-α), and the second largest subunit of RNA polymerase II (RPB2).

Materials and methods

Morphological studies

The studied specimens were deposited at the herbarium of the Institute of Microbiology, Beijing Forestry University (BJFC). Macro-morphological descriptions are based on the field notes and measurements of herbarium specimens. Color terms follow Petersen (1996). Micro-morphological data were obtained from the dried specimens and observed under a light microscope following Shen et al. (2019). Sections were studied at magnifications up to 1000× using a Nikon E80i microscope and phase contrast illumination (Nikon, Tokyo, Japan). Drawings were made with the aid of a drawing tube. Microscopic features, measurements, and drawings were made from slide preparations stained with cotton blue and Melzer's reagent. Spores were measured from sections cut from the tubes. In presenting the variation of spore size, 5% of measurements were excluded from each end of the range, and were given in parentheses. The following abbreviations were used: **KOH**, 5% potassium hydroxide; **IKI**, Melzer's reagent; **IKI-**, neither amyloid nor dextrinoid; **CB**, cotton blue; **CB+**, cyanophilous; **CB-**, acyanophilous; **L**, mean spore length (arithmetic average of all spores); **W**, mean spore width (arithmetic average of all spores); **Q**, variation in the L/W ratios between the specimens studied; ***n*** (a/b), number of spores (a) measured from given number (b) of specimens.

DNA extraction and sequencing

A CTAB rapid plant genome extraction kit (Aidlab Biotechnologies Co. Ltd, Beijing) was used to extract total genomic DNA from dried specimens, and performed the polymerase chain reaction (**PCR**) according to the manufacturer's instructions with

some modifications (Chen et al. 2015). The ITS region was amplified with primer pairs ITS5 and ITS4 (White et al. 1990). The nLSU region was amplified with primer pairs LR0R and LR7 (http://www.biology.duke.edu/fungi/mycolab/primers.htm). The mtSSU region was amplified with primer pairs MS1 and MS2 (White et al. 1990). Part of EF1-α was amplified with primer pairs EF1-983F and EF1-1567R (Rehner and Buckley 2005). RPB2 was amplified with primer pairs fRPB2-5F and fRPB2-7cR or bRPB2-6F and bRPB2-7R (Liu et al. 1999; Matheny 2005). The PCR procedure for ITS, mtSSU and EF1-α was as follows: initial denaturation at 95 °C for 3 min, followed by 34 cycles at 94 °C for 40 s, 54 °C for ITS and mtSSU, 54–56 °C for EF1-α for 45 s, 72 °C for 1 min, and a final extension of 72 °C for 10 min. The PCR procedure for nLSU was as follows: initial denaturation at 94 °C for 1 min, followed by 34 cycles at 94 °C for 30 s, 50 °C for 1 min, 72 °C for 1.5 min, and a final extension of 72 °C for 10 min. The PCR procedure for RPB2 was as follows: initial denaturation at 94 °C for 2 min, followed by 10 cycles at 94 °C for 40 s, 60 °C for 40 s and 72 °C for 2 min, then followed by 37 cycles at 94 °C for 45 s, 55–57 °C for 1.5 min and 72 °C for 2 min, and a final extension of 72 °C for 10 min. The PCR products were purified and sequenced at Beijing Genomics Institute, China, with the same primers. All newly generated sequences were submitted to GenBank (Table 1).

Phylogenetic analyses

Sequences used for phylogenetic analyses in this study are listed in Table 1. Sequences of ITS, nLSU, mtSSU, EF1-α, and RPB2 were aligned initially in MAFFT 7 (Katoh and Standley 2013; http://mafft.cbrc.jp/alignment/server/) and then manually adjusted in BioEdit (Hall 1999). Finally, these gene fragments were concatenated with Mesquite 3.2 (Maddison and Maddison 2017) for further phylogenetic analyses. Phylogenies were inferred from the combined 2-gene dataset (ITS+nLSU) and 5-gene dataset (ITS+nLSU+mtSSU+EF1-α+RPB2). *Heterobasidion annosum* (Fr.) Bref. and *Stereum hirsutum* (Willd.) Pers. obtained from GenBank were used as outgroups to root trees in the 2-gene based analysis. *Laetiporus montanus* Černý ex Tomšovský & Jankovský and *L. sulphureus* (Bull.) Murrill were selected as outgroups to root trees in the 5-gene based analysis. The final concatenated sequence alignments were deposited in TreeBase (https://treebase.org/treebase-web/home.html; submission ID 23521).

Phylogenetic analyses used in this study followed the approach of Zhu et al. (2019) and Song and Cui (2017). Maximum parsimony (**MP**) analysis was performed in PAUP* v. 4.0b10 (Swofford 2002). All characters were equally weighted and gaps were treated as missing data. Trees were inferred using the heuristic search option with TBR branch swapping and 1000 random sequence additions. Max-trees were set to 5000, branches of zero length were collapsed, and all parsimonious trees were saved. Clade robustness was assessed using a bootstrap (**BT**) analysis with 1000 replicates

Table 1. Species, specimens and GenBank accession numbers of sequences used in this study.

Species	Sample no.	Locality	GenBank accessions				
			ITS	nLSU	mtSSU	EF1-α	RPB2
Abortiporus biennis	EL 65-03	Sweden	JN649325	JN649325	–	–	–
Abundisporus fuscopurpureus	Cui 10950	China	KC456254	KC456256	KF051025	KF181154	–
A. pubertatis	Dai 11310	China	KC787568	KC787575	KF051031	KF181125	
	Dai 11927	China	KC787569	KC787576	KF051034	KF181128	–
A. sclerosetosus	MUCL 41438	Singapore	FJ411101	FJ393868	–	–	–
A. violaceus	Ryvarden 32807	Finland	KF018127	KF018135	KF051038	KF181132	–
Antrodia albida	CBS 308.82	USA	DQ491414	AY515348	–	–	–
A. macra	MUAF 887	Czech Republic	EU340898	–	–	–	–
Bjerkandera adusta	NBRC 4983	Unknown	AB733156	AB733333	–	–	–
Cinereomyces lindbladii	KHL 12078	Norway	FN907906	FN907906	–	–	–
Climacocystis borealis	KHL 13318	Estonia	JQ031126	JQ031126	–	–	–
Coriolopsis brunneoleuca	Cui 13911	China	MK116480[a]	MK116489[a]	MK116498[a]	–	MK124544[a]
C. brunneoleuca	Dai 12180	China	KC867414	KC867432	–	–	KF274655
C. polyzona	BKW004	Ghana	JN164978	JN164790	–	JN164881	JN164856
C. retropicta	Cui 13849	China	MK116481[a]	MK116490[a]	MK116499[a]	MK122979[a]	MK124545[a]
	Cui 14030	China	MK116482[a]	MK116491[a]	MK116500[a]	MK122980[a]	MK122987[a]
Crassisporus imbricatus	Cui 6556	China	KC867351	KC867426	–	–	–
C. imbricatus	Dai 10788	China	KC867350	KC867425	KX838374	–	–
C. leucoporus	Cui 16801	Australia	MK116488[a]	MK116497[a]	MK116507[a]	MK122986[a]	MK122993[a]
C. macroporus	Cui 14465	China	MK116485[a]	MK116494[a]	MK116504[a]	MK122983[a]	MK122990[a]
	Cui 14468	China	MK116486[a]	MK116495[a]	MK116505[a]	MK122984[a]	MK122991[a]
C. microsporus	Cui 16221	China	MK116487[a]	MK116496[a]	MK116506[a]	MK122985[a]	MK122992[a]
Daedaleopsis confragosa	Cui 6892	China	KU892428	KU892448	KX838381	KX838418	KU892507
D. hainanensis	Cui 5178	China	KU892435	KU892462	KX838413	KX838441	KU892495
Datronia mollis	RLG6304sp	USA	JN165002	JN164791	–	JN164901	JN164872
Earliella scabrosa	PR1209	Puerto Rico	JN165009	JN164793	–	–	JN164866
Fomes fomentarius	ES 2008-3	Sweden	JX109860	JX109860	–	–	–
Fomitella supina	JV0610	Guatemala	KF274645	KF274646	–	–	–
F. supina	Ryvarden 39027	Puerto Rico	KF274643	–	–	–	–
Fomitopsis betulina	Dai 11449	China	KR605798	KR605737	KR605998	KR610726	KR610816
F. pinicola	Cui 10405	China	KC844852	KC844857	KR605961	KR610690	KR610781
Fragiliporia fragilis	Dai 13080	China	KJ734260	KJ734264	–	–	–
F. fragilis	Dai 13559	China	KJ734261	KJ734265	–	–	–
	Yuan 5516	China	KJ734263	KJ734267	–	–	–
Funalia gallica	Dai 10977	China	KC867378	KC867452	–	–	KU182651
F. trogii	RLG4286Sp	USA	JN164993	JN164808	–	JN164898	JN164867
Gelatoporia subvermispora	BRNU 592909	Czech Republic	FJ496694	FJ496706	–	–	–
Grammethelopsis subtropica	Cui 9035	China	JQ845094	JQ845097	KF051030	KF181124	–
	Cui 9041	China	JQ845096	JQ845099	KF051039	KF181133	–
Haploporus latisporus	Dai 11873	China	KU941847	KU941871	KU941896	KU941934	KU941918
H. latisporus	Dai 10562	China	KU941848	KU941872	KU941897	KU941935	KU941919
H. odorus	Yuan 2365	China	KU941846	KU941870	KU941895	KU941933	KU941917
	Dai 11296	China	KU941845	KU941869	KU941894	KU941932	KU941916
H. subtrameteus	Dai 4222	China	KU941849	KU941873	KU941898	KU941936	KU941920
	Cui 10656	China	KU941850	KU941874	KU941899	KU941937	KU941921
Heterobasidion annosum	PFC 5327	Greece	KC492915	–	–	KC571655	–
Hexagonia apiaria	Cui 6447	China	KC867362	KC867481	MG847228	MG867697	KF274660
H. apiaria	Dai 10784	China	KX900635	KX900682	KX900732	KX900822	MG867677
H. hirta	Dai 5081	China	–	KC867486	–	–	–
	Cui 4051	China	KC867359	KC867471	–	–	–
Hornodermoporus latissimus	Cui 6625	China	HQ876604	JF706340	KF051040	KF181134	–
	Dai 12054	China	KX900639	KX900686	KF218297	KF286303	–

Species	Sample no.	Locality	GenBank accessions				
			ITS	nLSU	mtSSU	EF1-α	RPB2
H. martius	MUCL 41677	Argentina	FJ411092	FJ393859	–	–	–
	MUCL 41678	Argentina	FJ411093	FJ393860	–	–	–
Hydnopolyporus fimbriatus	LR 40855	Puerto Rico	JN649347	JN649347	–	–	–
Hypochnicium lyndoniae	NL 041031	UK	JX124704	JX124704	–	–	–
Laetiporus montanus	Cui 10011	China	KF951274	KF951315	KX354570	KX354617	KT894790
L. sulphureus	Cui 12388	China	KR187105	KX354486	KX354560	KX354607	KX354652
Lenzites betulina	HHB9942Sp	USA	JN164983	JN164794	–	JN164895	JN164860
Megasporia ellipsoidea	Cui 13854	China	MK116483[a]	MK116492[a]	MK116501[a]	MK122981[a]	MK122988[a]
M. major	Cui 10253	China	JQ314366	JQ780437	MK116502[a]	–	–
Megasporoporiella rhododendri	Cui 10745	China	MK116484[a]	MK116493[a]	MK116503[a]	MK122982[a]	MK122989[a]
M. subcavernulosa	Cui 14247	China	MG847213	MG847222	MG847234	MG867705	MG867685
Microporus affinis	Cui 7714	China	JX569739	JX569746	KX880696	–	KF274661
M. vernicipes	Dai 9283	China	KX880618	KX880658	KX880701	KX880926	–
M. xanthopus	Cui 8284	China	JX290074	JX290071	KX880703	KX880878	JX559313
Neodatronia sinensis	Dai 11921	China	JX559272	JX559283	–	–	JX559320
Neofomitella fumosipora	Cui 8816	China	JX569734	JX569741	KX900766	–	–
	Cui 13581a	China	KX900664	KX900714	KX900767	KX900848	KX900815
N. rhodophaea	TFRI 414	Unknown	EU232216	EU232300	–	–	–
Obba rivulosa	KCTC 6892	Canada	FJ496693	FJ496710	–	–	–
Perenniporia hainaniana	Cui 6364	China	JQ861743	JQ861759	KF051044	KF181138	–
P. hainaniana	Cui 6365	China	JQ861744	JQ861760	KF051045	KF181139	–
P. medulla-panis	MUCL 49581	Poland	FJ411088	FJ393876	–	–	–
	Cui 14515	China	MG847214	MG847223	–	MG867707	MG867687
P. substraminea	Cui 10177	China	JQ001852	JQ001844	KF051046	KF181140	–
	Cui 10191	China	JQ001853	JQ001845	KF051047	KF181141	–
Perenniporiella chaquenia	MUCL 47648	Argentina	FJ411084	FJ393856	–	HM467610	–
P. micropora	MUCL 43581	Cuba	FJ411086	FJ393858	–	HM467608	–
P. neofulva	MUCL 45091	Cuba	FJ411080	FJ393852	–	HM467599	–
P. pendula	MUCL 46034	Cuba	FJ411081	FJ393853	–	HM467601	–
Phanerochaete chrysosporium	BKM-F-1767	USSR	HQ188436	GQ470643	–	–	–
Phlebia unica	KHL 11786	Sweden	EU118657	EU118657	–	–	–
Pycnoporus cinnabarinus	Dai 14386	China	KX880629	KX880667	KX880712	KX880885	KX880854
Skeletocutis amorpha	Miettinen 11038	Finland	FN907913	FN907913	–	–	–
Stereum hirsutum	NBRC 6520	Unknown	AB733150	AB733325	–	–	–
Trametes conchifer	FP106793Sp	USA	JN164924	JN164797	–	JN164887	JN164849
T. pubescens	FP101414Sp	USA	JN164963	JN164811	–	JN164889	JN164851
T. tephroleuca	Cui 7987	China	KC848293	KC848378	KX880755	KX880934	KX880869
T. versicolor	FP135156Sp	USA	JN164919	JN164809	–	JN164878	JN164850
Truncospora detrita	MUCL 42649	French Guyana	FJ411099	FJ393866	–	–	–
T. macrospora	Cui 8106	China	JX941573	JX941596	KX880763	KX880920	KX880871
	Yuan 3777	China	JX941574	JX941597	–	–	–
T. ochroleuca	MUCL 39726	China Taiwan	FJ411098	FJ393865	–	–	–
	Cui 5671	China	JX941584	JX941602	KF218309	KF286315	–
T. ohiensis	MUCL 41036	USA	FJ411096	FJ393863	–	–	–
Tyromyces chioneus	Cui 10225	China	KF698756	KF698745	–	–	–
T. kmetii	Penttilä 13474	China	KF705040	KF705041	–	–	–
Vanderbylia fraxinea	DP 83	Italy	AM269789	AM269853	–	–	–
	MUCL 39326	France	FJ411094	FJ393861	–	–	–
V. robiniophila	Cui 5644	China	HQ876609	JF706342	KF051051	KF181145	MG867691
	Cui 7144	China	HQ876608	JF706341	KF051052	KF181146	–
V. vicina	MUCL 44779	Ethiopia	FJ411095	FJ393862	–	–	–
Whitfordia scopulosa	Dai 10739	China	KC867364	KC867482	KX880766	KX880922	MG867692

[a] Newly generated sequences for this study

(Felsenstein 1985). Descriptive tree statistics tree length (**TL**), consistency index (**CI**), retention index (**RI**), rescaled consistency index (**RC**) and homoplasy index (**HI**) were calculated for each maximum parsimonious tree generated.

RAxML v. 7.2.6 (Stamatakis 2006) was used to perform maximum likelihood (ML) analysis involved 200 ML searches under the GTR+GAMMA model and only the best tree from all searches was kept. In addition, 200 rapid bootstrap replicates were run with the GTR+CAT model to assess the reliability of the nodes.

MrModeltest v. 2.3 (Posada and Crandall 1998; Nylander 2004) was used to determine the best fit evolution model for the combined multi-gene dataset for Bayesian inference (BI). Bayesian inference was calculated with MrBayes v. 3.1.2 with a general time reversible (GTR) model of DNA substitution and a gamma distribution rate variation across sites (Ronquist and Huelsenbeck 2003). Four Markov chains were run for two runs from random starting trees for 2 million generations (ITS+nLSU), for 5 million generations (ITS+nLSU+mtSSU+EF1-α+RPB2) until the split deviation frequency value <0.01, and trees were sampled every 100 generation. The first quarter generations were discarded as burn-in. A majority rule consensus tree of all remaining trees was calculated.

Phylogenetic trees were viewed using FigTree v. 1.4.2 (http://tree.bio.ed.ac.uk/software/figtree/). Branches that received bootstrap support for maximum parsimony (MP), maximum likelihood (ML) and Bayesian posterior probabilities (BPP) greater than or equal to 75% (MP and ML) and 0.95 (BPP) were considered as significantly supported, respectively.

Results

Molecular phylogeny

The combined 2-gene dataset included sequences from 68 fungal samples representing 59 taxa. The dataset had an aligned length of 2111 characters, of which 1249 characters were constant, 196 were variable and parsimony-uninformative, and 666 were parsimony-informative. MP analysis yielded 37 equally parsimonious trees (TL = 4143, CI = 0.345, RI = 0.617, RC = 0.213, HI = 0.655). Best model for the combined 2-gene dataset estimated and applied in the BI was GTR+I+G, lset nst = 6, rates = invgamma; prset statefreqpr = dirichlet (1,1,1,1). MP, ML and BI analyses yielded similar tree topologies with an average standard deviation of split frequencies = 0.006293 (BI), and the ML topology is shown in Figure 1. The phylogeny (Fig. 1) inferred from the combined ITS+nLSU sequences demonstrated seven major clades for 59 species of the Polyporales. The new genus *Crassisporus* embed in the core polyporoid clade and grouped with *Haploporus* Bondartsev & Singer.

The combined 5-gene (ITS, nLSU, mtSSU, EF1-α, RPB2) dataset included sequences of 82 fungal samples representing 57 taxa. The dataset had an aligned

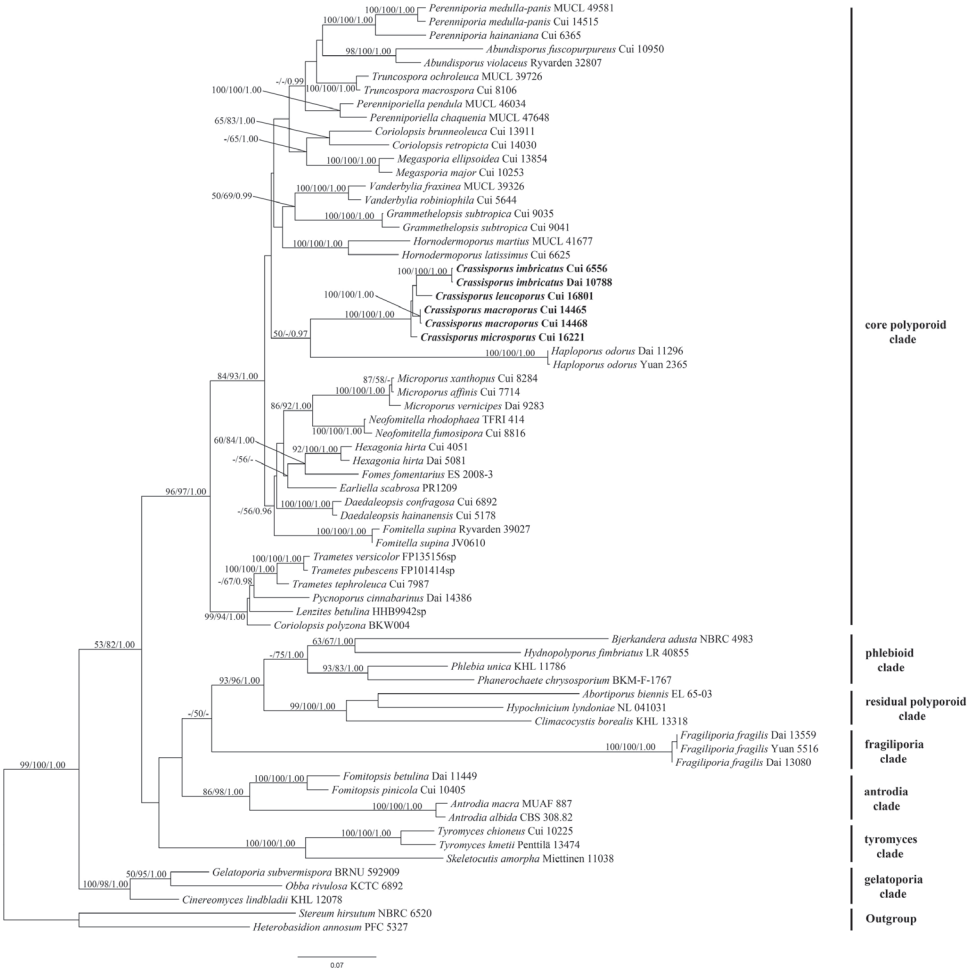

Figure 1. Phylogeny of *Crassisporus* and related genera in Polyporales based on combined ITS and nLSU sequences. Topology is from ML analysis with parsimony bootstrap support values (≥50 %), maximum likelihood bootstrap support values (≥50 %) and Bayesian posterior probability values (≥0.95).

length of 4306 characters, of which 2521 characters were constant, 258 were variable and parsimony-uninformative, and 1527 were parsimony-informative. MP analysis yielded 1 equally parsimonious tree (TL = 8989, CI = 0.339, RI = 0.620, RC = 0.210, HI = 0.661). Bayesian and ML analyses resulted in a similar topology as the MP analysis, with an average standard deviation of split frequencies = 0.006328 (BI); and the ML topology is shown in Figure 2. A further phylogeny (Fig. 2) inferred from the combined 5-gene dataset was obtained for more representative taxa in the Polyporaceae and showed that the new genus grouped with *Haploporus* clade but distinctly formed a monophyletic lineage.

Figure 2. Phylogeny of *Crassisporus* and related species obtained for more representative taxa in the Polyporaceae based on combined sequences dataset of ITS+nLSU+mtSSU+EF1-α+RPB2. Topology is from ML analysis with parsimony bootstrap support values (≥50 %), maximum likelihood bootstrap support values (≥50 %), and Bayesian posterior probability values (≥0.95).

Taxonomy

Crassisporus **B.K. Cui & Xing Ji, gen. nov.**
MycoBank: MB 828486

Notes. Differs from other genera by the combination of effused-reflexed to pileate basidiocarps, pale yellowish brown to yellowish brown, concentrically zonate or sulcate, velutinate pileal surface, a trimitic hyphal system with clamped generative hyphae, tissues darkening in KOH, and oblong to broadly ellipsoid, hyaline, smooth and slightly thick-walled basidiospores.

Etymology. *Crassisporus* (Lat.): referring to thick-walled basidiospores.

Type species. *Crassisporus macroporus* B.K. Cui & Xing Ji.

Basidiocarps annual, effused-reflexed to pileate. Pileal surface pale yellowish brown, yellowish brown to umber-brown when dry, concentrically zonate or sulcate, velutinate. Pore surface usually white, cream buff to cinnamon-buff when fresh, buff, pale yellowish brown to yellowish brown when dry. Context pale yellowish brown to yellowish brown, leathery to corky when dry. Tubes concolorous with the context, corky when dry. Hyphal system trimitic with clamped generative hyphae, skeletal hyphae hyaline to pale yellowish brown, binding hyphae hyaline to pale yellowish brown, negative in Melzer's reagent, tissues turning to black in KOH. Cystidia absent, thin-walled cystidioles usually present. Basidiospores oblong to broadly ellipsoid, hyaline, smooth, slightly thick-walled, IKI-, CB-. Causing a white rot.

Crassisporus imbricatus **B.K. Cui & Xing Ji, sp. nov.**
MycoBank: MB 828487
Figs 3, 4

Notes. *Crassisporus imbricatus* is characterized by imbricate basidiocarps, pale greyish-brown pore surface when dry, round to angular pores (3–5 per mm), and oblong ellipsoid basidiospores (10–14 × 4.5–6.2 μm).

Holotype. CHINA. Hainan Province, Changjiang County, Bawangling Nature Reserve, on dead angiosperm tree, 9 May 2009, Dai 10788 (BJFC).

Etymology. *Imbricatus* (Lat.): referring to the imbricate basidiocarps.

Description. Fruitbody: Basidiocarps annual, effused-reflexed to pileate, imbricate, soft corky, without odor or taste when fresh, leathery to corky upon drying. Pilei semicircular or elongated, projecting up to 1.5 cm, 3.5 cm wide, and 2.5 mm thick at base. Pileal surface yellowish brown, velutinate, concentrically zonate. Pore surface buff when fresh, becoming pale greyish brown when dry; sterile margin indistinct, pores round to angular, 3–5 per mm; dissepiments slightly thick, entire to slightly lacerate.

Figure 3. Basidiocarps of *Crassisporus imbricatus*. Scale bar: 2 cm.

Context yellowish brown, leathery, up to 2.5 mm thick. Tubes concolorous with context, corky, up to 1.5 mm long.

Hyphal structure: Hyphal system trimitic; generative hyphae bearing clamp connections; skeletal and binding hyphae IKI-, CB-; tissues turning to black in KOH.

Context: Generative hyphae infrequent, hyaline, thin-walled, unbranched, 2–3.5 μm in diam.; skeletal hyphae dominant, hyaline to pale yellowish brown, thick-walled with a narrow lumen to subsolid, rarely branched, straight, interwoven, occasionally simple-septate, 2.5–5.5 μm in diam.; binding hyphae hyaline to pale yellowish brown, thick-walled with a narrow lumen to subsolid, flexuous, frequently branched, interwoven, 1.2–2.5 μm in diam.

Tubes: Generative hyphae infrequent, hyaline, thin-walled, occasionally branched, 1.5–3 μm in diam.; skeletal hyphae dominant, hyaline to pale yellowish brown, thick-walled, occasionally branched, strongly interwoven, rarely simple-septate, 1.5–3.5 μm in diam.; binding hyphae hyaline to pale yellowish brown, thick-walled with a narrow lumen to subsolid, flexuous, frequently branched, interwoven, 1–2 μm in diam. Cystidia and cystidioles absent. Basidia clavate, bearing four sterigmata and a basal clamp connection, 19–32 × 9–12 μm; basidioles dominant, in shape similar to basidia, but distinctly smaller.

Spores: Basidiospores oblong ellipsoid, hyaline, slightly thick-walled, smooth, IKI-, CB-, 10–14(–15) × 4.5–6.2(–6.6) μm, L = 12.33 μm, W = 5.34 μm, Q = 2.27–2.36 (*n* = 60/2).

Type of rot. White rot.

Additional specimen (paratype) examined. CHINA. Hainan Province, Changjiang County, Bawangling Nature Reserve, on fallen branch of *Pinus latteri*, 10 May 2009, Cui 6556 (BJFC).

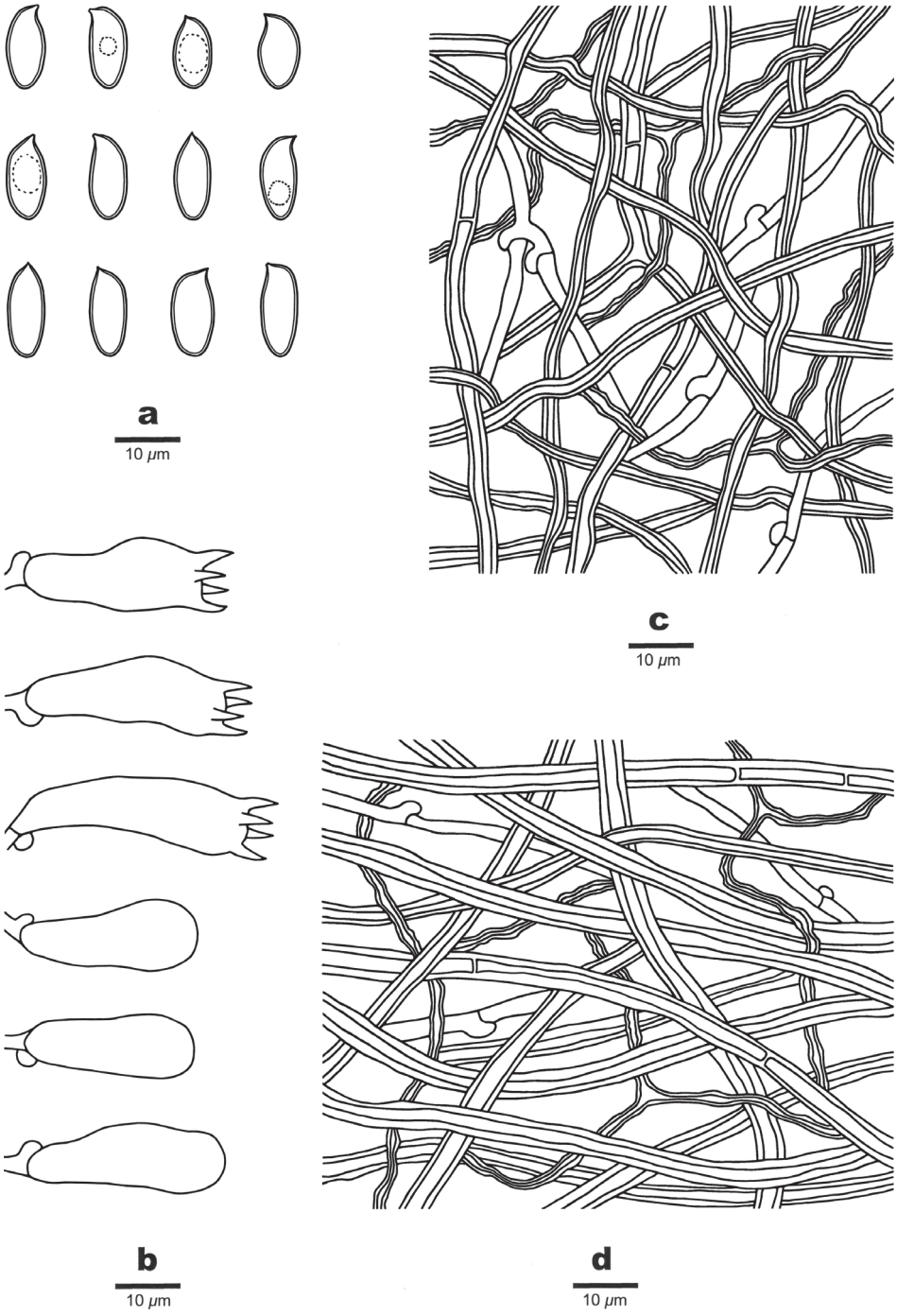

Figure 4. Microscopic structures of *Crassisporus imbricatus* (drawn from the holotype) **A** basidiospores **B** basidia and basidioles **C** hyphae from trama **D** hyphae from context.

Crassisporus leucoporus **B.K. Cui & Xing Ji, sp. nov.**
MycoBank: MB 828488
Figs 5, 6

Notes. *Crassisporus leucoporus* is characterized by a white pore surface when fresh, round to angular pores (3–4 per mm) and oblong ellipsoid basidiospores (8.4–11.2 × 4.2–5.4 μm).

Holotype. AUSTRALIA. Queensland, Cairns, Roadside of Mount Whitfield Park, on fallen angiosperm branch, 18 May 2018, Cui 16801 (BJFC).

Etymology. *Leucoporus* (Lat.): referring to the white pore surface when fresh.

Description. Fruitbody: Basidiocarps annual, effused-reflexed to pileate, corky, without odor or taste when fresh, soft leathery to corky upon drying. Pilei semicircular or elongated, projecting up to 1.5 cm, 3 cm wide, and 6 mm thick at base. Pileal surface yellowish brown to umber-brown, finely velutinate, concentrically sulcate. Pore surface white when fresh, becoming cream, clay buff to pale yellowish brown when dry; sterile margin distinct, cream to pale yellowish brown, up to 1.5 mm wide; pores round to angular, 3–4 per mm; dissepiments slightly thick, entire. Context pale yellowish brown to fulvous, leathery, up to 3 mm thick. Tubes pale yellowish brown, corky, up to 2.5 mm long.

Hyphal structure: Hyphal system trimitic; generative hyphae bearing clamp connections; skeletal and binding hyphae IKI-, CB-; tissues turning to black in KOH.

Context: Generative hyphae infrequent, hyaline, thin-walled, unbranched, 1.1–2.6 μm in diam.; skeletal hyphae in context dominant, pale yellowish brown, thick-walled with a narrow to wide lumen, unbranched, straight, interwoven, occasionally simple-septate, 1.8–3.9 μm in diam.; binding hyphae hyaline to pale yellowish brown, thick-walled with a narrow lumen to subsolid, flexuous, frequently branched, interwoven, 0.7–2.2 μm in diam.

Tubes: Generative hyphae infrequent, hyaline, thin-walled, occasionally branched, 1–2.8 μm in diam.; skeletal hyphae dominant, hyaline to pale yellowish brown, thick-walled with a narrow to wide lumen, occasionally branched, more or less straight, strongly interwoven, 0.9–3.3 μm in diam.; binding hyphae hyaline to pale yellowish brown, thick-walled with a narrow lumen to subsolid, flexuous, frequently branched, interwoven, 0.8–2.1 μm in diam. Cystidia absent, cystidioles fusoid, sometimes septate at the tips, hyaline, thin-walled, 16.7–28.1 × 5.1–6.3 μm. Basidia clavate, bearing four sterigmata and a basal clamp connection, 18.1–29.2 × 6.4–9.8 μm; basidioles dominant, in shape similar to basidia, but smaller.

Spores: Basidiospores oblong ellipsoid, hyaline, smooth, slightly thick-walled, IKI-, CB-, (7.9–)8.4–11.2(–11.5) × (4–)4.2–5.4(–5.7) μm, L = 9.49 μm, W = 4.79 μm, Q = 1.99 (*n* = 60/1).

Type of rot. White rot.

Figure 5. Basidiocarps of *Crassisporus leucoporus*. Scale bars: 1 cm (**A**); 2 cm (**B**).

Crassisporus macroporus **B.K. Cui & Xing Ji, sp. nov.**
MycoBank: MB 828489
Figs 7, 8

Notes. *Crassisporus macroporus* is characterized by cream-buff to cinnamon-buff colored pore surface with distinct sterile margin when fresh, large pores (2–3 per mm) with thin dissepiments, a trimitic hyphal system with cyanophilous skeletal hyphae, the presence of fusoid cystidioles, and oblong ellipsoid basidiospores (9.5–13.2 × 4–6.2 µm).

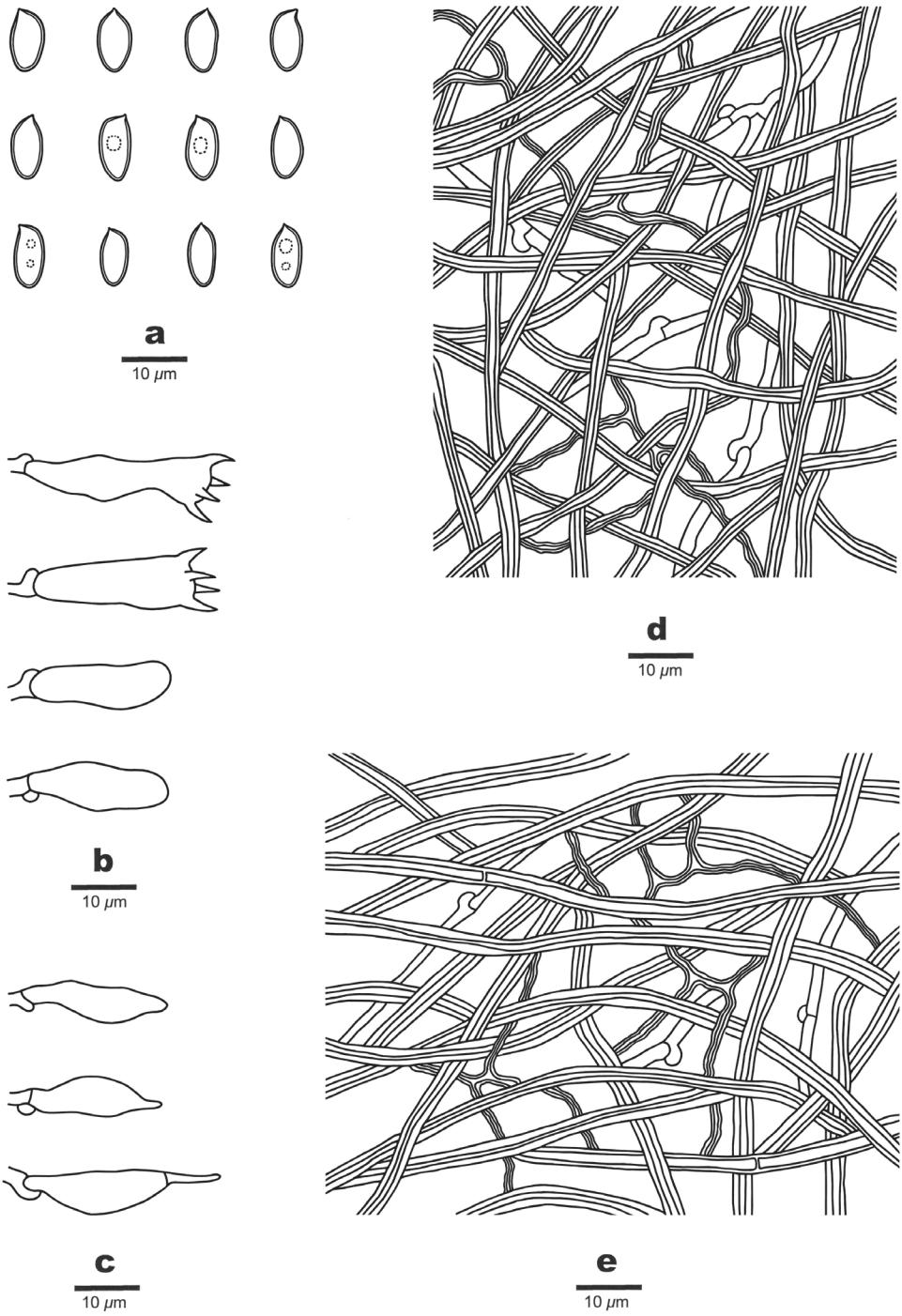

Figure 6. Microscopic structures of *Crassisporus leucoporus* (drawn from the holotype) **A** basidiospores **B** basidia and basidioles **C** cystidioles **D** hyphae from trama **E** hyphae from context.

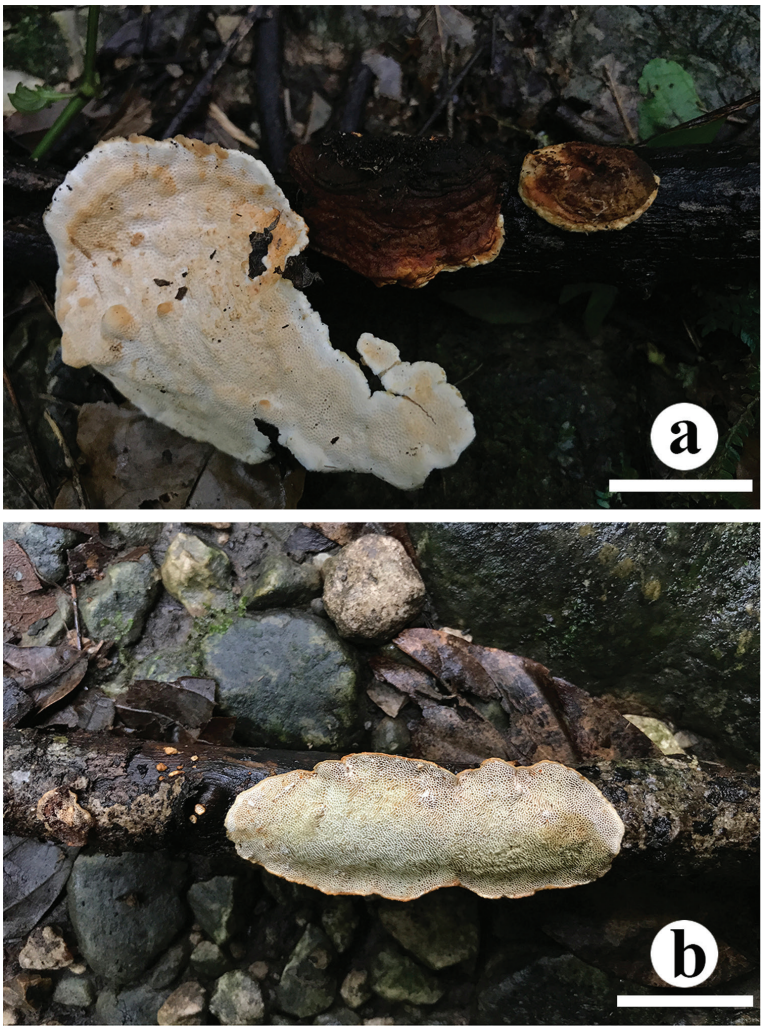

Figure 7. Basidiocarps of *Crassisporus macroporus*. Scale bars: 2 cm.

Holotype. CHINA. Guangxi Autonomous Region, Huanjiang County, Mulun Nature Reserve, on fallen angiosperm branch, 10 July 2017, Cui 14468 (BJFC).

Etymology. *Macroporus* (Lat.): referring to the large pores.

Description. Fruitbody: Basidiocarps annual, effused-reflexed to pileate, corky to leathery, without odor or taste when fresh, soft leathery upon drying. Pilei flabelliform, semicircular or elongated, projecting up to 1.5 cm, 4 cm wide and 5 mm thick at base; resupinate part up to 7 cm long, 4 cm wide, and 5 mm thick at center. Pileal surface buff to yellowish brown when fresh, becoming yellowish brown upon drying, finely velutinate, concentrically sulcate. Pore surface cream, buff to cinnamon-buff when fresh, becoming buff, pale yellowish brown to yellowish brown when dry; sterile margin distinct, buff to pale yellowish brown, up to 2 mm wide; pores round to angular,

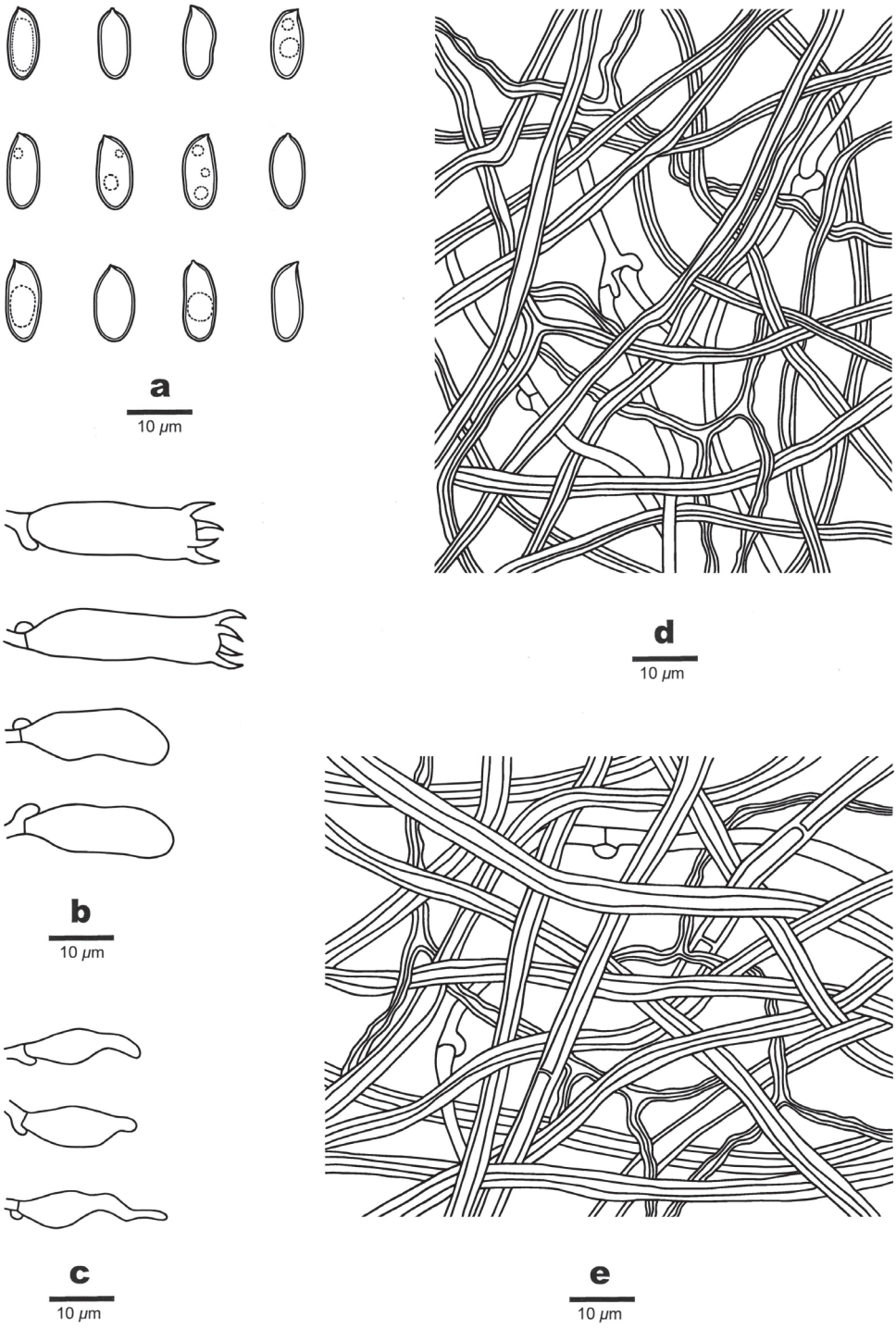

Figure 8. Microscopic structures of *Crassisporus macroporus* (drawn from the holotype) **A** basidiospores **B** basidia and basidioles **C** cystidioles **D** hyphae from trama **e** hyphae from context.

2–3 per mm; dissepiments thin, entire to lacerate. Context yellowish brown to pale yellowish brown, leathery, up to 1.5 mm thick. Tubes pale yellowish brown, corky, up to 2 mm long.

Hyphal structure: Hyphal system trimitic; generative hyphae bearing clamp connections; skeletal and binding hyphae IKI-, CB+; tissues turning to black in KOH.

Context: Generative hyphae infrequent, hyaline, thin-walled, unbranched, 1.5–3.5 μm in diam.; skeletal hyphae dominant, pale yellowish brown, thick-walled with a narrow lumen to subsolid, unbranched, more or less straight, interwoven, occasionally simple-septate, 2–5.5 μm in diam.; binding hyphae hyaline to pale yellowish brown, thick-walled with a narrow lumen to subsolid, flexuous, frequently branched, interwoven, 1–3 μm in diam.

Tubes: Generative hyphae infrequent, hyaline, thin-walled, occasionally branched, 1–2 μm in diam.; skeletal hyphae dominant, hyaline to pale yellowish brown, thick-walled with a narrow lumen to subsolid, occasionally branched, more or less straight, strongly interwoven, 1.5–3 μm in diam.; binding hyphae hyaline to pale yellowish brown, thick-walled with a narrow lumen to subsolid, flexuous, frequently branched, interwoven, 0.8–2 μm in diam. Cystidia absent, cystidioles fusoid, hyaline, thin-walled, 13–20 × 4.5–6 μm. Basidia clavate, bearing four sterigmata and a basal clamp connection, 17–28 × 7–8 μm; basidioles dominant, in shape similar to basidia, but smaller.

Spores: Basidiospores oblong ellipsoid, hyaline, smooth, slightly thick-walled, IKI-, CB-, 9.5–13.2(–14) × 4–6.2(–6.5) μm, L = 11.24 μm, W = 4.96 μm, Q = 2.26–2.31 (*n* = 60/2).

Type of rot. White rot.

Additional specimen (paratype) examined. CHINA. Guangxi Autonomous Region, Huanjiang County, Mulun Nature Reserve, on dead angiosperm tree, 10 July 2017, Cui 14465 (BJFC).

Crassisporus microsporus **B.K. Cui & Xing Ji, sp. nov.**
MycoBank: MB 828514
Figs 9, 10

Notes. *Crassisporus microsporus* is characterized by pileate basidiocarps, small pores (5–7 per mm), and small, broadly ellipsoid basidiospores (4–5 × 3–3.7 μm).

Holotype. CHINA. Yunnan Province, Ruili, Mori Tropical Rainforest Park, on living angiosperm tree, 17 September 2017, Cui 16221 (BJFC).

Etymology. *Microsporus* (Lat.): referring to the small basidiospores.

Description. Fruitbody: Basidiocarps annual, pileate, sessile, corky, without odor or taste when fresh, soft leathery to corky upon drying. Pilei semicircular, projecting up to 2 cm, 4 cm wide, and 4.5 mm thick at base. Pileal surface pale yellowish brown to yellowish brown, finely velutinate, concentrically sulcate. Pore surface cream, buff to cinnamon-buff when fresh, buff, pale yellowish brown to yellowish brown when dry; sterile margin distinct, buff, up to 1 mm wide; pores round to angular, 5–7 per mm;

Figure 9. Basidiocarps of *Crassisporus microsporus*. Scale bars: 1 cm.

dissepiments slightly thick, entire. Context pale yellowish brown to yellowish brown, leathery to corky when dry, up to 1.5 mm thick. Tubes concolorous with context, soft corky to corky, up to 3 mm long.

Hyphal structure: Hyphal system trimitic; generative hyphae bearing clamp connections; skeletal and binding hyphae IKI-, CB-; tissues turning to deep brown in KOH.

Context: Generative hyphae infrequent, hyaline, thin-walled, occasionally branched, 1.2–3.5 μm in diam.; skeletal hyphae dominant, hyaline to pale yellowish brown, thick-walled with a narrow lumen, rarely branched, straight, interwoven, occasionally simple-septate, 2.5–6 μm in diam.; binding hyphae hyaline to pale yellowish brown, thick-walled with a narrow lumen to subsolid, flexuous, frequently branched, interwoven, 0.8–2.5 μm in diam.

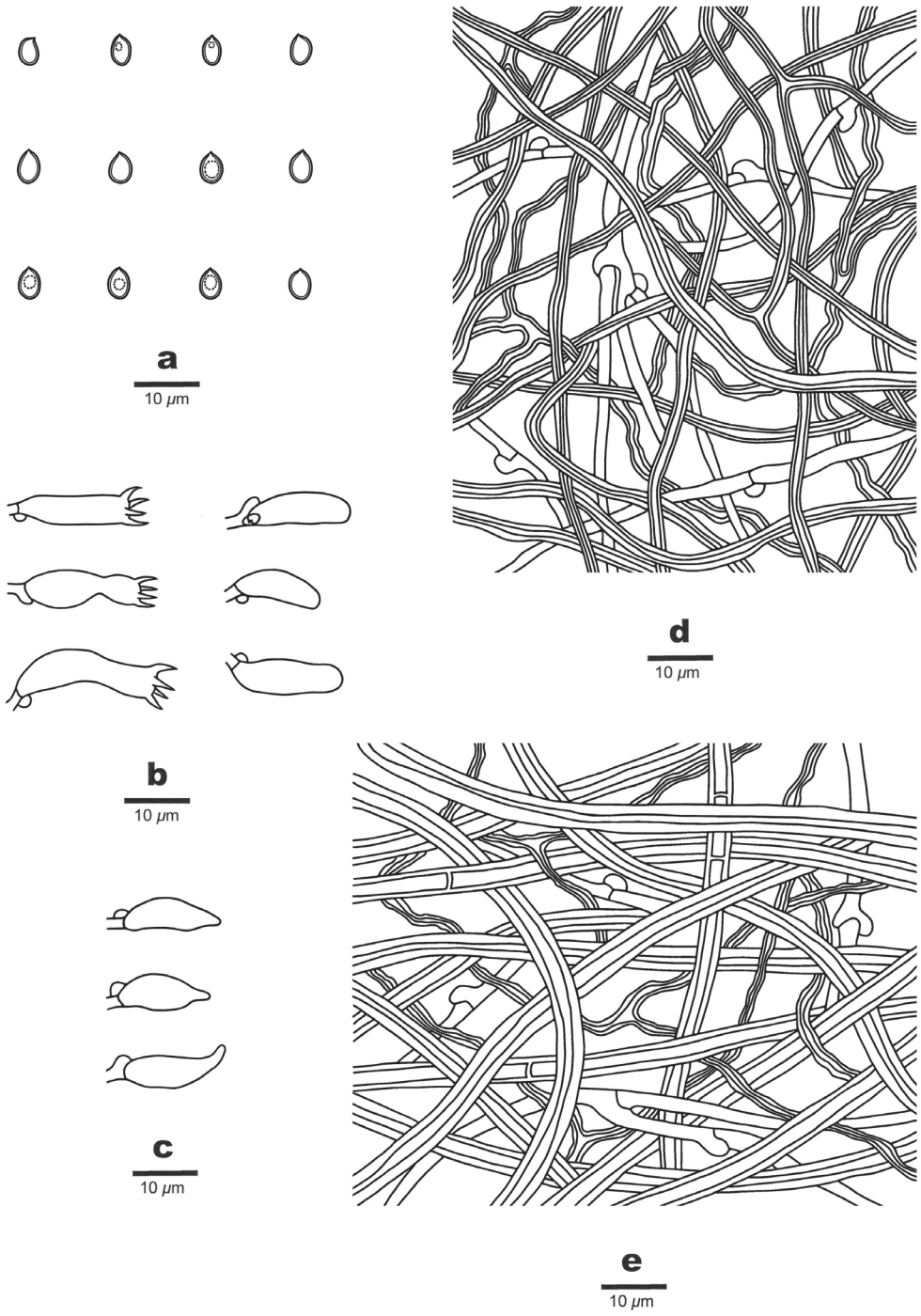

Figure 10. Microscopic structures of *Crassisporus microsporus* (drawn from the holotype) **A** basidiospores **B** basidia and basidioles **C** cystidioles **D** hyphae from trama **E** hyphae from context.

Tubes: Generative hyphae infrequent, hyaline, thin-walled, rarely branched, 1.2–3 μm in diam.; skeletal hyphae dominant, hyaline to pale yellowish brown, thick-walled with a narrow lumen to subsolid, moderately branched, more or less straight, strongly interwoven, 1.5–3 μm in diam.; binding hyphae hyaline to pale yellowish brown, thick-walled with a narrow lumen to subsolid, flexuous, frequently branched, interwoven, 0.8–2.5 μm in diam. Cystidia absent, cystidioles fusoid, hyaline, thin-walled, 12.5–18 × 4–5.5 μm. Basidia clavate, bearing four sterigmata and a basal clamp connection, 14–21 × 4.5–6 μm; basidioles in shape similar to basidia, but distinctly smaller.

Spores: Basidiospores broadly ellipsoid, hyaline, smooth, slightly thick-walled, IKI-, CB-, 4–5(–5.2) × (–2.8)3–3.7(–3.9) μm, L = 4.5 μm, W =3.23 μm, Q = 1.4 (*n* = 60/1).

Type of rot. White rot.

Discussion

In the present study, *Crassisporus* is proposed based on morphological characters and phylogenetic analyses. In the ITS+nLSU analysis, *Crassisporus* was nested in the core polyporoid clade with strong support (100% MP, 100% ML, 1.00 BPP; Fig. 1). A further study based on combined ITS+nLSU+mtSSU+EF1-α+RPB2 sequences data indicated that *Crassisporus* grouped with *Haploporus* with low support, but formed a monophyletic lineage with a strong support (100% MP, 100% ML, 1.00 BPP; Fig. 2). Morphologically, *Crassisporus* is characterized by the combination of an annual growth habit, effused-reflexed to pileate basidiocarps, pale yellowish brown to yellowish brown, concentrically zonate or sulcate pilei, velutinate pileal surface, a trimitic hyphal system with clamped generative hyphae, tissues turning to dark in KOH, oblong to broadly ellipsoid, hyaline, smooth and slightly thick-walled basidiospores.

Morphologically, the four *Crassisporus* species can be easily distinguished from each other. *Crassisporus microsporus* differs from other species by its small pores (5–7 per mm), and small broadly ellipsoid basidiospores (4–5 × 3–3.7 μm). Except for *C. imbricatus*, *C. leucoporus*, *C. macroporus*, and *C. microsporus*, all have fusoid cystidioles in the hymenium; moreover, *C. imbricatus* produces imbricate basidiocarps. Previously, the type specimen of *C. imbricatus* was identified as *Coriolopsis byrsina* (Mont.) Ryvarden based on morphological characters (Li and Cui 2010). After careful examination of the basidiospores along with DNA sequences analyses, the specimen was found to represent an unknown taxon. Here, we describe it as a new species of *Crassisporus* based on morphological characters and phylogenetic analysis. *Crassisporus macroporus* may be confused with *C. leucoporus* due to their similarity in effused-reflexed to pileate basidiocarps and oblong ellipsoid basidiospores, but *C. leucoporus* is distinguished from *C. macroporus* by its smaller pores (3–4 per mm), white pore surface when fresh, and acyanophilous skeletal and binding hyphae.

Phylogenetically, *Haploporus* groups together with *Crassisporus* (Figs 1, 2), but the former differs by its annual to perennial growth habit, dimitic to trimitic hyphal system, and ornamented, cyanophilous basidiospores (Shen et al. 2016; Cui et al. 2019).

Crassisporus is similar to *Hexagonia* Fr. and *Neofomitella* Y.C. Dai, Hai J. Li & Vlasák, because these genera share pileate brown basidiocarps, a trimitic hyphal system

with clamped generative hyphae, and tissues becoming dark in KOH. However, *Hexagonia* is distinguished from *Crassisporus* by its larger hexagonal pores and thin-walled basidiospores (Núñez and Ryvarden 2001). *Neofomitella* differs from *Crassisporus* in having crusted basidiocarps with the cuticle developing from base to margin, and smaller, thin-walled basidiospores (Li et al. 2014b).

Both *Perenniporia* Murrill and *Crassisporus* have hyaline and thick-walled basidiospores, but species of *Perenniporia* have cyanophilous, and variable dextrinoid skeletal hyphae. In addition, *Perenniporia* usually has truncate basidiospores (Gilbertson and Ryvarden 1987; Núñez and Ryvarden 2001; Zhao et al. 2013; Cui et al. 2019).

Truncospora Pilát is similar to *Crassisporus* in having pileate basidiocarps and variable presence of cystidioles. However, *Truncospora* is distinguished from *Crassisporus* by variable dextrinoid and cyanophilous skeletal hyphae and truncate, strongly dextrinoid basidiospores (Zhao and Cui 2013; Cui et al. 2019).

Abundisporus Ryvarden and *Crassisporus* share effused-reflexed or pileate basidiocarps, but *Abundisporus* differs by its pale-umber to deep-purplish-brown or greyish- to umber-brown context, dimitic hyphal system, and pale-yellowish basidiospores (Ryvarden 1998; Zhao et al. 2015; Cui et al. 2019).

Perenniporiella Decock & Ryvarden also has annual, pileate basidiocarps, and hyaline, thick-walled basidiospores, but it differs from *Crassisporus* in having a dimitic hyphal system (Decock and Ryvarden 2003).

Grammothelopsis Jülich is similar to *Crassisporus* in having thick-walled basidiospores; however, it differs from *Crassisporus* in its resupinate to effused basidiocarps with shallow irregular pores, and variable dextrinoid skeletal hyphae (Robledo and Ryvarden 2007; Zhao and Cui 2012).

Key to species of *Crassisporus*

1 Cystidioles absent ..... ***C. imbricatus***
– Cystidioles present **2**
2 Basidiospores broadly ellipsoid..... ***C. microsporus***
– Basidiospores oblong ellipsoid..... **3**
3 Pore surface cream, buff to cinnamon-buff when fresh, pores 2–3 per mm.... ..... ***C. macroporus***
– Pore surface white when fresh, pores 3–4 per mm..... ***C. leucoporus***

Acknowledgments

We express our gratitude to Drs Tom May (Royal Botanic Gardens Victoria, Australia) and Yu-Cheng Dai (Beijing Forestry University) for arrangement of and assistance during field collections. The research was financed by the National Natural Science Foundation of China (Project Nos. 31670016, 31870008) and Beijing Forestry University Outstanding Young Talent Cultivation Project (No. 2019JQ03016).

References

Chen JJ, Cui BK, Zhou LW, Korhonen K, Dai YC (2015) Phylogeny, divergence time estimation, and biogeography of the genus *Heterobasidion* (Basidiomycota, Russulales). Fungal Diversity 71: 185–200. https://doi.org/10.1007/s13225-014-0317-2

Chen YY, Wu F, Wang M, Cui BK (2017) Species diversity and molecular systematics of *Fibroporia* (Polyporales, Basidiomycota) and its related genera. Mycological Progress 16: 521–533. https://doi.org/10.1007/s11557-017-1285-1

Cui BK, Li HJ, Ji X, Zhou JL, Song J, Si J, Yang ZL, Dai YC (2019) Species diversity, taxonomy and phylogeny of Polyporaceae (Basidiomycota) in China. Fungal Diversity 97: 137–392. https://doi.org/10.1007/s13225-019-00427-4

Decock C, Ryvarden L (2003) *Perenniporiella* gen. nov. segregated from *Perenniporia*, including a key to Neotropical *Perenniporia* species with pileate basidiomes. Mycological Research 107 :93–103. https://doi.org/10.1017/S0953756202006986

Decock C, Stalpers J (2006) Studies in *Perenniporia*: *Polyporus unitus*, *Boletus medulla-panis*, the nomenclature of *Perenniporia*, *Poria* and *Physisporus*, and a note on European *Perenniporia* with a resupinate basidiome. Taxon 53: 759–778. https://doi.org/10.2307/25065650

Felsenstein J (1985) Confidence intervals on phylogenetics: an approach using bootstrap. Evolution 39: 783–791. https://doi.org/10.1111/j.1558-5646.1985.tb00420.x

Gilbertson RL, Ryvarden L (1987) North American Polypores. Vol. 2. Fungiflora, Oslo, 885 pp.

Hall TA (1999) Bioedit: a user-friendly biological sequence alignment editor and analysis program for Windows 95/98/NT. Nucleic Acids Symposium Series 41: 95–98.

Han ML, Chen YY, Shen LL, Song J, Vlasák J, Dai YC, Cui BK (2016) Taxonomy and phylogeny of the brown-rot fungi: *Fomitopsis* and its related genera. Fungal Diversity 80: 343–373. https://doi.org/10.1007/s13225-016-0364-y

Ji XH, Wu F (2017) *Pseudomegasporoporia neriicola* gen. et sp. nov. (Polyporaceae, Basidiomycota) from East Asia. Nova Hedwigia 105:435–443. https://doi.org/10.1127/nova_hedwigia/2017/0424

Katoh K, Standley DM (2013) MAFFT Multiple Sequence Alignment Software Version 7: Improvements in Performance and Usability. Molecular Biology and Evolution 30: 772–780. https://doi.org/10.1093/molbev/mst010

Kirk PM, Cannon PF, David JC, Minter DW, Stalpers JA (2008) Ainsworth and Bisby's Dictionary of the Fungi, 10th ed. CAB International Press, Wallingford, UK, 771 pp. https://doi.org/10.1079/9780851998268.0000

Li HJ, Cui BK (2010) Two species of polypores from Hainan new to China. Mycosystema 29: 824–827.

Li HJ, Cui BK (2013) Taxonomy and phylogeny of the genus *Megasporoporia* and its related genera. Mycologia 105: 368–383. https://doi.org/10.3852/12-114

Li HJ, Cui BK, Dai YC (2014a) Taxonomy and multi-gene phylogeny of *Datronia* (Polyporales, Basidiomycota). Persoonia 32: 170–182. https://doi.org/10.3767/003158514X681828

Li HJ, Li XC, Vlasák J, Dai YC (2014b) *Neofomitella polyzonata* gen. et sp. nov., and *N. fumosipora* and *N. rhodophaea* transferred from *Fomitella*. Mycotaxon 129: 7–20. https://doi.org/10.5248/129.7

Liu YL, Whelen S, Hall BD (1999) Phylogenetic relationships among Ascomycetes: evidence from an RNA polymerase II subunit. Molecular Biology and Evolution 16: 1799–1808. https://doi.org/10.1093/oxfordjournals.molbev.a026092

Maddison WP, Maddison DR (2017) Mesquite: a modular system for evolutionary analysis. Version 3.2. http://mesquiteproject.org

Matheny PB (2005) Improving phylogenetic inference of mushrooms with RPB1 and RPB2 nucleotide sequences (*Inocybe*, Agaricales). Molecular Phylogenetics and Evolution 35: 1–20. https://doi.org/10.1016/j.ympev.2004.11.014

Núñez M, Ryvarden L (2001) East Asian polypores 2. Polyporaceae s. lato. Synopsis Fungorum 14: 170–522.

Nylander JAA (2004) MrModeltest v2. Program distributed by the author. Evolutionary Biology Centre, Uppsala University.

Petersen JH (1996) Farvekort. The Danish Mycological Society's color chart. Foreningen til Svampekundskabens Fremme, Greve, 6 pp.

Posada D, Crandall KA (1998) Modeltest: testing the model of DNA substitution. Bioinformatics 14: 817–818. https://doi.org/10.1093/bioinformatics/14.9.817

Rehner SA, Buckley E (2005) A *Beauveria* phylogeny inferred from nuclear ITS and EF1-alpha sequences: evidence for cryptic diversification and links to *Cordyceps teleomorphs*. Mycologia 97: 84–98. https://doi.org/10.3852/mycologia.97.1.84

Robledo G, Ryvarden L (2007). The genus *Grammothelopsis* (Basidiomycota, aphyllophoroid fungi). Synopsis Fungorum 23: 7–12.

Ronquist F, Huelsenbeck JP (2003) Mrbayes 3: Bayesian phylogenetic inference under mixed models. Bioinformatics 19: 1572–1574. https://doi.org/10.1093/bioinformatics/btg180

Ryvarden L (1998) African polypores: a review. Paul Heinemann memorial symposium: systematics and ecology of the macromycetes. Belgian Journal of Botany 131: 150–155

Shen LL, Chen JJ, Wang M, Cui BK (2016) Taxonomy and multi-gene phylogeny of *Haploporus* (Polyporales, Basidiomycota). Mycological Progress 15: 731–742. https://doi.org/10.1007/s11557-016-1203-y

Shen LL, Wang M, Zhou JL, Xing JH, Cui BK, Dai YC (2019) Taxonomy and phylogeny of *Postia*. Multi-gene phylogeny and taxonomy of the brown-rot fungi: *Postia* (Polyporales, Basidiomycota) and related genera. Persoonia 42: 101–126. https://doi.org/10.3767/persoonia.2019.42.05

Song J, Cui BK (2017) Phylogeny, divergence time and historical biogeography of *Laetiporus* (Basidiomycota, Polyporales). BMC Evolutionary Biology 17: 102. https://doi.org/10.1186/s12862-017-0948-5

Stamatakis A (2006) RAxML-VI-HPC: maximum likelihood-based phylogenetic analyses with thousands of taxa and mixed models. Bioinformatics 22: 2688–2690. https://doi.org/10.1093/bioinformatics/btl446

Swofford DL (2002) PAUP*: phylogenetic analysis using parsimony (*and other methods). Version 4.0b10. Sinauer Associates, Sunderland, Massachusetts.

White TJ, Bruns T, Lee S, Taylor J (1990) Amplification and direct sequencing of fungal ribosomal RNA genes for phylogenetics. In: Innis MA, Gelfand DH, Sninsky JJ, White TJ (Eds) PCR Protocols: a Guide to Methods and Applications. Academic Press, San Diego, 315–322. https://doi.org/10.1016/B978-0-12-372180-8.50042-1

Zhao CL, Cui BK (2012) A new species of *Grammothelopsis* (Polyporales, Basidiomycota) from southern China. Mycotaxon 121: 291–296. https://doi.org/10.5248/121.291

Zhao CL, Cui BK (2013) *Truncospora macrospora* sp. nov. (Polyporales) from southwest China based on morphological and molecular data. Phytotaxa 87: 30–38. https://doi.org/10.11646/phytotaxa.87.2.2

Zhao CL, Cui BK, Dai YC (2013) New species and phylogeny of *Perenniporia* based on morphological and molecular characters. Fungal Diversity 58: 47–60. https://doi.org/10.1007/s13225-012-0177-6

Zhao CL, Chen H, Song J, Cui BK (2015) Phylogeny and taxonomy of the genus *Abundisporus* (Polyporales, Basidiomycota). Mycological Progress 14: 38. https://doi.org/10.1007/s11557-015-1062-y

Zhu L, Song J, Zhou JL, Si J, Cui BK (2019) Species diversity, phylogeny, divergence time and biogeography of the genus *Sanghuangporus* (Basidiomycota). Frontiers in Microbiology 10:812. https://doi.org/10.3389/fmicb.2019.00812

MycoKeys 57: 85–100 (2019)
doi: 10.3897/mycokeys.57.36416
http://mycokeys.pensoft.net

RESEARCH ARTICLE

A peer-reviewed open-access journal
MycoKeys
Launched to accelerate biodiversity research

Two new agaricoid species of the family Clavariaceae (Agaricales, Basidiomycota) from China, representing two newly recorded genera to the country

Ming Zhang[1], Chao-Qun Wang[1], Tai-Hui Li[1]

1 *State Key Laboratory of Applied Microbiology Southern China, Guangdong Provincial Key Laboratory of Microbial Culture Collection and Application & Guangdong Open Laboratory of Applied Microbiology, Guangdong Institute of Microbiology, Guangdong Academy of Sciences, Guangzhou 510070, China*

Corresponding author: *Tai-Hui Li* (mycolab@263.net)

Academic editor: *Zai-Wei Ge* | Received 22 May 2019 | Accepted 16 July 2019 | Published 21 August 2019

Citation: Zhang M, Wang C-Q, Li T-H (2019) Two new agaricoid species of the family Clavariaceae (Agaricales, Basidiomycota) from China, representing two newly recorded genera to the country. MycoKeys 57: 85–100. https://doi.org/10.3897/mycokeys.57.36416

Abstract

Two new lamellar species, *Camarophyllopsis olivaceogrisea* and *Hodophilus glaberripes*, of the family Clavariaceae were discovered in the subtropical zone of China. *Camarophyllopsis olivaceogrisea* is morphologically characterized by its hygrophanous basidiomata, greenish gray to dull green pileus, shortly decurrent lamellae, broadly elliptic basidiospores 4–5.5 × 3.5–4.5 µm in size, and cutis-like pileipellis composed of cylindrical cells. *Hodophilus glaberripes* is mainly characterized by its white to brownish pileus, glabrous stipe, slight yam bean smell, broadly elliptic basidiospores 5–6.5 × 4–5 µm in size, and epithelium-like pileipellis composed of inflated cells. Phylogenetic placement of the two species was determined by the combined analyses of a DNA data matrix containing ITS and LSU, and showed that collections of the two species formed two independent lineages in the *Camarophyllopsis* and *Hodophilus* clades respectively. The delimitation of *C. olivaceogrisea* and *H. glaberripes* were evaluated using molecular, morphological, and ecological methods. This is the first report of the genera *Camarophyllopsis* and *Hodophilus* in China.

Keywords

Camarophyllopsis, *Hodophilus*, phylogenetic analysis, subtropical zone, taxonomy

Introduction

Clavariaceae Chevall. (Agaricales, Basidiomycota) is a genetically monophyletic but morphologically diverse family. Members of this family show variations in the macromorphology of their sporocarps and are pendant-hydnoid, cylindrical, clavate, coralloid, resupinate, pileate, or lamellate-stipitate (Larsson et al. 2004; Dentinger and McLaughlin 2006; Matheny Curtis et al. 2006; Larsson 2007; Birkebak et al. 2013). Generally, Clavariaceae was known as a coral fungal group, including club-like (clavarioid) genera such as *Clavaria* Vaill. ex L., and *Clavulinopsis* Overeem, and branch-form (coralloid) genera, such as *Ramariopsis* (Donk) Corner (Birkebak et al. 2013, 2016). However, some agaricoid genera, such as *Camarophyllopsis* Herink, *Hodophilus* R. Heim ex R. Heim and *Lamelloclavaria* Birkebak & Adamčík, showed phylogenetic affinity within Clavariaceae (Matheny Curtis et al. 2006; Birkebak et al. 2013), thus have been added to the family based on phylogenetic analyses in recent years (Birkebak et al. 2016).

Camarophyllopsis can be easily distinguished from other genera in the family by its small agaricoid basidiomata, hygrophanous pileus, subglobose to broadly ellipsoidal basidiospores, and epithelium pileipellis composed of chains of erect, ascending or repent, subcylindrical to ellipsoid terminal cells (Arnolds 1986; Young 2005). *Hodophilus* differs from *Camarophyllopsis* in the hymeniderm pileipellis composed of typically perpendicular, broadly inflated, globose, and obpyriform to sphaero-pendunculate terminal elements (Birkebak et al. 2016). *Lamelloclavaria* can be distinguished from the above genera by its rimulose non-hygrophanous pileus and cutis pileipellis (Birkebak et al. 2016).

In this study, some agaricoid collections were identified in China. Morphological observation and phylogenetic analyses confirmed that they are two novel taxa in the genera *Camarophyllopsis* and *Hodophilus*. This is the first report of these two genera in China.

Materials and methods

Morphological studies

Photographs of basidiomata were taken in type localities when collected. Macro-morphological characteristics were recorded for fresh specimen. Specimens were dried and then deposited in the Fungal Herbarium of Guangdong Institute of Microbiology (GDGM). Methods used for morphological descriptions were followed Zhang et al. (2015). Colors were recorded and described in general terms according to the method of Kornerup and Wanscher (1978). Microstructures were observed from rehydrated materials, and the notation "basidiospores (n/m/p)" indicates that the measurements were conducted for n basidiospores from m basidiomata of p collections. Line drawings were prepared by free hand.

DNA extraction, PCR amplification, and sequencing

Total genomic DNA of each voucher specimen was extracted from silica-gel-dried materials using the Sangon Fungus Genomic DNA Extraction kit (Sangon Biotech, Shanghai, China) according to the manufacturer's instructions. Primer pairs ITS1/ITS4 (White et al. 1990) and LR0R/LR5 (Vilgalys and Hester 1990) were used to amplify the internal transcribed spacer (ITS) region and the large subunit nuclear ribosomal RNA (nrLSU) region, respectively. PCR protocol and sequencing were conducted following the method of Zhang et al. (2015).

Phylogenetic analyses

Newly generated sequences, related sequences used in previous studies (Adamčík et al. 2018) and a few sequences retrieved from GenBank by a Blast search were used to reconstruct phylogenetic trees. Detailed information on the newly sequenced samples, including the taxon names, voucher numbers, localities and GenBank accession numbers, is shown in Table 1.

ITS and LSU sequences were respectively aligned using Clustal X v1.81 (Thompson et al. 1997) and manually modified where necessary in Bioedit v7.0.9 (Hall 1999), and a combined matrix of ITS and LSU sequences was obtained. The combined dataset was then analyzed using RAxML v7.2.6 (Stamatakis 2006) and MrBayes v3.1.2 software (Ronquist and Huelsenbeck 2003) for maximum likelihood (ML) and Bayesian inference (BI) analyses, respectively. For both BI and ML analyses, the substitution model for the two gene partitions was individually determined using the Akaike Information Criterion (AIC) complemented in MrModeltest v2.3 (Nylander 2004). For ML analysis, all parameters were kept at default values, except for choosing the GTRGAMMAI model, and statistical support was obtained using rapid nonparametric bootstrapping with 1000 replicates. BI analysis using selected models and 4 chains was conducted by setting the number of generations to 3 million and stoprul com-

Table 1. Information on newly generated DNA sequences used in this study.

Taxon	Voucher	Country	ITS	LSU
Camarophyllopsis olivaceogrisea	GDGM44497	China	MK894563	MK894551
	GDGM44519	China	MK894564	MK894552
Camarophyllopsis sp.	GDGM44501	China	MK894565	MK894553
Hodophilus glaberripes	GDGM45940	China	MK894566	MK894554
	GDGM52374	China	MK894567	MK894555
	GDGM52530	China	MK894568	–
	GDGM52545	China	MK894569	MK894556
	GDGM52583	China	MK894570	MK894557
	GDGM55689	China	MK894571	MK894558
	GDGM70329	China	MK894572	MK894559
	GDGM70331	China	MK894573	MK894560
	GDGM72434	China	MK894574	MK894561
	GDGM72518	China	MK894575	MK894562

mand with the stopval value set to 0.01. Trees were sampled every 100 generations. The first 25% of generations were discarded as burn-ins and posterior probabilities (PP) were calculated from the posterior distribution of the retained Bayesian trees.

Results

Molecular phylogenetic results

For phylogenetic analyses, 25 sequences (13 ITS and 12 LSU) were newly generated from 13 collections, 219 related sequences (123 ITS and 96 LSU) were retrieved from GenBank, and *Ramariopsis corniculata* (Schaeff.) R.H. Petersen selected as an outgroup based on previous studies (Birkebak et al. 2016; Adamčík et al. 2016, 2018). The combined matrix of 137 samples with 1614 nucleotide sites was constructed for phylogenetic analyses and the final alignment was submitted to TreeBASE (Submission ID 24440). SYM+I and SYM+G were chosen as the best substitution models for ITS and LSU, respectively. The ML and BI analyses generated nearly identical tree topologies with minimal variation in statistical support values; thus, a ML tree was selected for display (Figure 1).

The tree topologies generated in this study are similar to those obtained by Adamčík et al. (2018) and are therefore not described in detail here, except for the results relevant to the two new species. The two monophyletic genera *Camarophyllopsis* and *Hodophilus* were highly supported (Figure 1). Two collections (GDGM44497 and GDGM44519) formed an independent lineage with strong statistical support (BS = 100, PP = 1), located within the *Camarophyllopsis* clade, and presented as a sister group to a collection numbered as GDGM44501 from China (with low statistical support). Ten collections (GDGM45940, GDGM52374, GDGM52530, GDGM52545, GDGM52583, GDGM55689, GDGM70329, GDGM70331, GDGM72434 and GDGM72518) were grouped together with strong statistical supports (BS = 100, PP = 1) and formed an independent lineage in the *Hodophilus* clade, and were revealed as a sister group to *H. indicus* K.N.A. Raj, K.P.D. Latha & Manim. with significant statistical support (BS = 100, PP = 1).

Taxonomy

Camarophyllopsis olivaceogrisea **Ming Zhang, C.Q. Wang & T.H. Li, sp. nov.**
MycoBank MB 831122
Figs 2a–b, 3

Etymology. The epithet "*olivaceogrisea*" refers to the olive-gray pileus color.

Diagnosis. This new species is morphologically distinguished from other taxa in the genus by its smaller basidiomata, greenish gray to dull green pileus, white and short decurrent lamellae, and broadly elliptic basidiospores.

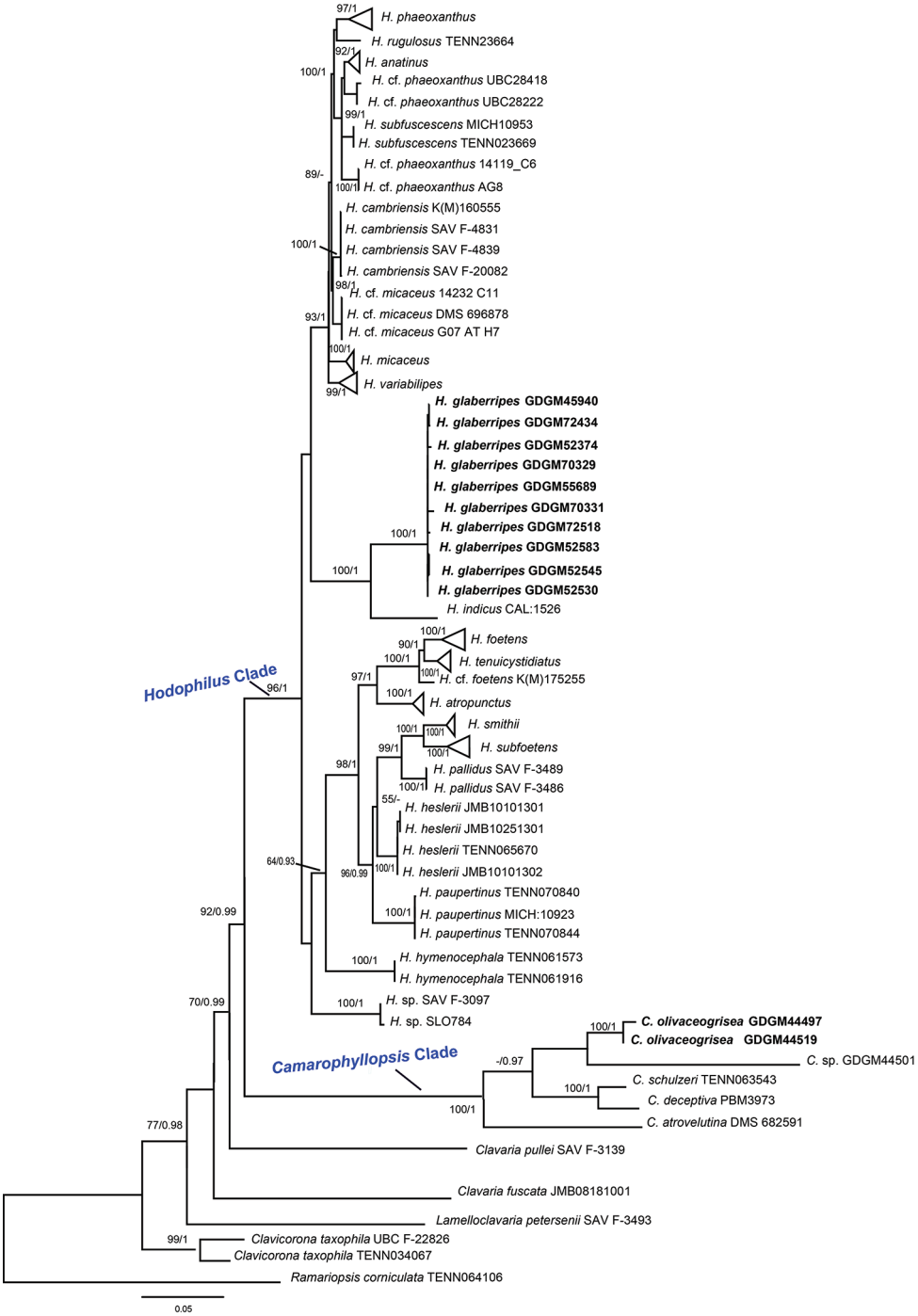

Figure 1. Phylogenetic placements of *Camarophyllopsis olivaceogrisea* and *Hodophilus glaberripes* inferred from the combined ITS and LSU dataset using RAxML. *Ramariopsis corniculata* was selected as an outgroup. The lineages with new species were shown in bold. BS ≥ 50% and PP ≥ 0.90 were indicated around the branches.

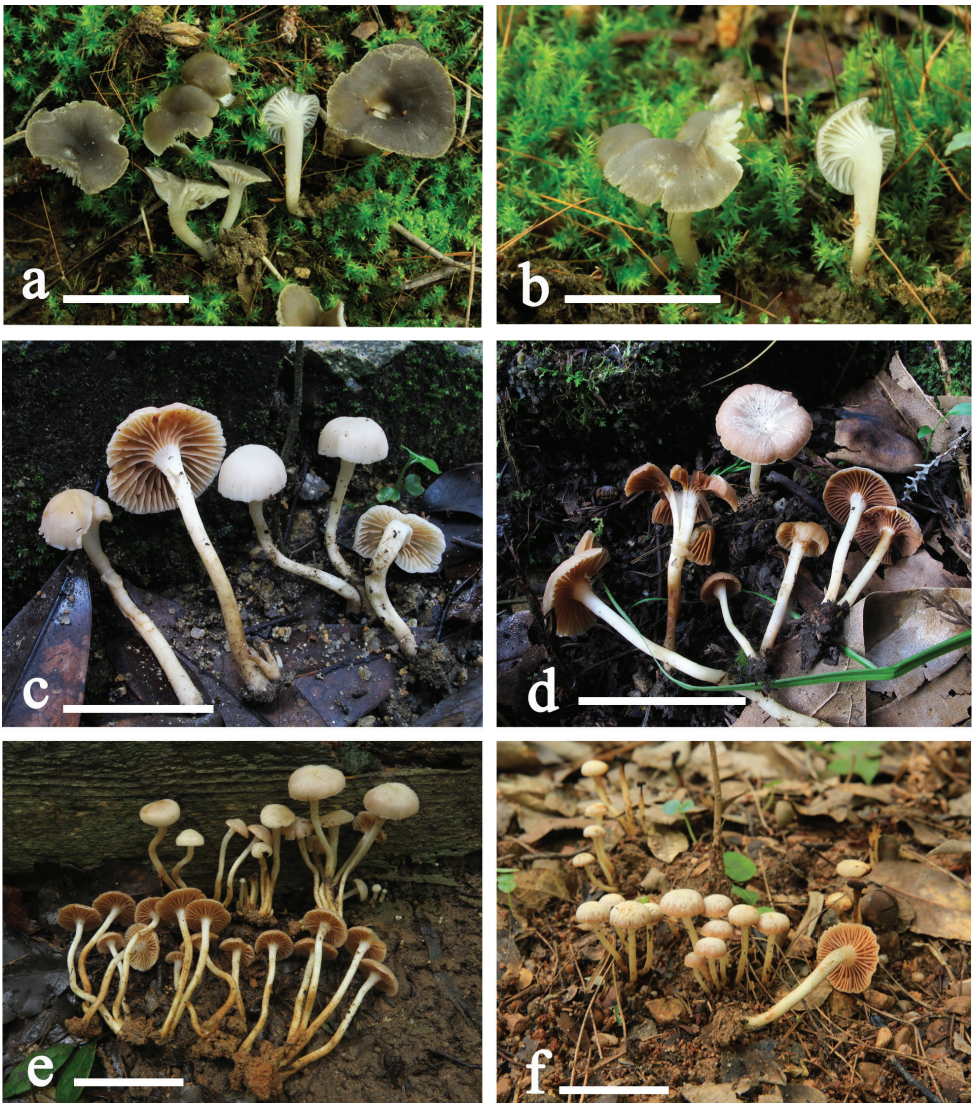

Figure 2. a, b Basidiomata of *Camarophyllopsis olivaceogrisea* (GDGM44519, holotype) **c–f** basidiomata of *Hodophilus glaberripes* (e. GDGM72518, holotype). Scale bars: 20 mm (**a, b**); 50 mm (**c–f**).

Type. CHINA. Guizhou Province: Leishan County, Leigongshan National Nature Reserve, alt. 1260 m, 22 July 2014, M. Zhang (holotype: GDGM44519!).

Description. Basidiomata small-sized. Pileus 7–12 mm broad, hemispherical, convex to plano-convex at first, then gradually applanate, becoming depressed at disc when mature, non-striate to weakly striate; margin slightly inflexed at first, soon straight, slightly crenate or lacerate when mature; surface matt, velvety, hygrophanous, greenish gray (or olive gray) to dull green (27D 2–30D2, 27D3–30D3, 27E2–30E2, 27E3–30E3), often paler at margin. Flesh 1–3 mm thick in the stipe, white to grayish

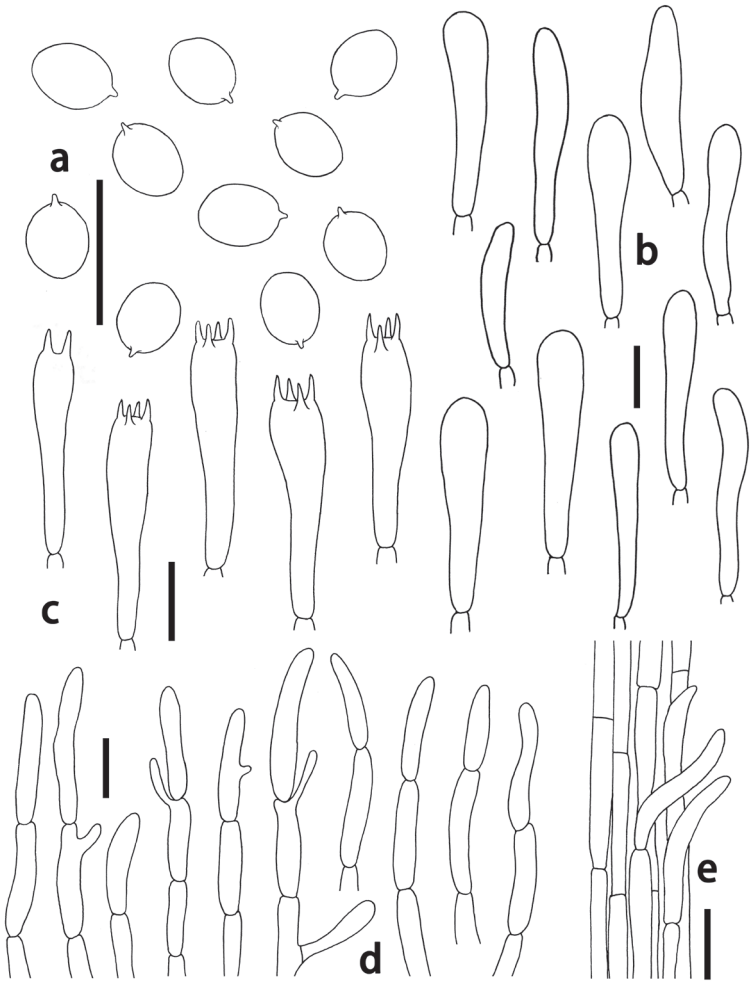

Figure 3. *Camarophyllopsis olivaceogrisea*. **a** Basidiospores **b** basidioles **c** Basidia **d** hyphal terminations in pileipellis **e** stipitipellis. Scale bars: 10 μm (**a–c**); 20 μm (**d, e**).

white, unchanging when exposed. Lamellae 1–2 mm deep, L = 20–34, l = 1–3, short to moderately decurrent, white to weakly grayish white (1A1–1B1) at first, white to weakly greenish white (27A2–30A2) when mature, unchanging when bruised; edge entire, concolorous with the sides. Stipe 13–25 × 1.5–2.5 mm, central, cylindrical and becoming narrower downwards; glabrous and shiny, hardly tomentulose or pruinose, hygrophanous, white to greenish white at first (28A1–28A2, 29A1–29A2), becoming greenish white to light greenish gray (28A2–28B2, 29A2–29B2) when mature and in dry condition. Odor none. Taste mild.

Basidiospores [60/2/2] 4–5.5(–6) × 3.5–4.5(–5) μm, av. 4.6 × 3.8 μm, Q = (1.12)1.14–1.28(1.43), av. Q = 1.21 ± 0.08, broadly ellipsoid, hyaline, smooth, inamyloid, thin-walled. Basidia 4-spored, occasionally 2-spored, (10–)15–26(–30) × 5–7 μm,

av. 24.5 × 5.8 μm, hyaline, narrowly clavate, attenuated and flexuous toward base, sterigmata up to 4 μm long. Basidioles cylindrical to narrowly clavate, often flexuous, obtuse, (18–)20–37.5(–40) × 6–8 μm, av. 23 × 6.8 μm. Pleurocystidia absent. Marginal cells on the lamellar edges not well differentiated, similar to basidioles on lamellar sides. Lamellar trama composed of sub-parallel or occasionally interwoven and irregularly inflated hyphae (23–)35–50(–104) × 4–8(–10) μm, av. 46.5 × 7 μm. Pileipellis a cutis of numerous repent branched hyphal 4–8 μm wide, with terminal chains of ellipsoid or cylindrical cells. Pileus trama composed of cylindrical and occasionally branched hyphae (23–)35–50(–70) × (4–)6–10 μm, av. 45.5 × 7.6 μm. Stipitipellis formed of parallel, thin-walled and narrow hyphae 3–8 μm diam. Caulocystidia not observed. Clamp connections absent in all tissues.

Habit, ecology and distribution. Solitary, scattered on soil in mixed forests; currently only known from the Guizhou Province of China.

Additional specimens examined. CHINA. Guizhou Province: Leishan County, Leigongshan National Nature Reserve, alt. 1120 m, 22 July 2014, J. Xu (GDGM44497).

Hodophilus glaberripes Ming Zhang, C.Q. Wang & T.H. Li, sp. nov.

MycoBank MB 831125
Figs 2c–f, 4

Etymology. The epithet refers to the glabrous stipe.

Diagnosis. This species is easily distinguished from other species in the genus *Hodophilus* by its larger basidiomata, white, brownish orange to brown pileus, glabrous stipe, slightly yam bean smell and broadly elliptic basidiospores.

Type. CHINA. Guangdong Province: Shaoguan City, Danxiashan National Nature Reserve, alt. 240 m, 10 May 2018, M. Zhang (holotype: GDGM72518!).

Description. Basidiomata small to medium-sized. Pileus 15–50 mm broad, hemispherical, convex to plano-convex at first, then becoming broadly convex or plano-convex but hardly fully expanded to plane, often depressed at disc when old; white to yellowish white at first, then gradually becoming orange white, pale yellow, pale orange, brownish orange, light brown, brown to reddish brown (5A2, 3A3–5A3, 5C4–7C4, 5D5–9D5) when mature and dry, hygrophanous; margin first slightly inflexed, soon straight, slightly crenate when mature, non-striate or indistinctly translucently striate up to one third when wet; surface matt, velvety and later with fine and darker granules or pruina, at first even, but becoming rugose or rough towards the center when mature, often concentrically cracked in dry conditions. Flesh 0.5–2 mm thick in half radius of the pileus, white, pinkish white to pale beige; Lamellae 3–5 mm deep, distant to subdistant, L = 21–32, l = 1–3, short decurrent, notched, orange white to pinkish white (5A2–10A2) when young, brownish orange, light brown, reddish brown to brownish red (5C4–7C4, 5D6–10D6) when mature, unchanging when bruised; edge entire, concolorous or slightly paler than lamella sides. Stipe (50) 80–100 × 3–5 mm, cental, usually flexuous, cylindrical and slightly

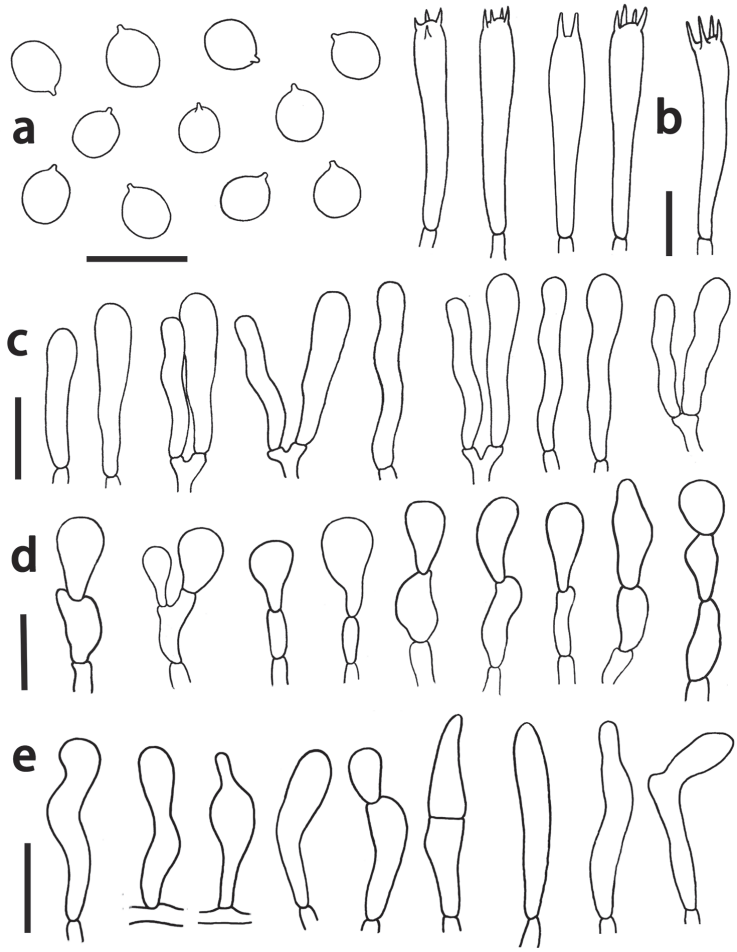

Figure 4. *Hodophilus glaberripes*. **a** Basidiospores **b** basidia **c** basidioles **d** hyphal terminations in pileipellis e hyphal terminations in stipitipellis. Scale bars: 10 μm (**a–c**); 20 μm (**d, e**).

narrower downwards; glabrous smooth and shiny, hygrophanous, white to yellowish white at first, becoming pale yellow to pale orange when mature and in dry condition. Odor none or slight yam bean smell, taste mild.

Basidiospores [210/9/9] (4.5)5–6.5(7) × 4–5(5.5) μm, av. 5.9 × 4.7 μm, Q = (1.0)1.11–1.37(1.4), av. Q = 1.20 ± 0.11, broadly ellipsoid to subglobose, hyaline, smooth, inamyloid, thin-walled. Basidia 4-spored, occasionally 2-spored, (32–)36–46(–66) × (4–)4.5–6(–7) μm, av. 39.5 × 5.9 μm, tenuated and flexuous towards base, with sterigmata up to 7 μm long. Basidioles cylindrical to narrowly clavate, obtuse, often flexuous, (31–)34–42(–60) × (4–)6–8(–10) μm, av. 40.5 × 6.9 μm. Pleurocystidia absent. Marginal cells on the lamellar edges usually not well differentiated, similar to basidioles on lamellar sides. Lamellar trama composed of sub-parallel or occasionally interwoven and irregularly inflated branched hyphae with elongate cells

(38–)52–98(–160) × (4–)6–14(–20) µm, av. 88 × 9.5 µm. Subhymenium poorly developed. Pileipellis a transition from hymeniderm to epithelium, with hyphal elements 3–10 µm wide, thin-walled, hyaline, terminations usually composed of 1–3 inflated cells; terminal cells obpyriform, subglobous or ellipsoid, rarely sphaero-pedunculate or broadly clavate, (15–)19–46(–50)× (7–)12–22(–30) µm, av. 38.5 × 18 µm. Pileus trama composed of subparallel hyphae (34–)46–89(–130) × (4–)5.5–10 µm, av. 74 × 7.6 µm. Stipitipellis formed of parallel, thin-walled and narrow hyphae 3–6 µm diam. Caulocystidia usually in dense fascicles or patches, thin-walled, repent or ascending; with terminal cells mainly clavate, occasionally subcapitate or obpyriform, obtuse, often pedicellate and flexuous, measuring (18–)22–53(–60)× (4–)5.5–13 µm, av. 43 × 7.5 µm. Clamp connections absent in all tissues.

Habit, ecology and distribution. Solitary, scattered on soil in broadleaf forests and mixed forests; currently only known from China.

Additional specimens examined. CHINA. Guangdong Province: Huizhou City, Xiangtoushan National Nature Reserve, alt. 640 m, 18 May 2016, H. Huang (GDGM45940); Shaoguan City, Nanling National Nature Reserve, 800 m, 29 July 2017, M. Zhang (GDGM70329 and GDGM70331); Shaoguan City, Danxiashan National Nature Reserve, 200 m, 27 April 2019, X.R. Zhong (GDGM76367 and GDGM76337), J.P. Li (GDGM76300); Jiangxi Province: Jinggangshan Botanical Garden, 884 m, 20 June 2016, H. Huang (GDGM52374), Z.P. Song (GDGM52545); same location, 21 June 2016, Z.P. Song (GDGM52530 and GDGM52583); Hunan Province: Chenzhou City, Jiulongjiang National Forest Park, alt. 230 m, 14 May 2018 X. R. Zhong (GDGM55689).

Discussion

Key to the species of *Camarophyllopsis* and *Hodophilus*

1 Basidiomata agaricoid; pileipellis an epithelium composed of chains of subcylindrical to ellipsoid terminal elements ..... **2 *Camarophyllopsis***
– Basidiomata agaricoid; pileipellis a hymeniderm composed of broadly inflated, globose, and obpyriform to sphaero-pendunculate terminal elements ..... **12 *Hodophilus***
2 Pileus diameter usually < 30 mm..... **3**
– Pileus diameter usually ≥ 30 mm..... **11**
3 Pileus hygrophanous or subhygrophanous..... **4**
– Pileus not hygrophanous..... **5**
4 Pileus greenish gray to dull green; lamellae white, decurrent; basidiospores 4–5.5 × 3.5–4.5 µm..... ***C. olivaceogrisea***
– Pileus rugulose, buffy brown to dark hazel; lamellae decurrent, pinkish to hazel; stipe olive brown or grayer; basidiospores globose av. 4 × 5 µm..... ***C. rugulosoides***

5 Lamellae always with pink tinct, pale pink to pink, decurrent; pileus pale pink to whitish, matt; stipe pale pink to whitish; basidiospores av. 7 × 4.5 µm .... ***C. roseola***
– Lamellae without pink tinct **6**
6 Lamellae white, unchanging when mature **7**
– Lamellae whitish to grayish or brownish **9**
7 Basidiospores < 6 µm; pileus brownish to dark brown, subtomentosus, depress in central when mature; stipe concolorous with pileus or slightly faded .... ***C. atrovelutina***
– Basidiospores usually ≥ 6 µm..... **8**
8 Pileus gray, manifestly cleaving at margin when dry; stipe white; basidiospores 5.5–8.5 × 4–5.5 µm ..... ***C. leucopus***
– Pileus gray, sub-velvety; stipe pale gray; basidiospores 7–8 × 5.5–6.5 µm .... ***C. tetraspora***
9 Basidiospores ≥ 7 µm; pileus fuliginous brown, subfibrillose to fibrillose, infundibuliform; lamellae deep decurrent; stipe brown..... ***C. araguensis***
– Basidospores < 7 µm **10**
10 Pileus dark brown, subtomentosus; lamellae light grayish, decurrent; stipe white, smooth, basidiospores 5–6.5 × 4–5 µm ..... ***C. albipes***
– Pileus yellowish cinnamon to brownish cinnamon or chocolate gray, silky-tomentose or velvet; lamellae decurrent, whitish to grayish or brownish; stipe concolorous with pileus; basidiospores 4–5 × 4–4.5 µm ..... ***C. schulzeri***
11 Pileus brownish gray to grayish brown; lamellae adnate to subdecurrent, white; stipe smooth, white; basidiospores 5–7 × 3.5–4.5 µm ..... ***C. pedicellata***
– Pileus pearl gray to drab, often rivulose-cracking; lamellae light gray; stipe light gray, slightly longitudinally fibrillose-striped; basidiospores 5–7 × 3.5–5.2 µm.... ..... ***C. dennisiana***
12 Basidiomata with a napthalene or an unpleasant odor..... ..... **see Adamčík et al. (2016, 2017)**
– Basidiomata without napthalene odor..... **13**
13 Stipe with dark dots on surface **14**
– Stipe never with dark dots on surface..... **16**
14 Lamellae white to grayish white, pileus pale brown; basidiospores 4.5–6 × 4.0–5 µm, pileipellis an epithelium composed of globose to pyriform elements .... ***'C. kearneyi'***
– Lamellae with orange, brown or light brown tinct..... **15**
15 Pileus yellowish gray to brown when fresh, light brown, orange gray to beige when mature; lamellae beige or orange gray at first, changing to brownish orange to yellowish brown when mature, basidiospores 4.6–5.4 × 3.5–4.2 µm ... ***H. atropunctus***
– Pileus dark brown to pale brown; lamellae light brown to grayish brown when young, changing brown to dark brown when mature; basidiospores 4.8–5.4 × 3.9–4.5 µm ..... ***H. variabilipes***
16 Stipe with yellow tinct..... **see Adamčík et al. (2018)**
– Stipe without yellow tinct **17**

17 Species has south hemisphere distribution, pileus creamy buff-brown or pinkish fawn; lamellae decurrent, pale pinkish; basidiosproes 4.5–6.0 × 4.5–5.5 μm; pileipellis an epithelium of globose or pyriform elements; known from Australia ..... ***'C. darminensis'***

– Species has north hemisphere distribution..... **18**

18 Pileus yellowish white, brownish orange to reddish brown; lamellae orange white to brownish red; basidiospores 5–6.5 × 4–5 μm; known from China ..... ***H. glaberripes***

– Pileus grayish brown to brownish orange; lamellae subdecurrent, pale orange; stipe grayish orange, glabrous; basidiospores 4–5 × 3–5 μm; known from India.. ***H. indicus***

Phylogenetic relationships of the genera within Clavariaceae have been investigated in several studies, and *Camarophyllopsis* and *Hodophilus* were well supported as two independent groups at generic level (Birkebak et al. 2013, 2016; Adamčík et al. 2017, 2018). In the present study, phylogenetic analyses based on ITS and LSU showed that the two clades *Camarophyllopsis* and *Hodophilus* were well supported with high phylogenetic values (BS/BPP = 100/1), and collections from China formed two strongly supported terminal branches in the two clades. The sequences generated in this study did not match any previously described sequences, validating with strong support the recognition of *C. olivaceogrisea* and *H. glaberripes* as two distinct species based on their phenotypic features.

According to the phylogram (Figure 1), *C. olivaceogrisea* nested well into the *Camarophyllopsis* clade and formed a sister group of an unidentified Chinese collection (GDGM44501) with low statistical support. Because of the low number of specimens, GDGM44501 was not described here, but it can be easily separated from *C. olivaceogrisea* by branch distance. The other three species in the phylogenetic tree, *C. atrovelutina*, *C. deceptive* and *C. schulzeri*, also can be easily separated from *C. olivaceogrisea*. The closest relatives of the new species remain unresolved in this study because of the lack of significant statistical supports and the few available sequences of *Camarophyllopsis* used in phylogenetic analysis.

In the *Hodophilus* clade, *H. glaberripes* is closely related to *H. indicus* K.N.A. Raj, K.P.D. Latha & Manim., and together formed a well-supported branch, which is a sister clade to the yellow stipe clade (or *H. micaceus* superclade) as defined by Adamčík et al. (2017, 2018), but with limited statistical support. However, the recently described Indian species, *H. indicus*, show smaller and brownish orange basidiomata, subdecurrent and pale orange lamellae, and slightly smaller basidiospores (4–5 × 3–5 μm) (Crous et al. 2017).

Morphologically, the most distinctive features of *C. olivaceogrisea* are the small basidiomata with a greenish gray to dull green pileus, white and decurrent lamellae, broadly ellipsoid basidiospores, narrowly clavate basidia, and a cutis pileipellis composed of chains of cylindrical cells. *Camarophyllopsis microspora* (A.H. Sm. & Hesler) Bon is similar to *C. olivaceogrisea* to some extent. However, *C. microspora*, originally

reported in Michigan, differs on account of its fuscous pileus and stipe, dark grayish context and smaller basidiospores (4–4.5 × 2.5–3 μm) (Hesler and Smith 1963). Considering species with a pileus diameter of 10–30 mm, *C. olivaceogrisea* is similar to *C. albipes* and *C. leucopus* (Singer) Boertm. However, *C. albipes* mainly differs on account of its brown and subtomentose pileus, grayish lamellae with slight veins at the margin, robust stipe, and slightly larger basidiospores (5–6.5 × 4–5 μm) (Singer 1973); *C. leucopus* mainly differs on account of its gray and sulcate pileus and larger basidiospores (5–8.5 × 4–5.5 μm) (Singer 1973).

Hodophilus glaberripes is characterized by its larger basidiomata, hygrophanous pileus with white, brownish orange to brown color, glabrous stipe, larger and broadly elliptic basidiospores, epithelium-like pileipellis with obpyriform or subglobous terminal cells, and slightly yam bean smell. The combination of these characteristics makes *H. glaberripes* easily distinguishable from other members of the genus. *Hodophilus glaberripes* is somewhat similar to *H. alboffloccipes* (Kovalenko, E.F. Malysheva & O.V. Morozova) Looney and Adamčík, *H. anatinus* Dima, Adamčík & Jančovičová, *H. subfoetens* Adamčík, Jančovičová & Looney, and *H. pallidus* Adamčík, Jančovičová & Looney in morphology. However, *H. alboffloccipes* mainly differs by its smaller baisdiomata, ochre or ochre yellow to pale olives pileus, yellow to brownish stipe covered with white pruina or squamula, smaller basidiospores (4–5.7 × 3.5–5 μm), and naphthalene-like odor (Kovalenko et al. 2012); *H. anatinus* differs by its smaller basidiomata, grayish brown pileus, grayish yellow to brown stipe, and smaller basidiospores (4.8–5.5 × 3.8–4.4 μm) (Adamčík et al. 2018); *H. subfoetens* differs by its smaller and grayish brown to brownish black basidiomata, with a naphthalene odor, and smaller basidiospores (5–5.7 × 3.9–4.5 μm) (Adamčík et al. 2017a); *H. pallidus* differs by its smaller basidiomata with a strong naphthalene odor, orange-gray to grayish orange pileus, orange gray to orange brown stipe, and smaller basidiospores (5.1–5.7 × 3.9–4.6 μm) (Adamčík et al. 2017a).

Ecologically, very little is known about the ecology of *Camarophyllopsis* species, as for most species only a few verified collections are known and little molecular data is available. *Camarophyllopsis* species are widely distributed in the southern and northern hemispheres, from tropical zones to cool temperate zones, and in monsoon forest, bushy forest, and grassland habitats, and some species have been shown to be saprotrophic (Young 1999, 2005; Boertmann 2002; Kovalenko et al. 2012). *Camarophyllopsis olivaceogrisea* was collected from subtropical regions in southwest China at altitudes of over 1000 m, and is typically found in wet areas with moss under mixed forest, which is mainly dominated by broadleaf plants (*Castanopsis* spp., *Fagus* spp. and *Schima* spp.) with few conifer (*Pinus massoniana* Lamb. and *Pinus* spp.). This study expands the geographic distribution of the genus *Camarophyllopsis* to China.

Hodophilus taxa were mainly reported in temperate to boreal zones of the northern hemisphere and can be found in forest, bushy forest margin, grassland and bare soil habitats (Adamčík et al. 2016, 2017a, 2017b, 2018), and a recent study reported a new tropical distribution in India (Crous et al. 2017). In this study, collections of *H. glaberripes* were distributed from 23°N to 26°N in the subtropical zone of southern

China and at altitudes of 200–800 m, mostly occurred in the margin of broadleaf forest (mainly dominated by Fagaceae, Hamamelidaceae and Theaceae plants) and mixed forest (dominated by broadleaf tree mixed with few conifer as *Pinus massoniana* Lamb., *Pinus* spp. and *Cunninghamia* spp.), commonly along the sides of cement road in the forest and preferentially in heavy clay soil to humus. This study revealed an expanded geographic distribution of *Hodophilus* species to subtropical regions.

Acknowledgments

Sincere acknowledgements are expressed to Dr. J. Xu, Mr. H. Huang, J.P. Li, Z.P. Song, X.R. Zhong and S.H. Zhou (Guangdong Institute of Microbiology, China) for their kind help during the field trips. This study was supported by the National Natural Science Foundation of China (Nos. 31700021, 31770014, 31670029), the Science and Technology Project of Guangdong Province (2017A030303050, 2018B030324001) and the GDAS' Special Project of Science and Technology Development (2019GDASYL-0104009).

References

Adamčík S, Dima B, Adamčíková K, Harries D, Læssøe T, Moreau PA, Jančovičová S (2018) European *Hodophilus* (Clavariaceae, Agaricales) species with yellow stipe. Mycological Progress 17: 1097–1111. https://doi.org/10.1007/s11557-018-1418-1

Adamčík S, Jančovičová S, Looney BP, Adamčíková K, Birkebak JM, Moreau PA, Vizzini A, Matheny PB (2017a) Circumscription of species in the *Hodophilus foetens* complex (Clavariaceae, Agaricales) in Europe. Mycological Progress 16: 47–62. https://doi.org/10.1007/s11557-016-1249-x

Adamčík S, Jančovičová S, Looney BP, Adamčíková K, Griffith GW, Læssøe T, Moreau PA, Vizzini A, Matheny PB (2017b) *Hodophilus* (Clavariaceae, Agaricales) species with dark dots on the stipe: more than one species in Europe. Mycological Progress 16: 811–821. https://doi.org/10.1007/s11557-017-1318-9

Adamčík S, Looney BP, Birkebak JM, Jančovičová S, Adamčíková K, Marhold K, Matheny PB (2016) Circumscription of species of *Hodophilus* (Clavariaceae, Agaricales) in North America with naphthalene odours. Botany 94: 941–956. https://doi.org/10.1139/cjb-2016-0091

Arnolds E (1986) Notes on Hygrophoraceae – VII. On the taxonomy and nomenclature of some species of *Hygrophorus*. Persoonia 13: 69–76.

Birkebak JM, Adamčík S, Matheny PB (2016) Multilocus phylogenetic reconstruction of the Clavariaceae (Agaricales) reveals polyphyly of the agaricoid members. Mycologia 108: 860–868. https://doi.org/10.3852/15-370

Birkebak JM, Mayor JR, Ryberg M, Matheny PB (2013) A systematic, morphological, and ecological overview of the Clavariaceae (Agaricales). Mycologia 105: 896–911. https://doi.org/10.3852/12-070

Boertmann D (2002) Index Hygrocybearum. A catalogue to names and potential names in tribus Hygrocybeae Kühner (Tricholomatales, Fungi). Bibliotheca Mycologica 192: 1–168.

Crous PW, Wingfield MJ, Burgess TI, Hardy GEStJ, Barber PA, Alvarado P, Barnes CW, Buchanan PK, Heykoop M, Moreno G, Thangavel R, van der Spuy S, Barili A, Barrett S, Cacciola SO, Cano-Lira JF, Crane C, Decock C, Gibertoni TB, Guarro J, Guevara-Suarez M, Hubka V, Kolařík M, Lira CRS, Ordoñez ME, Padamsee M, Ryvarden L, Soares AM, Stchigel AM, Sutton DA, Vizzini A, Weir BS, Acharya K, Aloi F, Baseia IG, Blanchette RA, Bordallo JJ, Bratek Z, Butler T, Cano-Canals J, Carlavilla JR, Chande J, Cheewangkoon R, Cruz RHSF, da Silva M, Dutta AK, Ercole E, Escobio V, Esteve-Raventós F, Flores JA, Gené J, Góis JS, Haines L, Held BW, Horta Jung M,Hosaka K, Jung T, Jurjević Ž, Kautman V, Kautmanova I, Kiyashko AA, Kozanek M, Kubátová A, Lafourcade M, La Spada F, Latha KPD, Madrid H, Malysheva EF, Manimohan P, Manjón JL, Martín MP, Mata M, Merényi Z, Morte A, Nagy I, Normand AC, Paloi S, Pattison N, Pawłowska J, Pereira OL, Petterson ME, Picillo B, Raj KNA, Roberts A, Rodríguez A, Rodríguez-Campo FJ, Romański M, Ruszkiewicz-Michalska M, Scanu B, Schena L, Semelbauer M, Sharma R, Shouche YS, Silva V, Staniaszek-Kik M, Stielow JB, Tapia C, Taylor PWJ, Toome-Heller M, Vabeikhokhei JMC, van Diepeningen AD, Van Hoa N, Van Tri M, Wiederhold NP, Wrzosek M, Zothanzama J, Groenewald JZ (2017) Fungal Planet description sheets: 558–624. Persoonia 38: 240–384. https://doi.org/10.3767/003158517X698941

Dentinger BTM, McLaughlin DJ (2006) Reconstructing the Clavariaceae using nuclear large subunit rDNA sequences and a new segregate genus from *Clavaria*. Mycologia 98:746–762. https://doi.org/10.1080/15572536.2006.11832646

Hesler LR, Smith AH (1963) North American species of *Hygrophorus*. The University of Tennessee Press, Knoxville, 1–416. https://doi.org/10.5962/bhl.title.61976

Kornerup A, Wanscher JH (1978) Methuen Handbook of Colour. Eyre Methuen: London, 1–252.

Kovalenko AE, Malysheva EF, Morozova OV (2012) The genus *Camarophyllopsis* in Russia: new records and new species *C. alboflоccipes*. Mikologiya I Fitopatologiya 43(1): 54–66. [in Russian]

Larsson KH (2007) Re-thinking the classification of corticioid fungi. Mycological Research 111: 1040–1063. https://doi.org/10.1016/j.mycres.2007.08.001

Larsson KH, Larsson E, Kóljalg U (2004) High phylogenetic diversity among corticioid homobasidiomycetes. Mycological Research 108: 983–1002. https://doi.org/10.1017/S0953756204000851

Matheny Curtis JM, Hofstetter V, Aime MC, Moncalvo JM, Ge ZW, Yang ZL, Slot JC, Ammirati JF, Baroni TJ, Bougher NL, Hughes KW, Lodge DJ, Kerrigan RW, Seidl MT, Aanen DK, DeNitis M, Daniele G, Desjardin DE, Kropp BR, Norvell LL, Parker A, Vellinga EC, Vilgalys R, Hibbett DS (2006) Major clades of Agaricales: a multilocus phylogenetic overview. Mycologia 98: 982–995. https://doi.org/10.1080/15572536.2006.11832627

Nylander JAA (2004) MrModeltest v2. Program distributed by the author. Evolutionary Biology Centre. Uppsala University, Uppsala.

Ronquist F, Huelsenbeck JP (2003) MrBayes 3: bayesian phylogenetic inference under mixed models. Bioinformatics 19:1572–1574. https://doi.org/10.1093/bioinformatics/btg180

Singer R (1973) Diagnoses fungorum novorum Agaricalium III. Beihefte zur Sydowia. 7: 1–106.

Stamatakis A (2006) RAxML-VI-HPC: maximum likelihood-based phylogenetic analyses with thousands of taxa and mixed models. Bioinformatics 22: 2688–2690. https://doi.org/10.1093/bioinformatics/btl446

Tamura K, Peterson D, Peterson N, Stecher G, Nei M, Kumar S (2011) MEGA5: molecular evolutionary genetics analysis using maximum likelihood, evolutionary distance, and maximum parsimony methods. Molecular biology and Evolution 28: 2731–2739. https://doi.org/10.1093/molbev/msr121

Thomson JD, Gibson TJ, Plewnlak F, Jianmougin F, Higgins DG (1997) The Clustal X windows interfaces: flexible strategies for multiple sequence alignment aided by quality analysis tools. Nucleic Acids Research 24: 4876–4882. https://doi.org/10.1093/nar/25.24.4876

Vilgalys R, Hester M (1990) Rapid genetic identification and mapping of enzymatically amplified ribosomal DNA from several *Cryptococcus* species. Journal of Bacteriology 172: 4238–4246. https://doi.org/10.1128/jb.172.8.4238-4246.1990

White TJ, Bruns T, Lee S, Taylor J (1990) Amplification and direct sequencing of fungal ribosomal RNA genes for phylogenies. In: Innis MA, Gelfand DH, Sninsky JJ, White TJ (Eds) PCR protocols, a guide to methods and applications. Academic Press, San Diego, 315–322. https://doi.org/10.1016/B978-0-12-372180-8.50042-1

Young AM (1997) Prelimnary observations on the limitations of the Australian Hygrophoraceae (Fungi, Agaricales). Muelleria 10: 131–138. https://doi.org/10.1071/SB96005

Young AM (1999) The Hygrocybeae (Fungi, Basidiomycota, Agaricales, Hygrophoraceae) of the Lane Cove Bushland Park, New South Wales. Austrobaileya 5: 535–564.

Young AM (2005) Fungi of Australia, Hygrophoraceae. Australian Biological Resources Study, Canberra; CSIRO Publishing, Melboune, 1–179.

Zhang M, Li TH, Wang CQ, Song B, Xu J (2015) *Aureoboletus formosus*, a new bolete species from Hunan Province of China. Mycological Progress 14: 1–7. https://doi.org/10.1007/s11557-015-1142-z

MycoKeys 57: 101–111 (2019)
doi: 10.3897/mycokeys.57.36376
http://mycokeys.pensoft.net

RESEARCH ARTICLE

A peer-reviewed open-access journal
MycoKeys
Launched to accelerate biodiversity research

Sanghuangporus toxicodendri sp. nov. (Hymenochaetales, Basidiomycota) from China

Sheng-Hua Wu[1], Chiung-Chih Chang[1], Chia-Ling Wei[1], Guo-Zheng Jiang[2], Bao-Kai Cui[3]

1 *Department of Biology, National Museum of Natural Science, Taichung 40419, Taiwan* **2** *Paoshantang Medicinal Herbs Development Co., Ltd, Xizang 850100,China* **3** *Institute of Microbiology, Beijing Forestry University, Beijing 100083, China*

Corresponding author: *Sheng-Hua Wu* (shwu@mail.nmns.edu.tw)

Academic editor: *Teodor T. Denchev* | Received 21 May 2019 | Accepted 12 August 2019 | Published 22 August 2019

Citation: Wu S-H, Chang C-C, Wei C-L, Jiang G-Z, Cui B-K (2019) *Sanghuangporus toxicodendri* sp. nov. (Hymenochaetales, Basidiomycota) from China. MycoKeys 57: 101–111. https://doi.org/10.3897/mycokeys.57.36376

Abstract

Sanghuangporus toxicodendri (Hymenochaetales) is described as new based on collections made from Shennongjia Forestry District, Hubei Province, China. All studied basidiocarps grew on living trunks of *Toxicodendron* sp. This new species is characterized by having perennial, effused-reflexed to pileate basidiocarps; pore surface brownish yellow or yellowish brown, pores 7–9 per mm; context 1–5 mm thick or almost invisible; setae ventricose, dark brown, 26–42 × 7–10 μm; basidia 4-sterigmate or occasionally 2-sterigmate; basidiospores broadly ellipsoid, smooth, brownish yellow, slightly thick-walled, mostly 3.5–4 × 2.8–3 μm. Maximum likelihood and Bayesian inference phylogenies inferred from internal transcribed spacer (ITS) region of rDNA indicated that *Sanghuangporus* spp. formed a monophyletic clade and resolved as a sister to *Tropicoporus* spp., and six strains of *S. toxicodendri* formed a monophyletic group which is sister to *S. quercicola*. An identification key to known species of *Sanghuangporus* is provided.

Keywords

Inonotus, taxonomy, *Tropicoporus*, wood-decaying fungi

Introduction

Sanghuangporus Sheng H. Wu et al. and *Tropicoporus* L.W. Zhou et al. were recently segregated from the broad generic concept of *Inonotus* P. Karst (Zhou et al. 2016). The former two genera differ from *Inonotus* s. str. chiefly in having dimitic hyphal system. *Sanghuangporus* is characterized by perennial and effused-reflexed to pileate

basidiomata, occurring in a variety of climate environment, whereas *Tropicoporus* is distinguished by annual to perennial basidiomata, and a tropical distribution (Zhou et al. 2016). Zhu et al. (2019) showed the molecular phylogeny strongly supports the monophyly of *Sanghuangporus* spp.; they also indicated that the maximum crown age of *Sanghuangporus* is approximately 30.85 million years, and East Asia is the likely ancestral area. *Sanghuangporus* spp. usually have host-specificity relationships with their host trees. *Sanghuangporus* accommodates some important medicinal fungal species generally are called "Sanghuang" (means yellow organism grows on *Morus*) in China and Korea, and "Meshimakobu" in Japan. *Sanghuangporus sanghuang* (Sheng H. Wu et al.) Sheng H. Wu et al., the generic type, was detected by Wu et al. (2012) as the genuine Sanghuang species growing exclusively on *Morus* in the wild. Before this study, 13 species of *Sanghuangporus* were known (Ghobad-Nejhad 2015; Tomsovsky 2015; Zhou et al. 2016; Zhu et al. 2017). In this study, we present a new species of *Sanghuangporus* sp. growing on *Toxicodendron* sp. collected from Shennongjia Forestry District, Hubei Province of China.

Materials and methods

Morphological studies

All studied specimens are deposited in the herbarium of National Museum of Natural Science, ROC (TNM). The description is based on dried basidiocarps. Freehand and thin sections of fruiting bodies were prepared in three media for microscopic studies: 5% (w/v) potassium hydroxide (KOH) with 1% (w/v) phloxine was used for observation and measurement of microscopic characters; Melzer's reagent was applied to check amyloidity and dextrinoidity; Cotton blue was used to test cyanophily. The abbreviations in the text were used as followed: L = mean spore length (arithmetical average for all spores), W = mean spore width (arithmetical average for all spores), *n* = total number of spores measured from a specimen, Q = variation in the L/W ratio between the studied specimens. When presenting the variation in the dimensions of spores, 5% of the measurements were rejected from each edge of the range and were given in parentheses.

DNA extraction and sequencing

Genomic DNA were extracted from dried samples with the Plant Genomic DNA Extraction Miniprep System (Viogene-Biotek Corp., New Taipei, Taiwan) following the manufacturer's protocol. Nuclear ribosomal internal transcribed spacer (ITS) region was amplified with primer pair ITS1/ITS4 (White et al. 1990). The PCR protocols for ITS regions were as follows: initial denaturation at 95 °C for 5 min, followed by 40 cycles at 94 °C for 45 s, 53 °C for 45 s and 72 °C for 45 s, and a final extension of 72 °C for 10 min. PCR products were purified and sequenced by the MB Mission Biotech Company (Taipei, Taiwan). Newly obtained sequences were assembled and manually

adjusted when necessary using BioEdit (Hall 1999). The sequences were then submitted to Genbank.

Alignment and phylogenetic analyses

Zhu et al. (2017) conducted ITS-based phylogenetic analysis for all previously known 13 species of *Sanghuangporus*. The ingroup strains of the *Sanghuangporus* spp. and *Tropicoporus* spp. employed in their analysis were basically adopted in the present analysis. We added newly generated sequences of six strains of the new species (Table 1). *Inonotus rickii* (Pat.) D.A. Reid, the outgroup in Zhu et al.'s analysis was not adopted, as this root failed to separate all *Sanghuangporus* spp. from the *Tropicoporus* spp. We consulted the study of Zhou et al. (2016) and chose *Inocutis tamaricis* (Pat.) Fiasson & Niemelä as the outgroup, which was successful in constructing the tree with a satisfactory result. The dataset was aligned using MAFFT 7 with Q-INS-i strategy. The aligned sequences were manually adjusted in BioEdit (Hall 1999) when necessary. Parsimony informative sites were calculated using MEGA 7 (Kumar et al. 2016). Phylogenetic trees were inferred from Bayesian inference (BI) and Maximum Likelihood (ML) methods using MrBayes v. 3.2.6. (Ronquist et al. 2012) at the CIPRES Science Gateway (http://www.phylo.org/) and PhyML 3.0 (Guindon et al. 2010), respectively. The best fit model for both algorithms was estimated by jModelTest2 (Darriba et al. 2012) using the Bayesian information criterion (BIC). For ML analysis, bootstrap (BS) values were calculated after running 1000 replicates. The BI analysis was conducted with 10 million generations initiated from random starting trees. Trees were sampled every 1000 generations, and the first 2500 trees were discards as burn-in. The Posterior Probability (PP) values were calculated from the remaining trees. Only the phylogram inferred from ML analysis was shown because both BI and ML analyses yield similar topologies. The statistical supports were shown on nodes of the ML tree when BS ≥ 70 and PP ≥ 0.7. The final phylogenetic trees and alignment were submitted to TreeBASE (submission number 24234; http://www.treebase.org).

Results

Phylogeny results

The ITS dataset consisted of 48 taxa and 1117 sites including gaps, of which 306 sites were parsimony informative. The HKY+G was selected as the best fit model for both the ML and BI analyses. The BI analysis was terminated when the average standard deviation of split frequencies fell to 0.009547. The ML tree shows that *Sanghuangporus* spp. formed a monophyletic clade (BS = 93%, PP = 1) and resolved as a sister to *Tropicoporus* spp. (BS = 92%, PP = 1) (Fig. 1). Six strains of *Sanghuangporus toxicodendri* formed a monophyletic group with statistical supports (BS = 78%, PP = 1), which was sister to *S. quercicola* L. Zhu & B.K. Cui with significant support (BS = 98%, PP = 1) (Fig. 1).

Table 1. List of species, specimens and ITS sequences used in this study. Sequences generated in this study are shown in boldface type.

Species name	Specimen or strain no.	Accession no.
Sanghuangporus alpinus	Cui9646	JQ860313
	Cui9658	JQ860310
	Cui9666	JQ860311
Sanghuangporus baumii	Cui11903	KY328305
	Dai3694	JN642569
	Dai3684	JN642568
Sanghuangporus ligneus	Ghobad-Nejhad 1157	KR073082
	Ghobad-Nejhad 1152	KR073081
Sanghuangporus lonicericola	Dai8376	JQ860308
	MG281	KU213574
	TAA55428	JN642575
Sanghuangporus microcystideus	AM19	JF895465
	AM-08	JF895464
Sanghuangporus pilatii	BRNM 771989	KT428764
Sanghuangporus quercicola	Li445	KY328311
	Li1149	KY328312
Sanghuangporus sanghuang	BZ-C	JN642587
	Dai12723	JQ860316
	Wu0903-1	JN794061
Sanghuangporus toxicodendri	**Wu 1805-2**	**MK400422**
	Wu 1805-3	**MK400423**
	Wu 1805-5	**MK400424**
	Wu 1807-2	**MK729538**
	Wu 1807-3	**MK729540**
	Wu 1807-4	**MK729539**
Sanghuangporus vaninii	Dai3624	JN642590
	SFC 20001106-7	AF534070
	SFCC 10209	AY558628
Sanghuangporus weigelae	Cui6012	JQ860319
	WD-1667	JN642594
	Dai11694	JQ860315
Sanghuangporus weirianus	CBS_618.89	AY558654
Sanghuangporus zonatus	Cui6631	JQ860305
	Dai10841	JQ860306
Tropicoporus cubensis	MUCL47079	JQ860325
Tropicoporus dependens	JV 1207/3.4-J	KC778779
Tropicoporus dependens	JV 0409/20-J	KC778778
Tropicoporus guanacastensis	O19228	KP030794
Tropicoporus linteus	JV0904/64	JQ860322
Tropicoporus pseudolinteus	JV 0312/22.10-J	KC778780
	JV0402/35-K	KC778781
Tropicoporus sideroxylicola	JV 1207/4.3-J	KC778783
	JV 0409/30-J	KC778782
Tropicoporus tropicalis	CBS-617.89	AF534077
Inonotus compositus	Wang 552	KP030781
Inonotus hispidus	PST4	EU918125
Inocutis tamaricis	CBS 384.72	AY558604

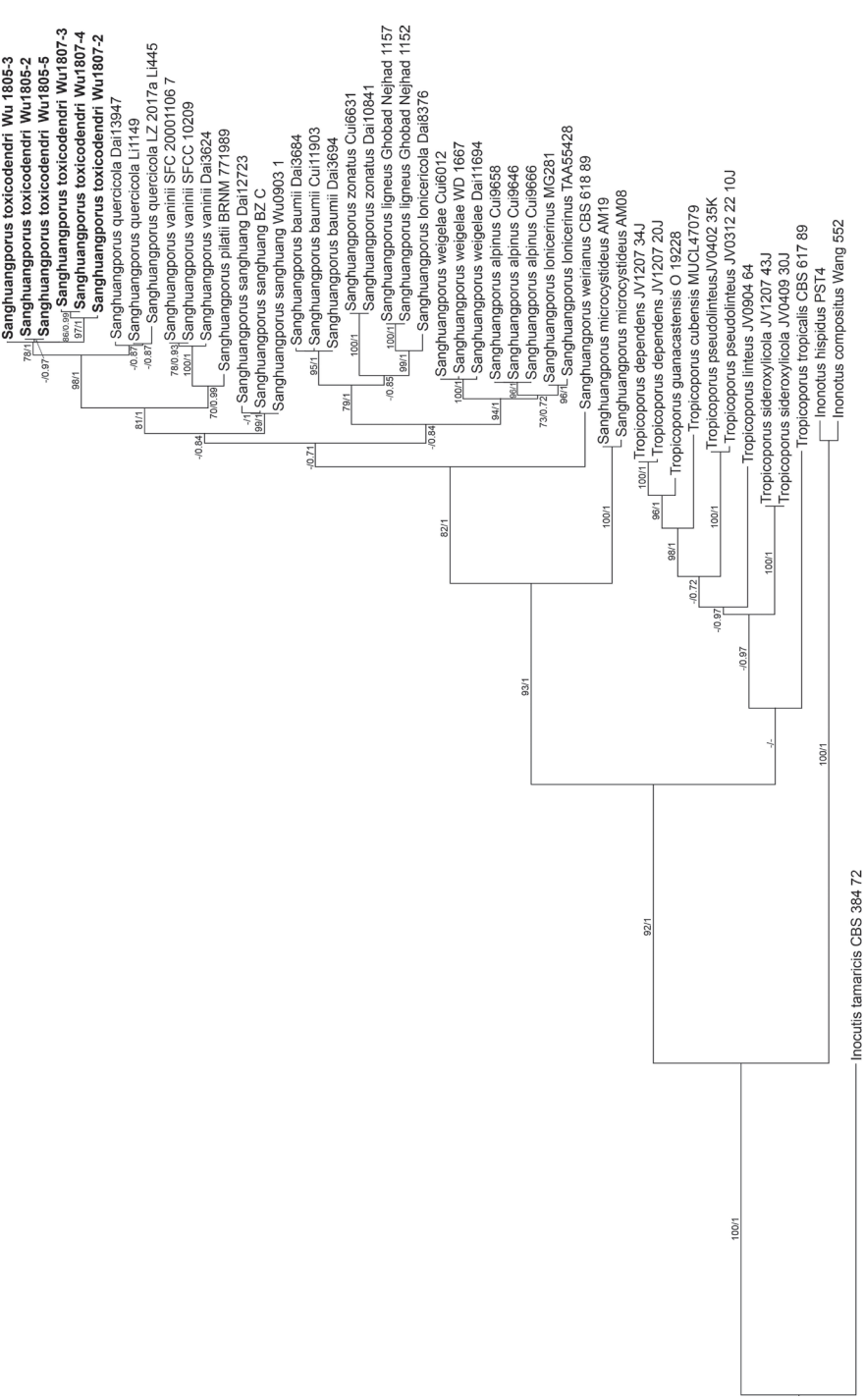

Figure 1. The phylogenetic tree inferred from maximum likelihood and Bayesian analyses of the ITS dataset of *Sanghuangporus toxicodendri* and related species. Statistic supports are shown on internodes with bootstrap values ≥70% and posterior probabilities ≥0.7. The presented new species are shown in boldface type.

Taxonomy

Sanghuangporus toxicodendri **Sheng H. Wu, B.K. Cui & Guo Z. Jiang, sp. nov.**
MycoBank MB 830791
Figures 2, 3

Type. CHINA. Hubei Province: Shennongjia Forestry District, Songbai Town, 1200 m, on living *Toxicodendron* sp. trunk, May 2018, *Wu 1805-3* (holotype, TNM F0032663).

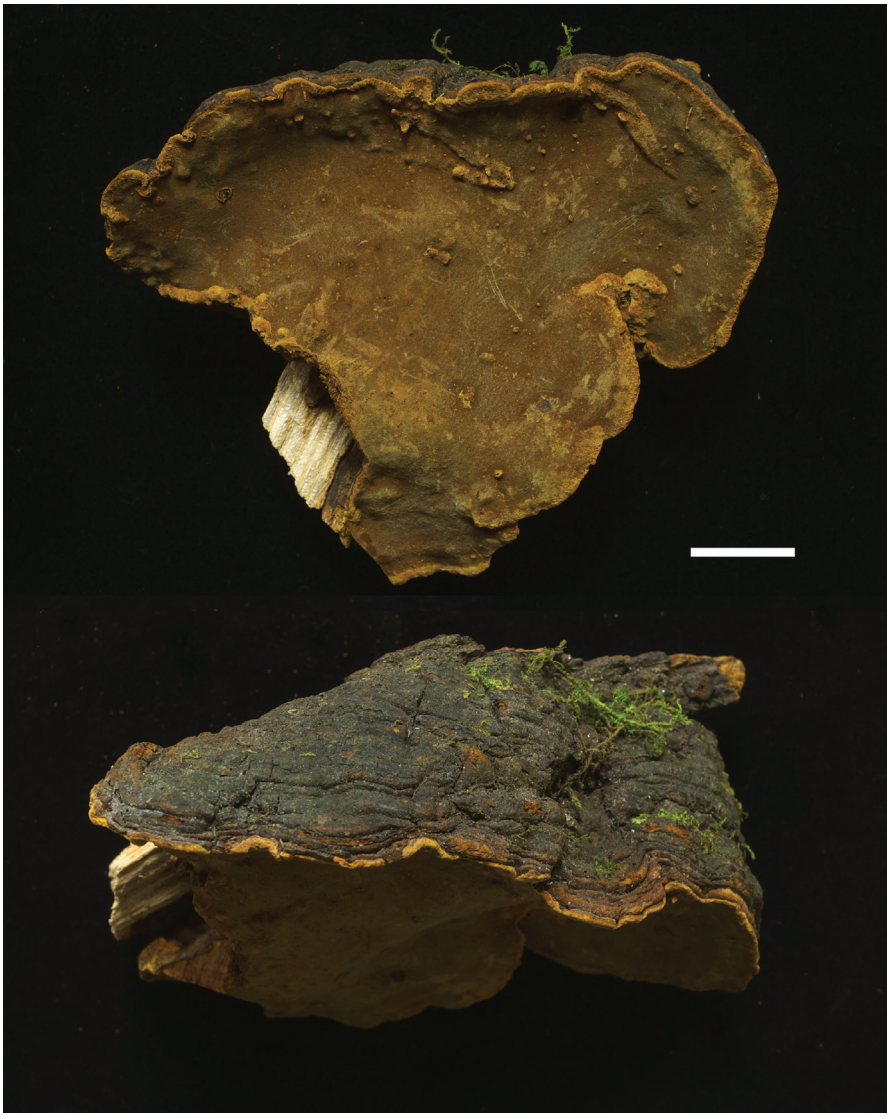

Figure 2. Basidiocarp. *Sanghuangporus toxicodendri* (holotype, *Wu 1805-3*).

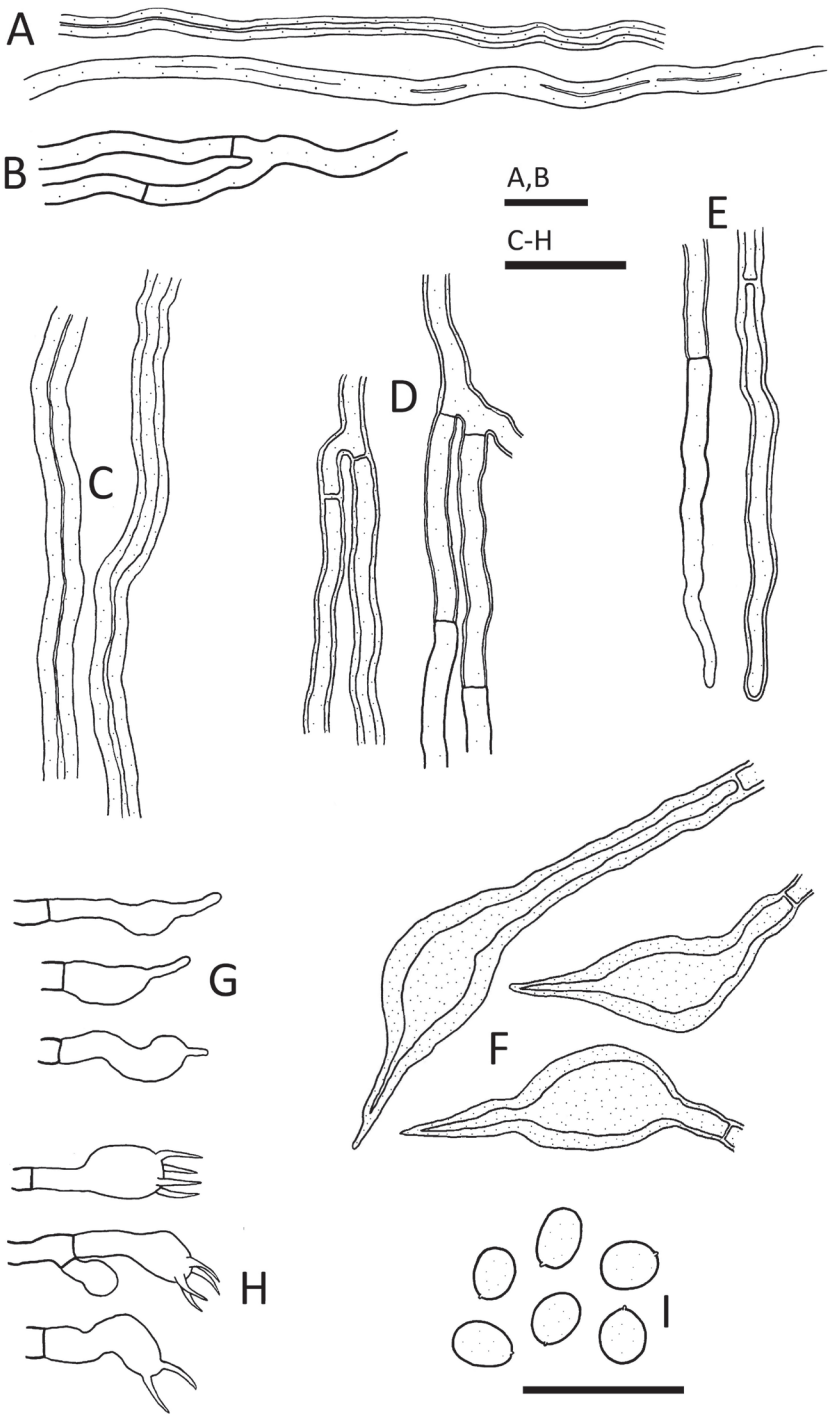

Figure 3. *Sanghuangporus toxicodendri* (holotype, *Wu 1805-3*) **A** skeletal hyphae from context **B** generative hyphae from context **C** skeletal hyphae from trama **D** generative hyphae from trama **E** generative hyphae from dissepiments **F** setae **G** cystidioles **H** basidia **I** basidiospores. Scale bars: 10 μm.

Etymology. The epithet refers to the host genus.

Description. Basidiocarps perennial, effused-reflexed to pileate, applanate, semicircular, adaxially slightly concave, woody hard. Pilei projecting 4–6 cm, up to 18 cm wide and up to 6 cm thick at base. Pileal surface grayish black to blackish brown, glabrous, occasionally cracked, concentrically zonate and sulcate; margin generally obtuse, concolorous or brownish yellow. Pore surface brownish yellow, yellowish brown, brownish or rusty brown, somewhat glancing, darkening in KOH; pores 7–9 per mm, circular. Context homogeneous, 1–5 mm thick or almost invisible, brownish yellow or brownish, with blackish crust at pileus parts. Tubes concolorous with pore surface, 1–5 cm thick, usually with several growth layers.

Hyphal system dimitic in both context and trama, generative hyphae simple-septate; tissue darkened in KOH. Context generative hyphae yellowish, brownish yellow or yellowish brown, moderately ramified, 2–3 μm diam., slightly thick-walled or with walls up to 1 μm thick; skeletal hyphae yellowish brown to brownish, fairly straight, rarely ramified, 2–4 μm diam., with 0.5–1.3 μm thick walls or subsolid. Tube generative hyphae yellowish brown to yellowish, moderately ramified, 2–3 μm diam., slightly thick-walled or with walls up to 1 μm thick; skeletal hyphae yellowish brown to brownish, fairly straight, rarely ramified, 2–4 μm diam., with 0.8–1.3 μm thick walls or subsolid. Hymenial setae ventricose, dark brown, 26–42 × 7–10 μm. Cystidioles with tapering or abruptly narrow apices, colorless, thin-walled, 10–20 × 3–3.5 μm. Basidia clavate, 10–12 × 4–4.5 μm, thin-walled, 4-sterigmate or occasionally 2-sterigmate; sterigmata up to 6 μm long. Basidiospores broadly ellipsoid, smooth, brownish yellow, slightly thick-walled, inamyloid, non-dextrinoid, somewhat cyanophilous, (3.2–)3.5–4 × (2.7–)2.8–3(–3.2) μm, L = 3.72±0.21 μm, W = 2.94±0.11 μm, Q = 1.27 (*n* = 30, holotype: *Wu 1805-3*).

Ecology and distribution. On trunk of *Toxicodendron* sp. Hitherto only known from Shennongjia Forestry District, Hubei province, China.

Additional specimens examined (paratypes). CHINA. Hubei Province: Shennongjia Forestry District, Songbai Town, 1200 m, on living *Toxicodendron* sp. trunk, May 2018, *Wu 1805-1* (TNM F0032661), *Wu 1805-2* (TNM F0032662), *Wu 1805-4* (TNM F0032664), *Wu 1805-5* (TNM F0032665); July 2018, *Wu 1807-2* (TNM F0032666), *Wu 1807-3* (TNM F0032667), *Wu 1807-4* (TNM F0032668).

Discussion

Zhu et al.'s (2019) phylogenetic study showed the monophyly of the genus *Sanghuangporus* spp., and the result coincides with the present study (Fig. 1). The genus *Sanghuangporus* comprises 14 species (Ghobad-Nejhad 2015; Tomsovsky 2015; Zhou et al. 2016; Zhu et al. 2017), after including *S. toxicodendri* presented here. It is not easy to identify some species of *Sanghuangporus* spp., as there are not that many good morphological characteristics to separate them. Distribution, climatic adaptation, host preference, and DNA sequences are important for species recognition, apart from morphological study.

The present phylogenetic study indicated that *S. toxicodendri* is sister to *S. quercicola* with significant support (Fig. 1). Both species are distributed in central China; the former grows on *Toxicodendron*, while the latter occurs on *Quercus*. However, two morphological features can separate these species. The yellow or brownish-yellow wide marginal zone on the pileus surface of *S. quercicola* (Zhu et al. 2017: figs A, B) is lacking in *S. toxicodendri*. Secondly, the basidiospores of *S. toxicodendri* are mostly longer than 2.8 µm, but are generally shorter than 2.8 µm in *S. quercicola*.

Sanghuangporus lonicericola (Parmasto) L.W. Zhou & Y.C. Dai, *S. quercicola*, *S. sanghuang*, *S. toxicodendri*, *S. vaninii* (Ljub.) L.W. Zhou & Y.C. Dai, and *S. zonatus* (Y.C. Dai & X.M. Tian) L.W. Zhou & Y.C. Dai have comparatively smaller pores (>6 per mm) than other species. *Sanghuangporus lonicericola* is distributed in northeast China and the Russian Far-East, growing exclusively on *Lonicera*; moreover, it has smaller setae (12–22 × 4–8 µm; Dai 2010) than *S. toxicodendri*. *Sanghuangporus sanghuang* grows only on *Morus* and has distinctly larger basidiospores (4–4.9 × 3.1–3.9 µm; Wu et al. 2012) than *S. toxicodendri*. *Sanghuangporus vaninii* grows on *Populus* and also resembles *S. quercicola* in having a wide marginal yellow zone on pileus surface, but it has larger basidiospores (3.8–4.4 × 2.8–3.7 µm; Dai 2010) than *S. toxicodendri*. *Sanghuangporus zonatus* is a tropical species distributed in southern China and differs from *S. toxicodendri* in having thicker context and shorter setae (Tian et al. 2013).

Several *Sanghuangporus* spp. are used for medicinal application in China, Korea, Japan, and South Asian countries. Wu et al. (2012) indicated that *S. sanghuang*, the only *Sanghuangporus* sp. growing on *Morus* in the wild, is the genuine Sanghuang species. Comparing health-care effectiveness among the so-called Sanghuang species, Lin et al. (2017) proved that *S. sanghuang* has better medicinal properties than two other commercial species: *S. baumii* (Pilát) L.W. Zhou & Y.C. Dai and *S. vaninii*. *Sanghuangporus vaninii* grows on *Populus davidiana* in the wild and is widely cultivated in China, Korea, and Japan as a medicinal fungus. *Sanghuangporus baumii*, which grows on *Syringa* in the wild, is also served as medicinal fungus in China. The medicinal properties of many *Sanghuangporus* spp. are not understood. It is noted that *S. toxicodendri* and the recently described *S. quercicola* are closely related to the medicinal species *S. sanghuang* and *S. vaninii* (Zhu et al. 2019; this study, Fig. 1). The medicinal properties of these two species are worth studying.

Key to the accepted species of *Sanghuangporus*

1 Pores 3–5 per mm **2**
– Pores > 5 per mm **3**
2 Basidiospores 3.5–4.5 × 3–3.5 µm; distribution in Central Asia .... ***S. lonicerinus***
– Basidiospores 4–4.8 × 3–3.8 µm; distribution in Europe ..... ***S. pilatii***
3 Pores 7–10 per mm **4**
– Pores 5–8 per mm **6**

4 Brownish yellow pileus surface marginal zone present; restricted to *Quercus*..... ..... ***S. quercicola***
– Brownish yellow pileus surface marginal zone not present; not on *Quercus*.....**5**
5 Setae >25 μm long; restricted to *Toxicodendron* ..... ***S. toxicodendri***
– Setae <25 μm long; restricted to *Lonicera* ..... ***S. lonicericola***
6 Context very thin, <3 mm **7**
– Context very thick, >10 mm **8**
7 Context duplex; distribution in the warm temperate zones ..... ***S. weigelae***
– Context homogeneous; distribution in alpinus zones ..... ***S. alpinus***
8 Setae mostly <20 μm long.....**9**
– Setae mostly >20 μm long.....**12**
9 Basidiomata with a sharp margin ..... ***S. zonatus***
– Basidiomata with an obtuse margin **10**
10 Basidiospores basically subglobose; distribution in Africa..... ***S. microcystideus***
– Basidiospores broadly ellipsoid; distribution in Asia.....**11**
11 Dissepiments distinctly thick; distribution in western Asia..... ***S. ligneus***
– Dissepiments distinctly thin to slightly thick (<¼ diameter of pores); distribution in eastern Asia..... ***S. baumii***
12 Basidiospores basically subglobose; restricted to *Juglans*..... ***S. weirianus***
– Basidiospores broadly ellipsoid; restricted to *Morus* or *Populus* **13**
13 Basidiospores 3.8–4.4 × 2.8–3.7 μm; restricted to *Populus* ..... ***S. vaninii***
– Basidiospores 4–4.9 × 3.1–3.9 μm; restricted to *Morus* ..... ***S. sanghuang***

Acknowledgements

This study was supported by a Grant-in-Aid for Scientific Research (no. 105-07.1-SB-18) from Council of Agriculture, Executive Yuan, ROC.

References

Dai YC (2010) Hymenochaetaceae (Basidiomycota) in China. Fungal Diversity 45: 131–343. https://doi.org/10.1007/s13225-010-0066-9

Darriba D, Taboada GL, Doallo R, Posada D (2012) jModelTest 2: more models, new heuristics and parallel computing. Nature Methods 9: 772–772. https://doi.org/10.1038/nmeth.2109

Ghobad-Nejhad M (2015) Collections on *Lonicera* in Northwest Iran represent an undescribed species in the *Inonotus linteus* complex (Hymenochaetales). Mycological Progress 14: 90. https://doi.org/10.1007/s11557-015-1100-9

Guindon S, Dufayard JF, Lefort V, Anisimova M, Hordijk W, Gascuel O (2010) New algorithms and methods to estimate maximum-likelihood phylogenies: assessing the performance of PhyML 3.0. Systematic Biology 59: 307–321. https://doi.org/10.1093/sysbio/syq010

Hall TA (1999) BioEdit: a user-friendly biological sequence alignment editor and analysis program for Windows 95/98/NT. Nucleic Acids Symposium Series 41: 95–98.

Kumar S, Stecher G, Tamura K (2016) MEGA7: molecular evolutionary genetics analysis version 7.0 for bigger datasets. Molecular Biology and Evolution 33: 1870–1874. https://doi.org/10.1093/molbev/msw054

Lin WC, Deng JS, Huang SS, Wu SH, Lin HY, Huang GJ (2017) Evaluation of antioxidant, anti-inflammatory and anti-proliferative activities of ethanol extracts from different varieties of *Sanghuang* species. RSC Advances 7: 7780–7788. https://doi.org/10.1039/C6RA27198G

Ronquist F, Teslenko M, van der Mark P, Ayres DL, Darling A, Hohna S, Larget B, Liu L, Suchard MA, Huelsenbeck JP (2012) MrBayes 3.2: Efficient Bayesian phylogenetic inference and model choice across a large model space. Systematic Biology 61: 539–542. https://doi.org/10.1093/sysbio/sys029

Tomsovsky M (2015) *Sanghuangporus pilatii*, a new combination, revealed as European relative of Asian medicinal fungi. Phytotaxa 239: 82–88. https://doi.org/10.11646/phytotaxa.239.1.8

Tian XM, Yu HY, Decock C, Vlasák J, Dai YC (2013) Phylogeny and taxonomy of the *Inonotus linteus* complex. Fungal Diversity 58: 159–160. https://doi.org/10.1007/s13225-012-0202-9

White TJ, Bruns T, Lee S, Taylor JW (1990) Amplification and direct sequencing of fungal ribosomal RNA genes for phylogenetics. In: Innis MA, Gelfand DH, Sninsky JJ, White TJ (Eds) PCR Protocols: A Guide to Methods and Applications. Academic Press, San Diego 315–322. https://doi.org/10.1016/B978-0-12-372180-8.50042-1

Wu SH, Dai YC, Hattori T, Yu TW, Wang DM, Parmasto E, Chang HY, Shih SY (2012) Species clarification for the medicinally valuable 'sanghuang' mushroom. Botanical Studies 53: 135–149.

Zhou LW, Vlasák J, Decock C, Assefa A, Stenlid J, Abate D, Wu SH, Dai YC (2016) Global diversity and taxonomy of the *Inonotus linteus* complex (Hymenochaetales, Basidiomycota): *Sanghuangporus* gen. nov., *Tropicoporus excentrodendri* and *T. guanacastensis* gen. et spp. nov., and 17 new combinations. Fungal Diversity 77: 335–347. https://doi.org/10.1007/s13225-015-0335-8

Zhu L, Song J, Zhou JL, Si J, Cui BK (2019) Species diversity, phylogeny, divergence time, and biogeography of the genus *Sanghuangporus* (Basidiomycota). Frontiers in Microbiology 10: 812. https://doi.org/10.3389/fmicb.2019.00812

Zhu L, Xing JH, Cui BK (2017) Morphological characters and phylogenetic analysis reveal a new species of *Sanghuangporus* from China. Phytotaxa 311: 270–276. https://doi.org/10.11646/phytotaxa.311.3.7

MycoKeys 57: 113–127 (2019)
doi: 10.3897/mycokeys.57.35448
http://mycokeys.pensoft.net

RESEARCH ARTICLE

A peer-reviewed open-access journal
MycoKeys
Launched to accelerate biodiversity research

Diaporthe species in south-western China

Hui Long[1], Qian Zhang[1], Yuan-Yuan Hao[4], Xian-Qiang Shao[5], Xiao-Xing Wei[6], Kevin D. Hyde[7], Yong Wang[1,2], De-Gang Zhao[2,3]

1 *Department of Plant Pathology, College of Agriculture, Guizhou University, Guiyang, Guizhou 550025, China* **2** *Guizhou Key Laboratory Agro-Bioengineering, Guizhou University Guiyang, Guizhou, 550025, China* **3** *Guizhou Academy of Agricultural Sciences, Guiyang 550006, China* **4** *Administration Center of the Yellow River Delta Sustainable Development Institute of Sandong Province, Dongying, 257091, China* **5** *Dejiang County Chinese herbal medicine industry development office, Tongren, 565200, China* **6** *Academy of Animal and Veterinary Sciences, Qinghai University (Qinghai Academy of Animal and Veterinary Sciences), Xining, China* **7** *Center of Excellence in Fungal Research and School of Science, Mae Fah Luang University, Chiang Rai, 57100, Thailand*

Corresponding author: *Yong Wang* (yongwangbis@aliyun.com); *De-Gang Zhao* (dgzhao@gzu.edu.cn)

Academic editor: *Andrew Miller* | Received 15 April 2019 | Accepted 15 July 2019 | Published 23 August 2019

Citation: Long H, Zhang Q, Hao Y-Y, Shao X-Q, Wei X-X, Hyde KD, Wang Y, Zhao D-G (2019) *Diaporthe* species in south-western China. MycoKeys 57: 113–127. https://doi.org/10.3897/mycokeys.57.35448

Abstract

Three strains of the genus *Diaporthe* were isolated from different plant hosts in south-western China. Phylogenetic analyses of the combined ITS, *β*-tubulin, *tef*1 and calmoudulin dataset indicated that these strains represented three independent lineages in *Diaporthe*. *Diaporthe millettiae* **sp. nov.** clustered with *D. hongkongensis* and *D. arecae*, *Diaporthe osmanthi* **sp. nov.** grouped with *D. arengae*, *D. pseudomangiferae* and *D. perseae* and *Diaporthe* strain GUCC9146, isolated from *Camellia sinensis*, was grouped in the *D. eres* species complex with a close relationship to *D. longicicola*. These species are reported with taxonomic descriptions and illustrations.

Keywords

Diaporthe, phylogeny, taxonomy, 2 new taxa

Introduction

Genus *Diaporthe* has been well-studied in recent years by Udayanga et al. (2011, 2012), incorporating morphological and molecular data and recommending appropriate genes to resolve species limitations in the genus. Since these revolutionary papers, 43 novel *Diaporthe* species have been described from China with morphological and

phylogenetic evidence (Huang et al. 2013, 2015; Fan et al. 2016; Gao et al. 2014, 2015, 2016, 2017; Yang et al. 2017a,b, 2018; Yang et al. 2016; Du et al. 2016; Dissanayake et al. 2017a). Dissanayake et al. (2017b) provided an update of the genus with additional 15 species (7 new and 8 known species) from Italy based on molecular evidence. New records and species have also been reported by Hyde et al. (2016), Rossman et al. (2016), Chen and Kirschner (2017), Guarnaccia et al. (2018), Perera et al. (2018), Tibpromma et al. (2018) and Wanasinghe et al. (2018).

Three strains of *Diaporthe* were isolated from different medicinal plants collected in Guizhou and Guangxi during a survey of fungal diversity in south-western China. All the strains produced conidiomata containing alpha- and beta-conidia, typical of *Diaporthe*. This paper describes these three collections using molecular evidence, based on the analysis of combined ITS, *β*-tubulin, *tef*1 and calmoudulin datasets, as *Diaporthe millettiae* sp. nov. and *D. osmanthi* sp. nov. and *D. longicicola* with a new host record from *Camellia sinensis*.

Materials and methods

Isolation and morphological studies

The samples were collected from Guizhou and Guangxi provinces. The *Diaporthe* strains were isolated using the single-spore method (Chomnunti et al. 2014). Colonies, growing from single spores, were transferred to potato-dextrose agar (PDA) and incubated at room temperature (28 °C). Following 2–3 weeks of incubation, morphological characters were recorded as in Udayanga et al. (2011, 2015). Conidia and conidiophores were observed using a compound microscope (Olympus BX53). The holotype specimens are deposited in the Herbarium of Department of Plant Pathology, Agricultural College, Guizhou University (HGUP). Ex-type cultures are deposited in the Culture Collection at the Department of Plant Pathology, Agriculture College, Guizhou University, China (GUCC). Taxonomic information of the new taxa was submitted to MycoBank (http://www.mycobank.org) and Facesoffungi (http://www.facesoffungi.org).

DNA extraction and sequencing

Fungal cultures were grown on PDA medium until they nearly covered the whole Petri-dish (90 mm diam.) at 28 °C. Fresh fungal mycelia were scraped from the surface with sterilised scalpels. A BIOMIGA Fungus Genomic DNA Extraction Kit (GD2416) was used to extract fungal genome DNA. DNA amplification was performed in a 25 µl reaction volume system which contained 2.5 µl 10 × PCR buffer, 1 µl of each primer (10 µM), 1 µl template DNA and 0.25 µl Taq DNA polymerase (Promega, Madison, WI, USA). Primers ITS4 and ITS5 (White et al. 1990) were used to amplify the ITS region. Three protein-coding gene fragments (*β*-tubulin, *tef*1 and

calmoudulin) were amplified by the primers Bt2a/Bt2b (Glass and Donaldson 1995), CAL228F/CAL737R and EF1-728F/EF1-986R (Carbone and Kohn 1999). Gene sequencing was performed with an ABI PRISM 3730 DNA autosequencer using either a dRhodamine terminator or Big Dye Terminator (Applied Biosystems Inc., Foster 19 City, California). The sequences of both strands of each fragment were determined for sequence confirmation. The DNA sequences were submitted to GenBank and their accession numbers were provided in Table 1.

Table 1. GenBank accession numbers of isolates include in this study.

Species	Culture no.	GenBank no.			
		ITS	*tef*1	*β*-tubulin	calmoudulin
Diaporthe alleghaniensis	CBS 495.72	KC343007	KC343733	KC343975	KC343249
D. ambigua	CBS 114015	AF230767	GQ250299	KC343978	KC343252
D. anacardii	**CBS 720.97***	KC343024	KC343750	KC343992	KC343266
D. arecae	**CBS 161.64**	KC343032	KC343758	KC344000	KC343274
D. arengae	**CBS 114979**	KC343034	KC343760	KC344002	KC343276
D. baccae	**CBS 136972**	KJ160565	KJ160597	MF418509	MG281695
D. beilharziae	**BRIP 54792**	JX862529	JX862535	KF170921	–
D. betulae	CFCC 50470	KT732951	KT733017	KT733021	KT732998
D. bicincta	CBS 121004	KC343134	KC343860	KC344102	KC343376
D. biguttusis	**CGMCC 3.17081**	KF576282	KF576257	KF576306	–
D. celastrina	**CBS 139.27**	KC343047	KC343773	KC344015	KC343289
D. celeris	**CBS 143349**	MG281017	MG281538	MG281190	MG281712
D. charlesworthii	BRIP 54884m*	KJ197288	KJ197250	KJ197268	–
D. cinerascens	CBS 719.96	KC343050	KC343776	KC344018	KC343292
D. cotoneastri	CBS 439.82	FJ889450	GQ250341	JX275437	JX197429
D. decedens	CBS 109772	KC343059	KC343785	KC344027	KC343301
D. elaeagni	CBS 504.72	KC343064	KC343790	KC344032	KC343306
D. ellipicola	**CGMCC 3.17084**	KF576270	KF576245	KF576291	–
D. eres	**CBS 138594**	KJ210529	KJ210550	KJ420799	KJ434999
D. foeniculina	**CBS 187.27**	KC343107	KC343833	KC344075	KC343349
D. goulteri	**BRIP 55657a**	KJ197289	KJ197252	KJ197270	–
D. helianthi	**CBS 592.81**	KC343115	GQ250308	KC343841	JX197454
D. hongkongensis	**CBS 115448**	KC343119	KC343845	KC344087	KC343361
D. inconspicua	**CBS 133813**	KC343123	KC343849	KC344091	KC343365
D. longicicola	GUCC9146	MK398676	MK480611	MK502091	MK502088
D. longicicola	**CGMCC 3.17091**	KF576267	KF576242	KF576291	–
D. macinthoshii	BRIP 55064a*	KJ197290	KJ197251	KJ197269	–
D. millettia	**GUCC9167**	MK398674	MK480609	MK502089	MK502086
D. oncostoma	CBS 589.78	KC343162	KC343888	KC344130	KC343404
D. osmanthusis	**GUCC9165**	MK398675	MK480610	MK502090	MK502087
D. perseae	CBS 151.73	KC343173	KC343899	KC344141	KC343415
D. phragmitis	**CBS 138897**	KP004445	–	KP004507	–
D. pseudomangiferae	**CBS 101339**	KC343181	KC343907	KC344149	KC343423
D. pseudophoenicicola	**CBS 462.69**	KC343184	KC343910	KC344152	KC343426
D. rosicola	MFLU 17.0646	NR157515	MG829270	MG843877	MG829274
D. saccarata	**CBS 116311**	KC343190	KC343916	KC344158	KC343432
D. stitica	CBS 370.54	KC343212	KC343938	KC344180	KC343454
D. vaccinii	CBS 160.32	AF317578	GQ250326	KC344196	KC343470
Valsa ambiens	CFCC 89894	KR045617	KU710912	KR045658	–

Ex-type isolates were labeled with bold.

Phylogenetic analyses

DNA sequences from our three strains and reference sequences downloaded from GenBank (Dissanayake et al. 2017a, b), Guarnaccia et al. (2018) and Wanasinghe et al. (2018) were analysed by maximum parsimony (MP) and maximum likelihood (ML). Sequences were optimised manually to allow maximum alignment and maximum sequence similarity, as detailed in Manamgoda et al. (2012). MP analyses were performed in PAUP v. 4.0b10 (Swofford 2003), using the heuristic search option with 1,000 random taxa additions and tree bisection and re-connection (TBR) as the branch swapping algorithm. Maxtrees = 5000 was set to build the phylogenetic tree. The characters of the alignment document were ordered according to ITS+*tef*1+β-tubulin+CAL for GUCC9165 and GUCC9167 and *tef*1+β-tubulin for GUCC9146 with equal weight and gaps were treated as missing data. The Tree Length (TL), Consistency Indices (CI), Retention Indices (RI), Rescaled Consistency Indices (RC) and Homoplasy Index (HI) were calculated for each tree generated. The resulting Phylip file was used to make ML and Bayesian trees by the CIPRES Science Gateway (https://www.phylo.org/portal2/login.action) and RAxML-XSEDE with 1000 bootstrap inferences.

Results

Phylogenetic analyses

Three *Diaporthe* strains isolated from different plant hosts were sequenced. PCR products of 456–465 bp (ITS), 292–303 bp (*tef*1), 666–690 bp (β-tubulin) and 336–345 bp (CAL) were obtained. By alignment with the single gene region and then combination according to the order of ITS, *tef*1, β-tubulin and CAL with *Valsa ambiens* (CFCC 89894), only 1833 characters were obtained, viz. ITS: 1–492, *tef*1: 493–801, β-tubulin: 802–1469, CAL: 1470–1833, with 500 parsimony-informative characters. This procedure yielded eleven parsimonious trees (TL = 2169, CI = 0.58, RI = 0.71, RC = 0.41 and HI = 0.42), the first one being shown in Figure 1. All *Diaporthe* species clustered together, although without credible support for bootstrap and BPP values (Figure 1). Phylogenetic analysis of strains GUCC9165 and GUCC9167, using the four gene loci, confirmed them as well-resolved species (Figure 1). Strain GUCC 9165 formed an independent branch adjacent to *D. arecae* and *D. hongkongensis* (MP: 100%, ML: 94% and BPP: 1). Strain GUCC 9167 grouped with the branch which included *D. arengae*, *D. perseae* and *D. pseudomangiferae* (MP: 92%, ML: 98% and BPP: 1). Strain GUCC 9146 was aligned to the branch having *D. longicicola* and *D. rosicola* in the *Diaporthe eres* species-complex (Figure 2), with high statistical support (MP: 84%, ML: 93% and BPP: 1). This strain also showed a close relationship to *D. eres* and *D. cotoneastri*. In addition, we also compared the DNA base pair differences between our strains and related species in different gene regions (Suppl. material 1: Table S1). In *Diaporthe* strain GUCC9165, the four genes had 64 base pair differ-

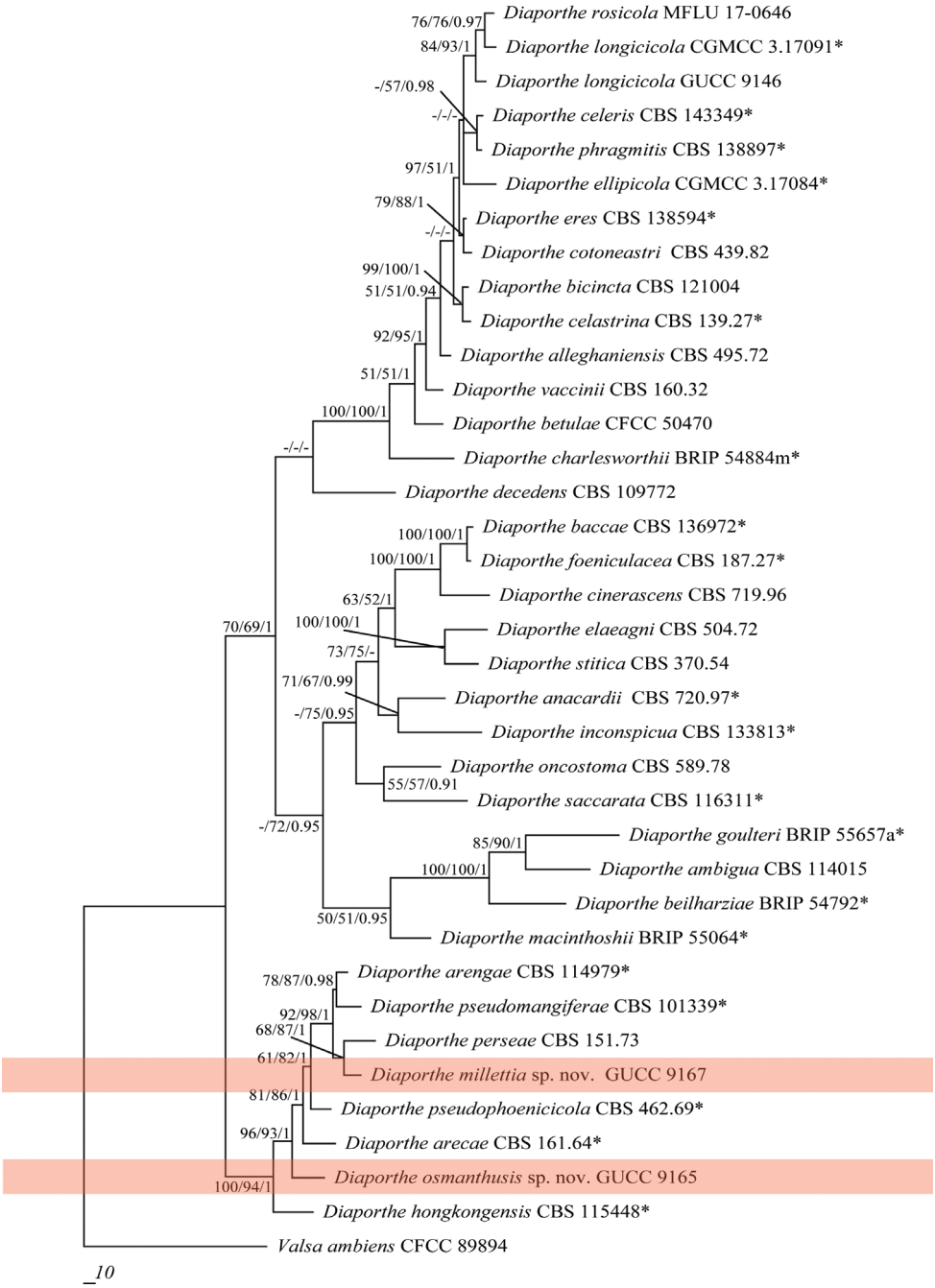

Figure 1. Parsimonious tree obtained from a combined analyses of an ITS, β-tubulin, calmoudulin and *tef*1 sequence dataset. MP, ML above 50% and BPP values above 0.90 were placed close to topological nodes and separated by "/". The bootstrap values below 50% and BPP values below 0.90 were labelled with "-". The tree is rooted with *Valsa ambiens* (CFCC89894). The branch of our new *Diaporthe* species is in pink.

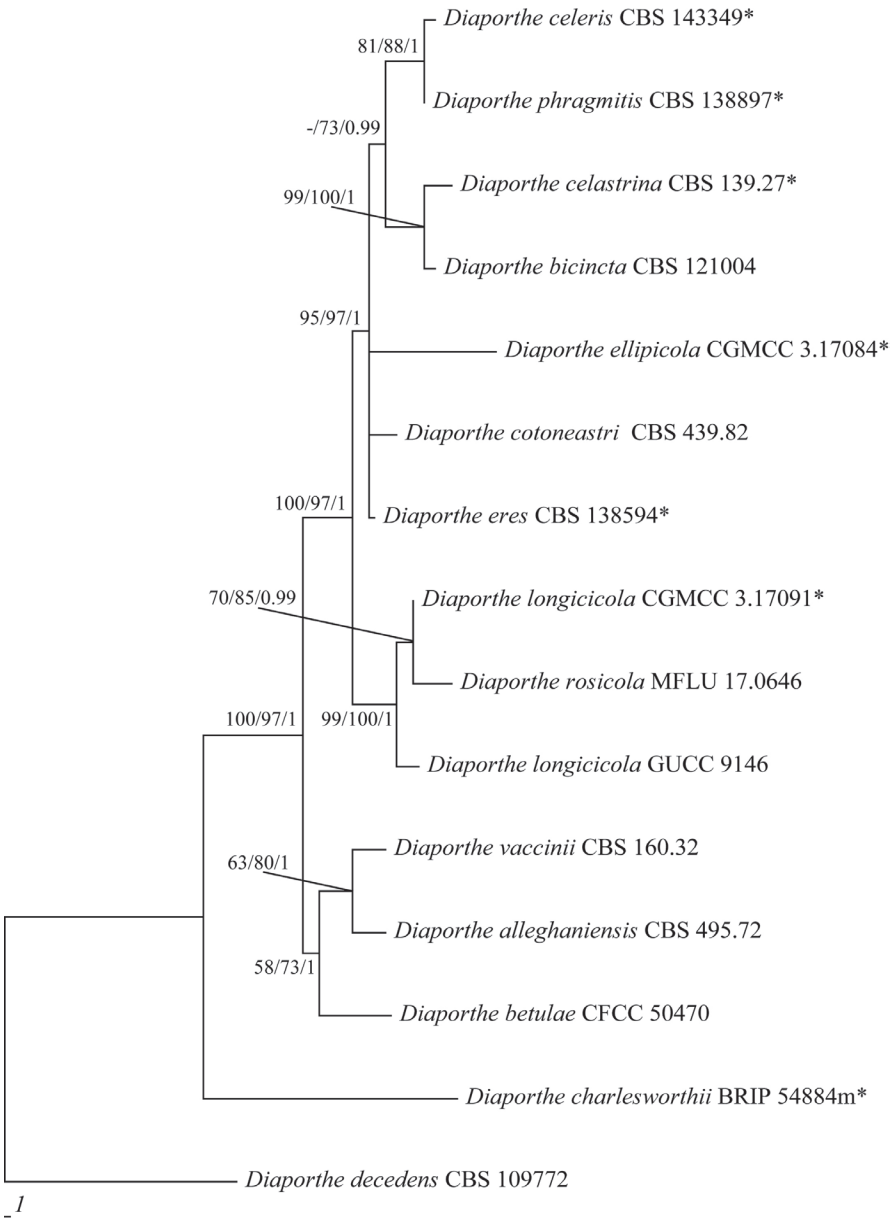

Figure 2. Parsimonious tree obtained from a combined analyses of a β-tubulin and *tef*1 sequence dataset (TL = 265, CI = 0.89, RI = 0.76, RC = 0.68 and HI = 0.11). MP, ML above 50% and BPP values above 0.90 were placed close to topological nodes and separated by "/". The bootstrap values below 50% and BPP values below 0.90 were labelled with "-". The tree is rooted with *Diaporthe decedens* (CBS 109772).

ences with *D. arecae* and 119 with *D. hongkongensis*, the main differences being with β-tubulin and *tef*1. Strain GUCC9167 had 52 base pair differences with *D. arengae*, 61 with *D. perseae* and 64 with *D. pseudomangiferae*, wherein the base distinction was

primarily in the *β*-tubulin and *tef*1 gene region. The *β*-tubulin sequences of *D. eres* and *D. longicicola* were apparently shorter than in strain GUCC 9146. The CAL sequences of *D. rosicola* were shorter than GUCC 9146. The DNA sequence of CAL for *Diaporthe longicicola* was not available (Gao et al. 2015). Integrating available DNA information, we discovered that 28 base pair differences were shown between GUCC 9146 and *D. eres*, 51 between GUCC 9146 and *D. cotoneastri*, 26 between GUCC 9146 and *D. rosicola* and 22 (only three genes) between GUCC 9146 and *D. longicicola*. Meanwhile, the phylogenetic analysis, based on only *tef*1 and *β*-tubulin for the *D. eres* species-complex (Figure 2), also indicated that GUCC 9146 clustered with *D. longicicola* and *D. rosicola* which obtained support values of MP: 99%, ML: 100% and BPP: 1 and maintained a closer relationship with *D. longicicola*.

Taxonomy

Diaporthe millettiae **H. Long, K.D. Hyde & Yong Wang bis, sp. nov.**
MycoBank MB 829563
Figure 3

Diagnosis. Characterised by larger J-shaped β-conidia.

Type. China, Guangxi Province, Nanning City, from leaves of *Millettia reticulata*, 20 September 2016, Y. Wang, HGUP 9167, holotype, ex-type living culture GUCC 9167.

Description. *Colonies* on PDA attaining 9 cm diam. after 10 days; coralloid with feathery branches at margin, adpressed, with apparent aerial mycelium, with numerous irregularly zonate dark stromata, isabelline becoming lighter towards the margin; reverse similar to surface, with zonations. *Conidiomata* pycnidial, multilocular, scattered, abundant on PDA after 3 wks, subglobose to irregular, 1.5–1.8 mm diam., ostiolate, with up to 1 mm necks when present. *Conidiophores* formed from the inner layer of the locular wall, sometimes reduced to conidiogenous cells, when present 1-septate, hyaline to pale yellowish-brown, cylindrical, 10–23 × 1–2.5 µm. *Conidiogenous cells* cylindrical to flexuous, tapered towards apex, hyaline, 8–18 × 1.5–3 µm. *Alpha conidia* abundant, fusiform, narrowed towards apex and base, mostly biguttulate, hyaline, 4.5–9 × 2–3.5 µm. *Beta conidia* scarce to abundant, flexuous to J-shaped, hyaline, 17.5–32 × 1–2 µm. *Perithecia* not seen.

Habitat and distribution. Isolated from leaves of *Millettia reticulata* in China

Etymology. Species epithet *millettiae*, referring to the host, *Millettia reticulata* from which the strain was isolated.

Notes. Phylogenetic analysis combining four gene loci showed that *Diaporthe millettiae* (strain GUCC 9167) displayed a close relationship with *D. arengae*, *D. pseudomangiferae* and *D. perseae* with high bootstrap values (Figure 1). We compared the DNA base pair differences of the four gene regions, the main differences being in the *β*-tubulin and *tef*1 genes, especially *tef*1. *Diaporthe millettiae* produced two types of conidia (α, β), whereas *D. pseudomangiferae* only produced *alpha conidia* and *D. perseae*

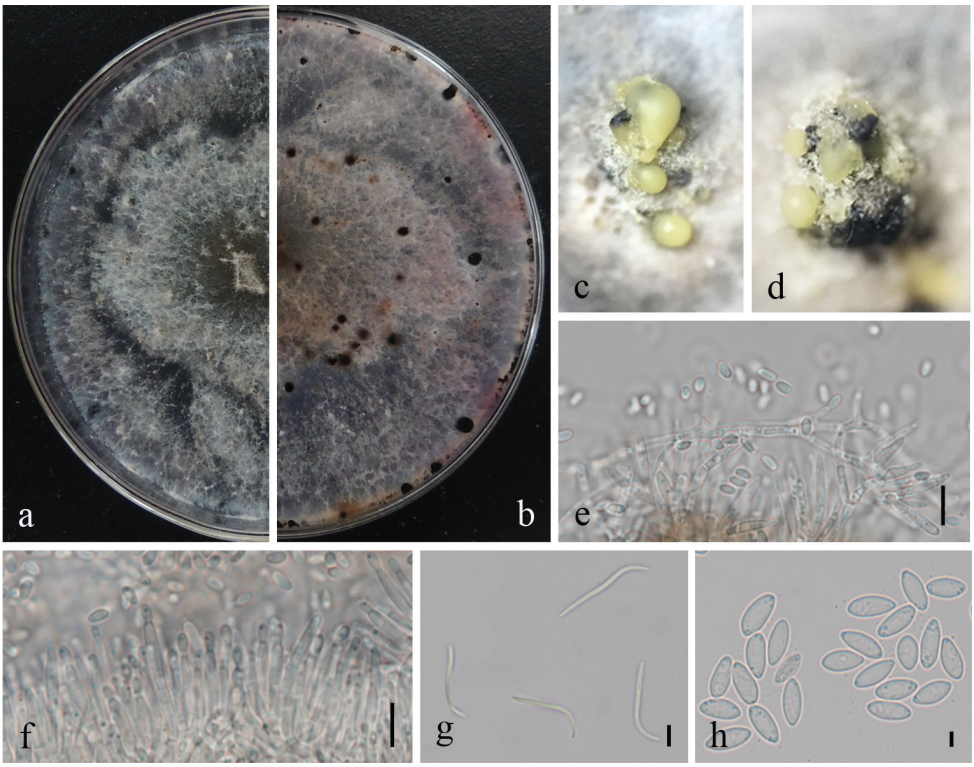

Figure 3. *Diaporthe millettiae* (GUCC9167). **a–b** upper (**a**) and lower (**b**) surface of colony on PDA **c–d** conidiomata **e–f** conidiophores, conidiogenous loci and conidia **g** β-conidia **h** α-conidia. Scale bars: 20 μm (**e, f**), 10 μm (**g, h**).

produced three types of conidia (α, β, γ). The β-conidia of *D. arengae* were smaller (20–25 × 1.5 μm) than those of *Diaporthe millettiae* (17.5–32 × 1–2 μm). The shape of β-conidia was also different. Conidiophores of *D. arengae* (10–60 μm) with more septa (0–6), were longer than those of *D. millettiae* (10–23 × 1–2.5 μm; 0-1-septate) (Gomes et al. 2013).

Diaporthe osmanthi H. Long, K.D. Hyde & Yong Wang bis, sp. nov.

MycoBank MB 829564
Figure 4

Diagnosis. Characterised by size of α-conidia and β-conidia.

Type. China, Guangxi province, Nanning City, from leaves of *Osmanthus fragrans*, 20 September, 2016, Y. Wang, HGUP 9165, holotype, ex-type living culture GUCC 9165.

Description. *Colonies* on PDA attaining 9 cm diam. after 10 days; coralloid with feathery branches at margin, adpressed, without aerial mycelium, with numerous irregularly zonated dark stromata, isabelline becoming lighter towards the margin; re-

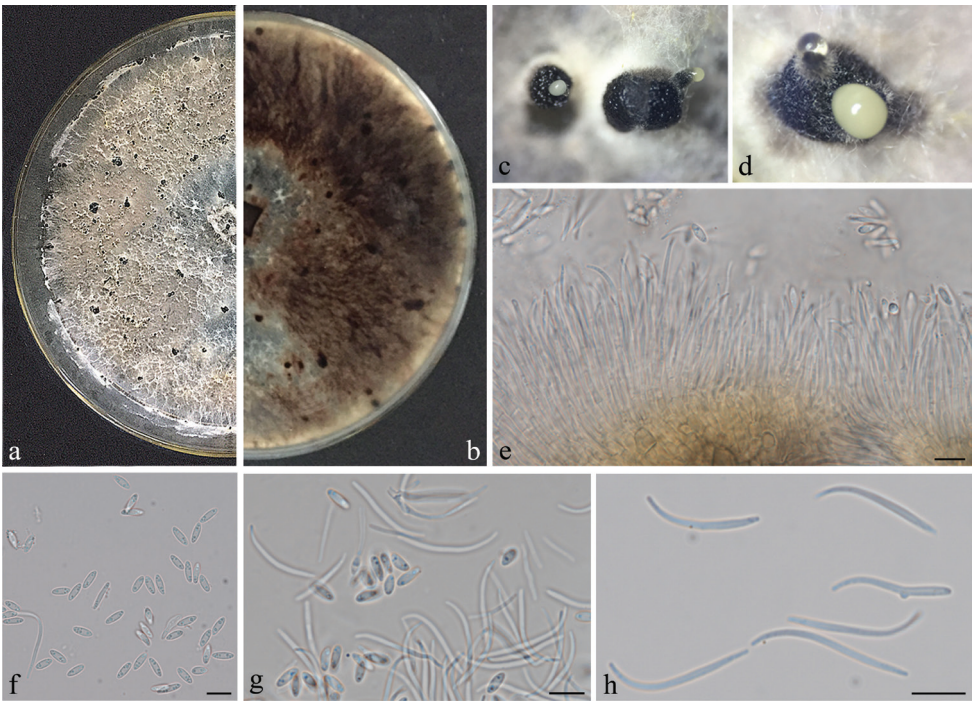

Figure 4. *Diaporthe osmanthi* (GUCC9165). **a–b** upper (**a**) and lower (**b**) surface of colony on PDA **c–d** conidiomata **e** conidiophores, conidiogenous loci and conidia **f** α-conidia **g** two types of conidia **h** β-conidia. Scale bars: 10 μm (**e, f, g, h**).

verse similar to the surface with zonations more apparent. *Conidiomata* pycnidial and multilocular, scattered, abundant on PDA after 3 wks, globose, subglobose or irregular, up to 1–1.5 mm diam., ostiolate, necks absent or up to 1 mm. *Conidiophores* formed from the inner layer of the locular wall, reduced to conidiogenous cells or 1-septate, hyaline to pale yellowish-brown, cylindrical, 20.5–61 × 1–3 μm. *Conidiogenous cells* cylindrical to flexuous, tapered towards apex, hyaline, 10–15 × 1.5–3 μm. *Alpha conidia* abundant, fusiform, narrowed towards the apex and base, apparently biguttulate, hyaline, 5.5–8.5 × 2–3 μm. *Beta conidia* scarce to abundant, flexuous to J-shaped, hyaline, 20–31.5 × 1–2.5 μm. *Perithecia* not seen.

Habitat and distribution. Isolated from leaves of *Osmanthus fragrans* in China.

Etymology. Species epithet *osmanthi*, referring to the host, *Osmanthus fragrans* from which our strain was isolated.

Notes. *Diaporthe osmanthi* (strain GUCC9165) formed an independent lineage, but was also related to *D. arecae* and *D. hongkongensis* (Figure 1). The sequences of *β*-tubulin and *tef*1 included about two-three differences between *D. osmanthi* (GUCC9165) and *D. arecae* (42) and *D. hongkongensis* (78) and thus they were different species according to the guidelines of Jeewon and Hyde (2016). Additionally, *Diaporthe hongkongensis* produced three types of conidia, but *Diaporthe osmanthi* did

not produce γ-conidia. In addition, β-conidia of *D. hongkongensis* (18–22 μm) were shorter than those of *Diaporthe osmanthi* (Gomes et al. 2013). According to original description Srivastava et al. (1962), *D. arecae* also produced two types of conidia. The α-conidia (7.2–9.6 × 2.4 μm) were longer than in *Diaporthe osmanthi*, but its β-conidia (14.4–24 × 1.2 μm) were shorter and their shape also had some differences.

Diaporthe longicicola **Y.H. Gao & L. Cai, Fungal Biology 119(5): 303 (2015)**
Figure 5

Description. *Colonies* on PDA attaining 9 cm diam. in 10 days; coralloid with feathery branches at margin, adpressed, without aerial mycelium, without numerous irregularly zonated dark stromata, isabelline becoming lighter towards the margin; reverse similar to the surface with zonations more apparent. *Conidiomata* pycnidial and multilocular, scattered, abundant on PDA after 20 d, subglobose or irregular, 1.5–1.8 mm diam., ostiolate and up to 1 mm long. *Conidiophores* formed from the inner layer of the locular wall, densely aggregated, hyaline to pale yellowish-brown, cylindrical, tapering towards the apex, 15–25 × 1.5–2 μm. *Alpha conidia* abundant, ellipsoid to fusiform, apparently biguttulate, hyaline, 6–9 × 2–3 μm. *Beta conidia* scarce to abundant, flexuous to J-shaped, hyaline, 25.5–35.5 × 1–2.5 μm.

Habitat and distribution. Isolated from leaves of *Camellia sinensis* in Duyun, Guizhou Province, China

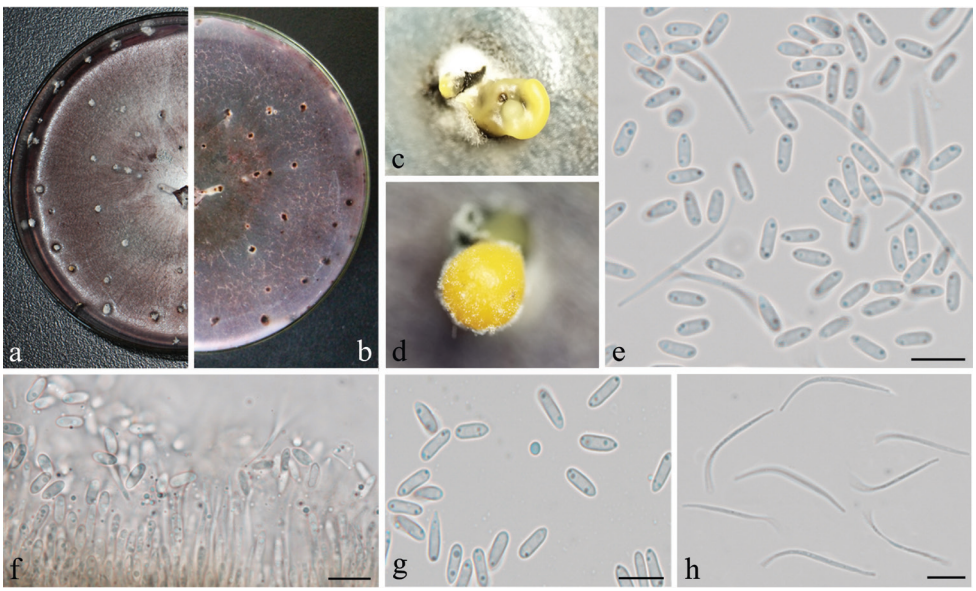

Figure 5. *Diaporthe longicicola* (GUCC9146). **a–b** upper (**a**) and lower (**b**) surface of colony on PDA **c–d** conidiomata **e** two types of conidia **f** conidiophores, conidiogenous loci and conidia **g** α-conidia **h** β-conidia. Scale bars: 10 μm (**e, f, g, h**).

Notes. Phylogenetic analyses (Figures 1, 2) indicated that GUCC 9146 has a close relationship with *D. longicicola*, *D. rosicola*, *D. eres* and *D. cotoneastri*. Morphological comparison indicated that this strain was most similar to *D. longicicola* but not a related species by the width of alpha conidia and length of beta conidia (Udayanga et al. 2014; Gao et al. 2015).

Discussion

Phylogenetic analysis and morphology provide evidence for the introduction of *Diaporthe millettiae* and *D. osmanthi* as new species. In order to support the validity of these new species, we followed the guidelines of Jeewon and Hyde (2016) in comparing base pair differences (Suppl. material 1: Table S1). In accordance with Udayanga et al. (2014), we also believed that the ITS fragment was problematic for the *D. eres* species-complex. When not considering ITS, integration with morphological comparison was helpful and we concluded that GUCC 9146 is *D. longicicola. Diaporthe longicicola* was firstly reported on *Lithocarpus glabra* in Zhejiang Province, but our strain (GUCC 9146) was recovered from *Camellia sinensis* in Guizhou Province. Thus, this is the report of a new host and new location in China for *D. longicicola*.

Acknowledgements

This research is supported by the project funding of National Natural Science Foundation of China (No. 31560489), Genetically Modified Organisms Breeding Major Projects of China [2016ZX08010-003-009], Agriculture Animal and Plant Breeding Projects of Guizhou Province [QNYZZ2013-009], Key Laboratory of Superior Forage Germplasm in the Qinghai-Tibetan Plateau (2017-ZJ-Y12), Talent project of Guizhou science and technology cooperation platform ([2017]5788-5 and [2019]5641) and Guizhou science, technology department international cooperation base project ([2018]5806) and postgraduate education innovation programme of Guizhou Province (ZYRC[2014]004). Dr Kevin D. Hyde would like to thank "the future of specialist fungi in a changing climate: baseline data for generalist and specialist fungi associated with ants, *Rhododendron* species and *Dracaena* species (DBG6080013)" and "Impact of climate change on fungal diversity and biogeography in the Greater Mekong Subregion (RDG6130001)".

References

Carbone I, Kohn LMA (1999) A method for designing primer sets for speciation studies in filamentous ascomycetes. Mycologia 91(3): 553–556. https://doi.org/10.2307/3761358

Chen KL, Kirschner R (2017) Fungi from leaves of lotus (*Nelumbo nucifera*). Mycological Progress 17: 275–293. https://doi.org/10.1007/s11557-017-1324-y

Chomnunti P, Hongsanan S, Aguirre-Hudson B, Tian Q, Persoh D, Dhami MK, Alias AS, Xu JC, Liu XZ, Stadler M (2014) The sooty moulds. Fungal Diversity 66: 1–36. https://doi.org/10.1007/s13225-014-0278-5

Dissanayake AJ, Zhang W, Liu M, Hyde KD, Zhang W, Yan JY, Li XH (2017a) *Diaporthe* species associated with peach tree dieback in Hubei, China. Mycosphere 8, 533–549. https://doi.org/10.5943/mycosphere/8/5/4

Dissanayake AJ, Phillips AJL, Hyde KD, Yan JY, Li XH (2017b) The current status of species in *Diaporthe*. Mycosphere 8: 1106–1156. https://doi.org/10.5943/mycosphere/8/5/5

Du Z, Fan XL, Hyde KD, Yang Q, Liang YM, Tian CM (2016) Phylogeny and morphology reveal two new species of *Diaporthe* from *Betula* spp. in China. Phytotaxa 269: 90–102. https://doi.org/10.11646/phytotaxa.269.2.2

Fan XL, Hyde KD, Udayanga D, Wu XY, Tian CM (2016) *Diaporthe rostrata*, a novel ascomycete from *Juglans mandshurica* associated with walnut dieback. Mycological Progress 14: 82. https://doi.org/10.1007/s11557-015-1104-5

Gao YH, Sun W, Su YY, Cai L (2014) Three new species of *Phomopsis* in Gutianshan Nature Reserve in China. Mycological Progress 13: 111–121. https://doi.org/10.1007/s11557-013-0898-2

Gao YH, Su YY, Sun W (2015) *Diaporthe* species occurring on *Lithocarpus glabra* in China, with descriptions of five new species. Fungal Biology 119: 295–309. https://doi.org/10.1016/j.funbio.2014.06.006

Gao YH, Liu F, Cai L (2016) Unravelling *Diaporthe* species associated with *Camellia*. Systematics and Biodiversity 14: 102–117. https://doi.org/10.1080/14772000.2015.1101027

Gao YH, Liu F, Duan W, Crous PW, Cai L (2017) *Diaporthe* is paraphyletic. IMA fungus 8: 153–187. https://doi.org/10.5598/imafungus.2017.08.01.11

Glass NL, Donaldson GC (1995) Development of primer sets designed for use with the PCR to amplify conserved genes from filamentous ascomycetes. Applied and Environmental Microbiology 61: 1323–1330.

Gomes RR, Glienke C, Videira SIR, Lombard L, Groenewald JZ, Crous PW (2013) *Diaporthe*: a genus of endophytic, saprobic and plant pathogenic fungi. Persoonia- Molecular Phylogeny and Evolution of Fungi 31: 1–41. https://doi.org/10.3767/003158513X666844

Guarnaccia V, Groenewald JZ, Woodhall J, Armengol J, Cinelli T, Eichmeier A, Ezra D, Fontaine F, Gramaje D, Gutierrez-Aguirregabiria A, Kaliterna J, Kiss L, Larigno P (2018) *Diaporthe* diversity and pathogenicity revealed from a broad survey of grapevine diseases in Europe. Persoonia - Molecular Phylogeny and Evolution of Fungi 40: 135–153. https://doi.org/10.3767/persoonia.2018.40.06

Huang F, Hou X, Dewdney MM, Fu YS, Chen GQ, Hyde KD, Li HY (2013) *Diaporthe* species occurring on citrus in China. Fungal Diversity 61: 237–250. https://doi.org/10.1007/s13225-013-0245-6

Huang F, Udayanga D, Wang XH, Hou X, Mei XF, Fu YS, Hyde KD, Li HY (2015) Endophytic *Diaporthe*, associated with citrus: a phylogenetic reassessment with seven new species from China. Fungal Biology,119: 331–347. https://doi.org/10.1016/j.funbio.2015.02.006

Hyde KD, Hongsanan S, Jeewon R, Bhat DJ, McKenzie EHC, Jones EBG, Phookamsak R, Ariyawansa HA, Boonmee S, Zhao Q, Abdel-Aziz FA, Abdel-Wahab MA, Banmai S, Chomnunti P, Cui BK, Daranagama DA, Das K, Dayarathne MC, de Silva NI, Dis-

sanayake AJ, Doilom M, Ekanayaka AH, Gibertoni TB, Goes-Neto A, Huang SK, Jayasiri SC, Jayawardena RS, Konta S, Lee HB, Li WJ, Lin CG, Liu JK, Lu YZ, Luo ZL, Manawasinghe IS, Manimohan P, Mapook A, Niskanen T, Norphanphoun C, Papizadeh M, Perera RH, Phukhamsakda C, Richter C, Santiago ALCM de A, Ricardo DS, Senanayake IC, Tanaka K, Tennakoon TMDS, Thambugala KM, Tian Q, Tibpromma S, Thongbai B, Vizzini A, Wanasinghe D, Wijayawardene NN, Wu HX, Yang J, Zeng XY, Zhang, H, Zhang JF, Bulgakov T, Camporesi E, Bahkali AH, Amoozegar M, Araujo-Neta LS, Ammirati JF, Baghela A, Bhatt RP, Bojantchev D, Buyck B, da Silva GA, Ferreira de Lima, Catarina Leticia, Vilela de Oliveira RJ, Fragoso de Souza CA, Dai YC, Dima B, Duong TT, Ercole E, Mafalda-Freire F, Ghosh A, Hashimoto A, Kamolhan S, Kang, JC, Karunarathna, Samantha C, Kirk PM, Kytovuori I, Lantieri A, Liimatainen K, Liu ZY, Liu XZ, Lucking R, Medardi G, Mortimer PE, Thi TTN, Promputtha I, Raj KNA, Reck MA, Lumyong S, Shahzadeh-Fazeli SA, Stadler M, Soudi MR, Su HY, Takahashi T, Tangthirasunun N, Uniyal P, Wang Y, Wen TC, Xu JC, Zhang ZK, Zhao YC, Zhou JL, Zhu L (2016) Fungal diversity notes 367–490: taxonomic and phylogenetic contributions to fungal taxa. Fungal Diversity 80: 1–270. https://doi.org/10.1007/s13225-016-0366-9

Jeewon R, Hyde KD (2016) Establishing species boundaries and new taxa among fungi: recommendations to resolve taxonomic ambiguities. Mycosphere 7: 1669–1677. https://doi.org/10.5943/mycosphere/7/11/4

Manamgoda DS, Cai L, Bahkali AH, Chukeatirote E, Hyde KD (2011) *Cochliobolus*: an overview and current status of species. Fungal Diversity 51: 3–42. https://doi.org/10.1007/s13225-011-0139-4

Manamgoda DS, Cai L, McKenzie EHC, Crous PW, Madrid H, Chukeatirote E, Shivas RG, Tan YP, Hyde KD (2012) A phylogenetic and taxonomic re-evaluation of the *Bipolaris-Cochliobolus-Curvularia* complex. Fungal Diversity 56: 131–144. https://doi.org/10.1007/s13225-012-0189-2

Nilsson RH, Hyde KD, Pawlowska J, Ryberg M, et al. (2014) Improving ITS sequence data for identification of plant pathogenic fungi. Fungal Diversity 67: 11–19. https://doi.org/10.1007/s13225-014-0291-8

Perera RH, Hyde KD, Dissanayake AJ, Jones EBG, Liu JK, Wei D, Liu ZY (2018) *Diaporthe collariana* sp. nov., with prominent collarettes associated with *Magnolia champaca* fruits in Thailand. Studies in Fungi 3: 141–151. https://doi.org/10.5943/sif/3/1/16

Rossman AY, Allen WC, Braun U, Castlebury LA, Chaverri P, Crous PW, Hawksworth DL, Hyde KD, Johnston P, Lombard L, Romberg M, Samson RA, Seifert KA, Stone JK, Udayanga D, White JF (2016) Overlooked competing asexual and sexually typified generic names of Ascomycota with recommendations for their use or protection. IMA Fungus 7: 289–308. https://doi.org/10.5598/imafungus.2016.07.02.09

Srivastava HC, Zakia B, Govindarajan VS (1962) Fruit rot of areca nut caused by a new fungus. Mycologia 54: 5–11. https://doi.org/10.1080/00275514.1962.12024974

Swofford D (2003) PAUP* – Phylogenetic analysis using parsimony (*and other methods). Version 4. Sinauer Associates, Sunderland.

Tibpromma S, Hyde KD, Bhat JD, Mortimer PE, Xu JC, Promputtha I, Doilom M, Yang JB, Tang AMC, Karunarathna SC (2018) Identification of endophytic fungi from leaves of

Pandanaceae based on their morphotypes and DNA sequence data from southern Thailand. Mycokeys 33: 25–67. https://doi.org/10.3897/mycokeys.32.23670

Udayanga D, Liu XZ, McKenzie EHC, Chukeatirote E, Bahkali AH, Hyde KD (2011) The genus *Phomopsis*: biology, applications, species concepts and names of common phytopathogens. Fungal Diversity 50: 189–225. https://doi.org/10.1007/s13225-011-0126-9

Udayanga D, Liu XZ, Crous PW, McKenzie EHC, Chukeatirote E, Hyde KD (2012) A multilocus phylogenetic evaluation of *Diaporthe* (*Phomopsis*). Fungal Diversity 56: 157–171. https://doi.org/10.1007/s13225-012-0190-9

Udayanga D, Castlebury LA, Rossman AY, Chukeatirote E, Hyde KD (2014) Insights into the genus *Diaporthe*: phylogenetic species delimitation in the *D. eres* species complex. Fungal Diversity 67: 203–229. https://doi.org/10.1007/s13225-014-0297-2

Udayanga D, Castlebury LA, Rossman AY, Hyde KD (2015) Species limits in *Diaporthe*: molecular re-assessment of *D. citri*, *D. cytosporella*, *D. foeniculina* and *D. rudis*. Persoonia 32: 83–101. https://doi.org/10.3767/003158514X679984

Wanasinghe DN, Phukhamsakda C, Hyde KD, Jeewon R, Lee HB, Jones EBG, Tibpromma S, Tennakoon DS, Dissanayake AJ, Jayasiri SC, Gafforov Y, Camporesi E, Bulgakov TS, Ekanayake AH, Perera RH, Samarakoon MC, Goonasekara ID, Mapook A, Li WJ, Senanayake IC, Li JF, Norphanphoun C, Doilom M, Bahkali AH, Xu JC, Mortimer PE, Tibell L, Tibell S, Karunarathna SC (2018) Fungal diversity notes 709–839: taxonomic and phylogenetic contributions to fungal taxa with an emphasis on fungi on *Rosaceae*. Fungal Diversity 89: 1–236. https://doi.org/10.1007/s13225-018-0395-7

White TJ, Bruns TD, Lee S, Taylor J (1990) Amplification and direct sequencing of fungal ribosomal genes for phylogenetics. In: Gelfand M, Sninsky JI, White TJ (Eds) PCR protocols: a guide to methods and applications, Academic Press, USA, 315–322. https://doi.org/10.1016/B978-0-12-372180-8.50042-1

Yang Q, Fan X, Du Z, Liang Y, Tian C (2017a). *Diaporthe camptothecicola* sp. nov. on *Camptotheca acuminata* in China. Mycotaxon 132: 591–601. https://doi.org/10.5248/132.591

Yang Q, Fan XL, Du Z, Tian CM (2017b) *Diaporthe juglandicola* sp. nov. (*Diaporthales*, Ascomycetes) evidenced by morphological characters and phylogenetic analysis. Mycosphere 8: 817–826. https://doi.org/10.5943/mycosphere/8/5/3

Yang Q, Du Z, Tian CM (2018) Phylogeny and morphology reveal two new species of *Diaporthe* from Traditional Chinese Medicine in Northeast China. Phytotaxa 336: 159–170. https://doi.org/10.11646/phytotaxa.336.2.3

Yang Y, Guo YX, Zhang YK, WuH, Zhang M (2016) *Diaporthe henanensis* sp. nov. an endophytic fungus in *Ziziphus jujuba* from China. Mycotaxon 131: 645–652. https://doi.org/10.5248/131.645

Supplementary material 1

The DNA bases difference between our strains and related taxa on four gene regions

Authors: Hui Long, Qian Zhang, Yuan-Yuan Hao, Xian-Qiang Shao, Xiao-Xing Wei, Kevin D. Hyde, Yong Wang, De-Gang Zhao

Data type: molecular data

Link: https://doi.org/10.3897/mycokeys.57.35448.suppl1